INVESTIGATING THE ROLE OF GUT HORMONES IN ENERGY AND GLUCOSE HOMEOSTASIS

Sofia Asim Rahman

A thesis submitted to University College London for the

Doctorate of Philosophy degree

MRC-Industrial Collaborative Award in Science and Engineering (CASE) with GlaxoSmithKline

Supervisors:

Dr Rachel Batterham

Centre for Obesity Research

UCL Division of Medicine

Dr Khalid Hussain

Clinical and Molecular Genetics Unit

UCL Institute of Child Health

Declaration of work

'I, Sofia Asim Rahman, confirm that the work presented in this thesis is my own. Where information has been derived from other sources, I confirm that this has been indicated in the thesis'

Chapter 3

Pdxcre transgenic mice were generated and generously donated as a gift by Professor Pedro Herrera.

Several of the animal studies were conducted with the assistance of Dr E. Irvine, Dr K. Piipari, Dr E. Karra, Ms Q. Millet, Mr M. Gordon and UCL BSU facility staff.

Chapter 4

Several of the studies were carried out with the assistance of Dr E. Kleymenova, Dr J. Way and Ms D. Danger.

Chapter 5

The studies in human subjects were conducted with the assistance of the Histopatholgy Unit at the Camelia Botnar Labs, CHI specialist Nurses and Dr K. Hussain.

Gene expression assays were conducted by Dr S. Senniappan.

Acknowledgements

I would like to thank Dr. Rachel Batterham for providing me with this project, for her advice during my PhD and for getting me this far. In addition, thanks to the members of the Centre for Obesity Research for their practical and theoretical help towards this report. I would like to extend my gratitude to the members of the Metabolic Pathways Enteroendocrine DPU at GlaxoSmithKline NC, USA and especially Drs. Derek Nunez and Kathleen Brown, from whom I have gained unconditional support. Additionally, to Dede who has been my support network from the time I most needed it.

I am also ever so grateful for the support, guidance and supervision that Dr Khalid Hussain has provided to me during my crucial final year.

I would like to truly thank and dedicate this PhD to my greatest support network; my family. Abu, you always knew how to make me smile, Maryam, for being the sister I needed, and my husband, Asim, who stands by me and always inspires me to do great things and has been an endless source of wisdom. Most importantly, I would like to show my appreciation for the two strongest women in my life; Zahida and Shahida. You have collectively shown me how to grow, develop and learn to become ambitious. You always told me I could get through it and I would be grateful once I had finished, all I want to say now is….. I did it!

وقُلْ ربِّ زدْني عِلْماً

This thesis was supported and co-funded by the Medical Research Council (MRC) Industrial Collaborative Award in Science and Engineering (CASE) and GlaxoSmithKline (GSK).

Abstract

Obesity is strongly associated with type-2 diabetes mellitus (T2DM). Gut hormones are peptides secreted from the gut in response to nutrient intake that act to regulate appetite, food intake, energy and glucose homeostasis. Thus, alterations in gut hormone abundance and/or signalling can contribute to the development of the obese and T2DM phenotype. The incretin hormones glucagon-like peptide-1 (GLP-1) and glucose-dependent insulinotropic hormone (GIP) augment glucose-mediated insulin secretion. Peptide YY (PYY) is released from the gut post-prandially and acts primarily as a satiety signal. Recently studies have highlighted a potent role for PYY in regulating glucose homeostasis, which however to date remains partially understood. Dipeptidyl peptidase-4 (DPP-4) is involved in the biological inactivation of the incretins hence; DPP-4 inhibition is used for the treatment of T2DM. DPP-4 also mediates the enzymatic processing of the full length PYY 1-36 to the truncated isoform PYY 3-36. Thus, DPP-4 inhibition may potentially impact on pancreatic PYY function and signalling and may alter the effects of the PYY system on glucose homeostasis by shifting the balance between the PYY isoforms. In addition, gut peptides have been identified as possible contributors to cases of hyperinsulinaemic-hypoglycaemia (HH) resulting from bariatric surgery. Therefore, this thesis aimed to (1) determine the contribution of pancreatic PYY deletion to the intra-islet PYY system; glucose homeostasis and body weight phenotype and (2) establish the impact of hyperinsulinism (HI) on DPP-4 and its gut hormone substrates. To address the first point, pancreatic-specific *Pyy* null (*PdxPyy* KO) mice were phenotyped for changes in the pancreatic endocrine system, followed by body weight and glucose metabolism, *in vivo*. Further investigations measuring gut hormone mRNA suggested the intra-islet system was contributing to the observed reduction in weight gain and HI. Finally, patients with congenital forms of HI (in particular K_{ATP}HI) were evaluated for PYY, GLP-1 and GIP and their enzyme. This study highlighted a role for DPP-4, PYY and GIP in mediating HI. In conclusion, this thesis demonstrates a role for gut hormones in energy and glucose homeostasis. Further work is required to understand the interaction of gut peptides on islet function. This will provide the essential understanding to develop tissue-specific targeted treatment for obesity and T2DM.

Contents

Figure list

Table list

Abbreviations

3V	Third cerebral ventricle
18s	18s ribosomal RNA
ACTB	β-actin
ADP/ATP	Adenosine bi/triphospate
AgRP	Agouti-related peptide
ANOVA	Analysis of variance
ANS	Autonomic nervous system
ARC	Arcuate nucleus
AU	Arbitrary unit(s)
AUC	Area under curve
BAT	Brown adipose tissue
BBB	Blood brain barrier
BMI	Body mass index
Bo	RIA reference tube
BrdU	Bromodeoxyuridine
BSA	Bovine serum albumin
BSU	Biological Services Unit
BW	Body weight
Ca^{2+}	Calcium ion
cAMP	Adenosine 3', 5' –cyclic monophosphate
CART	Cocaine- and amphetamine-regulated transcript
CCK	Cholesytokinin
cDNA	Complementary deoxyribonucleic acid
CHI	Congenital form of hyperinsulinism
CNS	Central Nervous System
Ct	Cycle threshold
DAPI	4',6-diamidino-2-phenylindole
D-CHI	Diffuse disease
DIO	Diet-induced Obesity
DM	Diabetes mellitus
DMEM	Dulbecco's modified eagle medium

DMH	Dorsomedial Hypothalamus
DNA	Deoxyribonucleic acid
DPP-4	Dipeptidyl Peptidase-4
EDTA	ethylene diaminetetraacetic acid
ELISA	Enzyme linked-Immunosorbent Assay
ER	endoplasmic reticulum
FBS	Foetal Bovine Serum
F-CHI	Focal disease
FU	Fluorescent units
GAPDH	Glyceraldehyde-3-phosphate dehydrogenase
GBP	Gastric bypass
GCG	Glucagon
GCGR	Glucagon receptor
GCK	Glucokinase
GHIH	Growth hormone inhibiting hormone
GHSR	Growth hormone secretagogue receptor
GI	Gastrointestinal
GIP	Glucose-dependent peptide
GIPR	Glucose-dependent peptide receptor
GLP-1/2	Glucagon-like peptide-1/2
GLP-1R	Glucagon-like peptide-1 receptor
GLUD1	Glutamate dehydrogenase
GLUT	Glucose transporter type
GPCR	G-Protein Coupled Receptor
GOSH	Great Ormond Street Hospital
GSIS	Glucose-stimulated insulin secretion
HADH	3-hydroxyacyl-CoA dehydrogenase
H&E	Haematoxylin and eosin
HFD	High-fat diet
HI	Hyperinsulinaemia/Hyperinsulinism
HH	Hyperinsulinaemia Hypoglycaemia
HNF4α	Hepatocyte nuclear factor-4α
HPRT	Hypoxyanthine guanine phosphoribosyl transferase

HPS	Hypothalamic-pituitary-somatotropin axis
HPT	Hypothalamic-pituitary-thyroid axis
IHC	Immunohistochemistry
IGF	Insulin-like growth factor
IL2	Interleukin 2
Ins/INS	Insulin
i.p.	Intraperitoneal
IPGTT	Intraperitoneal glucose tolerance test
ir	Immunoreactivity
IR	Insulin receptor
IRS	Insulin receptor substrate
i.v.	Intravenous
IVC	Individually Ventilated Cages
K_{ATP}	ATP-sensitive potassium channels
Kir	Potassium inward-rectifying subunit
KO	Knock-out
LHA	Lateral hypothalamic areas
Lepr	Leptin receptor
MC(1-5)R	Melanocortin Receptor (1-5)
MBH	Medial basal portions of the hypothalamus
MCT	Monocarboxylase transporter
NBF	Neutral buffered formalin
NFW	Nuclease-free water
NIPHS	Noninsulinoma pancreatogenous hypoglycaemia syndrome
NPY	Neuropeptide Y
NRES	National research ethics
NSB	Non-specific binding
NTS	Nucleus of the solitary tract
OFC	Orbital frontal cortex
OGTT	Oral glucose tolerance test
OGSIS	Oral glucose-stimulated insulin secretion
OXM	Oxyntomodulin
PBS	Phosphate buffered saline

PC	Proconvertase
PCR	Polymerase chain reaction
Pdx	Pancreatic-duodenal homeobox
PKA	Protein kinase A
POMC	Proopiomelanocortin
PP	Pancreatic polypeptide
Ppx	Pancreatectomy
PVN	Paraventricular nucleus
PYY	Peptide YY
qRTPCR	Quantitative real-time PCR
rcf	Relative centrifugal field
RIA	Radioimmunoassay
RIN	RNA integrity number
RM-ANOVA	Repeated measures analysis of variance
RPM	Revolutions per minute
RT	Reverse transcription
SD	Standard deviation
SEM	Standard error mean
SPF	Specific pathogen free
SRIF	Somatostatin release inhibitory factor
SST	Somatostatin
SSTR	Somatostatin receptor
STZ	Streptozotocin
SUR	Sulphonylurea
T2DM	Type-2 diabetes mellitus
t	Time
TAE	Tris-acetate EDTA
TC	Total count
Ubc	Ubiquitin C
UCP	Uncoupling protein
VGCC	Voltage-gated calcium channels
VMH	Ventromedial hypothalamus
WAT	White adipose issue

WHO	World health organisation
WT	Wild-type
w/v	weight/volume
YR	PYY receptor
YFP	Yellow fluorescent protein

Chapter 1

Introduction

1. Introduction

1.1. Energy and glucose homeostasis

Energy balance is required for an array of homeostatic functions essential for survival. The fine tuning of this control is achieved through interactions of complex feedback systems from neuronal inputs to the gut-brain axis regulating what and when we eat (Murphy and Bloom, 2006). However, it is not the dysfunction of one of these specific steps that has caused obesity and diabetes pandemics, but a regulatory system that is finding the demand too great.

Obesity is characterised as a condition where stores of fat exceed normal and healthy limits. This is crudely but clinically defined as a body mass index (BMI) of 30 kg/m^2 or more in adults. In school-aged children and adolescents, this is measured by growth references matched for age and sex. Two standard deviations from the normal distribution is characterised as obese.

The modern age supply of cheap and highly calorific dense food and sedentary lifestyles are forcing malfunctions in this otherwise stable and constant metabolic homeostatic setting (Hill et al., 2003). Obesity is a multifaceted condition with pathogenic contributions occurring via physical, psychological and social involvements (Moore et al., 1962). It appears to have no boundaries, virtually affecting all individuals regardless of age or socioeconomic group in the developing and developed world. According to 2008 statistics from the World Health Organisation (WHO), it was estimated that 500 million adults across the globe were obese, which is over 10% of the world's adult population. 40 million under-5s were also classified as overweight by 2011 with 30 million of this number being from developing countries (WHO, 2013). In general, the incidence of obesity is higher in females, but poses a very high and serious risk of other conditions such as cardiovascular diseases, several forms of cancers (Calle and Thun, 2004) and most notably type-2 diabetes mellitus (T2DM) to both sexes (Haslam, 2010). Maintenance of energy balance; energy intake (food intake) and expenditure

(metabolism) must be homeostatically matched (Morton et al., 2006). Traditional exercising and dieting methods are failing to control obesity, making it essential to improve our understanding of the mechanisms implicated in body weight changes in the bid to solve the soaring obesity crisis seen worldwide.

Glycaemic control is important in maintaining the storage of fuels, in particular glucose. Glucose is stored in tissues from ingested carbohydrates. The stomach and remaining gastrointestinal tract (GI) break down the carbohydrates eaten and absorb the glucose molecules, which circulate in the periphery. The increase in plasma glucose levels promotes glucose-stimulated insulin secretion (GSIS). Insulin; a pancreatic β-cell hormone aids in the transport of glucose to tissues. Like the dysregulation of energy homeostasis, imbalances in glucose control can also be detrimental, leading to a severe condition known as diabetes mellitus (DM). Normally fasted blood glucose concentrations in adult humans are maintained within a very tight and narrow range of 3.9 to 5.5 mM. DM arises in individuals where there is a resistance for insulin to function normally (also known as 'insulin resistance'), which is termed as T2DM. T2DM is hyperinsulinaemia (HI)-induced insulin resistance and thus, promotion of hyperglycaemia.

'Diabesity' (Astrup and Finer, 2000), a term used to link obesity to diabetes is thought to be caused by the build-up of fat surrounding tissues (visceral fat) and thus, prevents insulin from functioning. This inhibits an intake of glucose into the tissue causing blood glucose concentration to remain high. As the tissue appears to be deficient in fuel required for cellular activity, it continues to send signals to the pancreas to produce more insulin; this results in exertion of the insulin-producing pancreatic β-cells. This eventually leads to β-cell failure with a subsequent reduction and sometimes loss of insulin production. This can eventually result in the individual going from insulin resistance to an insulin deficient state.

Currently, predictions are that more than half of obese persons will eventually be diagnosed with T2DM. Shaw et al. (Shaw et al., 2010) predicted that the prevalence of adult diabetes was 6.4% in 2010, worldwide. A further 20 years will apparently see this figure go to 7.7%. Disturbingly, it is estimated a rise in the number of adults with DM will occur; an increase by 20% in developed countries and 73% in the developing world. Thus, it is fundamental that we progress to understanding and treating the root cause of this metabolic imbalance.

1.2. The central regulatory circuits of appetite and body weight control

During the 1950s, Stellar identified the hypothalamus and the brainstem as the central homeostatic sites of energy balance (Grill and Kaplan, 2002). These feeding sites receive both endocrine and neural inputs from the periphery to adjust to both the short-term nutritional status and the long-term tissue stores. The non-homeostatic regions of the central nervous system (CNS) such as the orbital frontal cortex (OFC) have also been implicated in feeding behaviour (Batterham et al., 2007). This is thought to be an adaptation to our current environment and lifestyles. A prominent role of the brain and in particular the hypothalamus in regulating the feeding behaviour was established about 50 years ago, however the last 20 years have provided the milestones in our major developmental understandings of how the brain exerts control over energy balance (Murphy and Bloom, 2006). Taken from the Greek (*hypo*- below; below thalamus), the hypothalamus (Figure 1.1) is a major centre for the regulation of food intake and energy balance (Harrold, 2004). The hypothalamus is present in all mammals; it occupies the midbrain below the thalamus and lies on either side of the third ventricle (3V). It also plays an important role in hormonal regulation and links the nervous system to the endocrine system via the pituitary gland. Whilst the hypothalamus is a simple looking structure, it is integrated into numerous complex neuronal systems. These neuronal circuits interchange regulatory factors, which causes subsequent changes in food intake and fat deposition. Identified through classical lesioning experiments, the hypothalamic

regions involved in the regulation of energy balance and food intake have led to observations of certain phenotypes in rodents (Morton et al., 2006). Lesions to the medial basal portions of the hypothalamus (MBH) results in increased adiposity; whereas damage to the lateral hypothalamic areas (LHA) produces a reduction in food intake and body weight (Hetherington and Ranson, 1940). Further work demonstrated the primary region of the MBH area that was disrupted and caused hyperphagia and obesity was in fact the ventromedial hypothalamus (VMH), and hence, was appropriately named the 'satiety' centre. In contrast, the LHA was termed the 'feeding' centre and taken together led to the 'dual centre' hypothesis (King, 2006).

The hypothalamic control of feeding is now well-known to be far more sophisticated and complex than previously thought. For example, lesions to other MBH subnuclear areas, such as the paraventricular nuclei (PVN) and arcuate nucleus (ARC) led to hyperphagia and weight gain (Elfers et al., 2011). However, lesions restricted to the dorsomedial hypothalamus (DMH) resulted in hypophagia, without producing changes to body weight (Bellinger and Bernardis, 2002). This identified the role of many hypothalamic nuclei in controlling body weight and energy stores.

Post-prandially, the hypothalamus senses the changes in metabolic status from both central and peripheral factors (Table 1.1). Circulating factors appear to be released in response to adiposity, in addition to secretion of satiety factors from the GI tract in response to nutrient-intake (Cuomo et al., 2011). This hypothalamic-gut crosstalk governs the regulation and expression of central mediators involved in energy balance. The orexigenic mediators act to stimulate food intake and reduce energy expenditure, causing an increase in adiposity (Tiesjema et al., 2007). However, after a meal and/or when adiposity is above physiological requirements, the satiety factors (anorectic factors) act to reduce feeding and increase the body's natural thermogenic pathways to remove excess stores. These anorectic factors provide negative feedback to the hypothalamic regions that control food intake (Xu et al., 2011).

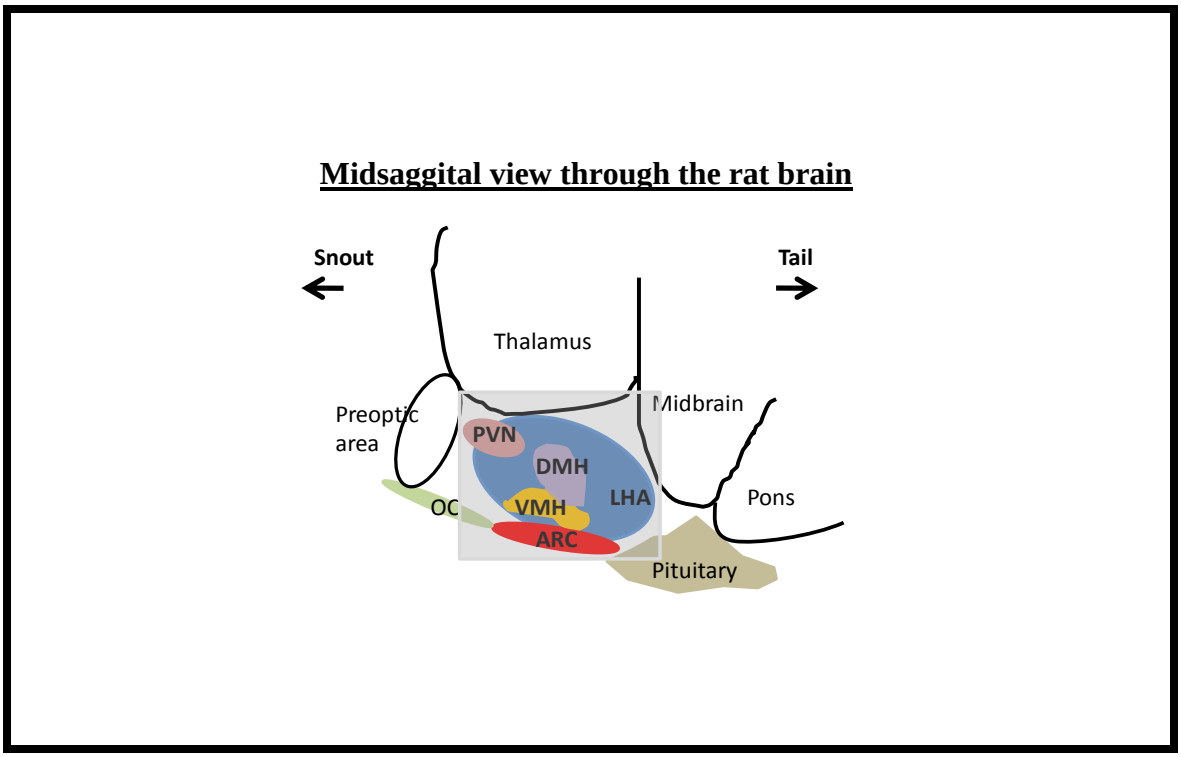

Figure 1.1: Diagrammatic representation of the hypothalamic nuclei involved in energy homeostasis (grey box) (Schwartz et al., 2000). ARC: arcuate nucleus; PVN: paraventricular nucleus; VMH: ventromedial hypothalamus; DMH: dorsomedial hypothalamus; LH: lateral hypothalamic area; OC: optic chiasm.

	Orexigenic peptides	**Anorectic/Anorexigenic peptides**
Peripheral	Ghrelin	Peptide YY (PYY) Insulin Leptin Glucagon-like Peptide- 1/2 (GLP-1/2) Oxyntomodulin (OXM) Cholecystokinin (CCK)
Central	Neuropeptide Y (NPY) Agouti- Related Peptide (AgRP)	Melanocortins Cocaine- and Amphetamine- Related Transcript (CART)

Table 1.1: Regulatory factors involved in the control of food intake and energy balance. The orexigenic mediators act to stimulate food intake and reduce energy release, thus, increasing adiposity. However, after a meal and/or when adiposity is above physiological requirements, the satiety factors (anorectic) act to reduce feeding and increase the body's natural thermogenic pathways to remove excess stores. These anorectic factors provide negative feedback to the hypothalamic regions that control food intake. This energy homeostatic mechanism is fine-tuned to a 'set' balance, ensuring the stores are sufficient for physiological requirements.

1.3. Leptin

Leptin is an adipocyte-derived hormone that acts to reduce food intake by inducing a feeling of 'satiety' (Wang et al., 1997). Leptin is a 167 amino acid hormone, which was discovered by Friedman, Leibel and Coleman whist working with leptin mutant mice (Coleman, 1978, Green et al., 1995). These mice were spontaneously found in the Jackson Laboratories as obese and hyperphagic. Further work led to finding of the gene that encoded leptin (*Ob* gene) and the leptin receptor (Lepr) gene; *Lepr*. The anorectic action of leptin is partially mediated via the down-regulation of hypothalamic orexigen neuropeptide Y (NPY). Central leptin receptors (Lepr) are expressed on neurones in the ARC, PVN and DMH, including the NPY/AgRP (agouti-related peptide: orexigen peptide) neurones. After a fatty meal, adiposity increases and with this the adipocytes release leptin to provide a negative feedback to areas expressing the Lepr, including the hypothalamic feeding and satiety centres (Zhang et al., 1997). Leptin crosses the blood-brain barrier (BBB) and enters the CNS via a saturable transport system (Banks et al., 2000).

The NPY/AgRP neurones are negatively regulated by leptin, consequently causing a reduction in *Npy* mRNA and inhibiting the stimulation to eat. Peripherally, leptin increases energy expenditure by stimulating uncoupling protein (UCP) -1 in brown adipose tissue (BAT) (Wang et al., 1997). However, obese individuals appear to become leptin-resistant, a phenomenon that remains unknown (Myers et al., 2010).

Apart from the hypothalamus, satiety factors signal from the periphery to other central regions of the brain, including the brainstem. These central sites are linked via neuronal projections that have yet to be identified and characterised (Thorens, 2012). It was recently demonstrated that the brainstem exhibits superior homeostatic control than the hypothalamic circuits (Williams and Schwartz, 2011). Transgenic mice deficient in *Lepr* within the nucleus of the solitary tract (NTS) of the hindbrain (*Phox2b Cre Lepr(flox/flox*) display hyperphagia, increased weight gain as seen in the hypothamlamic-specific *Lepr*KO^{VMH} mice (Bingham et al., 2008); however, unlike the

*Lepr*KO^{VMH} mice, the increases in metabolic rate seen in the Phox2b Cre *Lepr*(*flox/flox*) mice produced a compensatory increase in food intake but prevented the development of obesity (Scott et al., 2011).

1.4. The enteroinsular axis: A bidirectional interaction of the gut & pancreas

In 1902, the first description of a connection between the gut and the pancreas was established by Bayliss and Starling who demonstrated that a factor in intestinal mucosa extracts, which they named as 'secretin' (Bayliss and Starling, 1902, Hirst, 2004). Secretin acted via blood to stimulate the pancreatic exocrine secretions (Chey and Chang, 2003). This was followed by Perley and Kipnis showing that ingested nutrients increased the stimulation of insulin release more potently than intravenous administration of glucose (Perley and Kipnis, 1967). Creutzfeldt then labelled this effect as an *'incretin'* effect, i.e. a GI hormone that is released due to enteral stimulation which in turn augments insulin release (Figure 1.2) (Creutzfeldt, 1979). The link between the gut and pancreas was referred to as the 'enteroinsular axis' (Unger and Eisentraut, 1969).

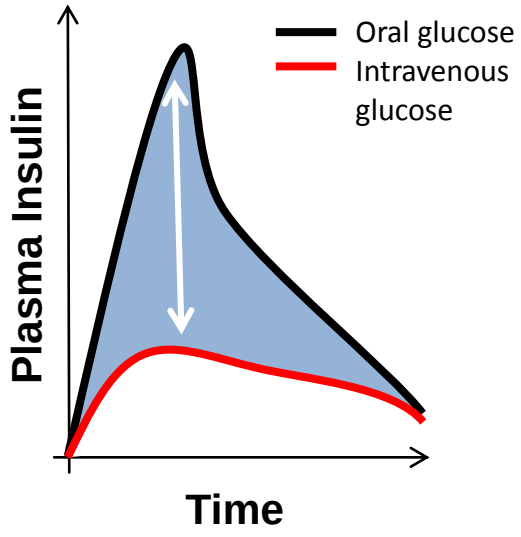

Figure 1.2: Graphical illustration of the incretin effect. This figure illustrates the difference in insulin response to oral versus intravenous glucose load. This difference between the insulinotropic effect is the incretin effect. Adapted from (Nauck et al., 1986).

1.4.1. Insulin

Apart from glucose, insulin secretion is also stimulated by other factors including the autonomic nervous system (ANS) and gut peptides. However the ANS mechanisms are not fully understood (Rodriguez-Diaz and Caicedo, 2013). Proinsulin is synthesised from the human *INS* or rodent *Ins* gene and via proconvertase- (PC-) 1, 2 and carboxypeptidase activity yields the mature insulin and C-peptide. Post-prandial glucose enters the β-cells via the glucose transporter type-2 (GLUT2) transporter. Glucose then enters glycolysis and respiratory cycles and yields the high-energy molecule, ATP. The ATP molecules travel to and inhibit the potassium-dependent ATP channels (K_{ATP}) resulting in depolarisation of the cell membrane via its two subunits: sulphonylurea receptor-1 (SUR-1) and inward rectifying potassium channels (Kir6.2). This triggers voltage-gated calcium channels (VGCC) to open and an influx of calcium (Ca^{2+}) occurs. The Ca^{2+} promotes exocytosis of the pre-packaged mature insulin and active C-peptide, which are released into the circulation (Figure 1.3). Hence, C-peptide is used as a surrogate marker for insulin resistance. Pancreatic β-cells release insulin in two phases. The first phase release is rapid and mediated by increases in blood glucose concentrations. Whereas, the second phase of insulin secretion is glucose-independent. This is much slower and more sustained as newly synthesised insulin-containing vesicles are released (Seino et al., 2011).

Insulin has an oscillation phase; it increases and then steadily decreases levels every 3-6 minutes. This rhythmic delivery keeps the body in fine balance and is thought to prevent insulin resistance occurring. Insulin travels to responsive tissues, typically the liver, muscle and adipocytes and binds to its receptor; the insulin receptor (IR); a tyrosine kinase receptor. IR activates kinases to phosphorylate insulin receptor substrate-1 (IRS-1) to induce the translocation of GLUT4 to the outer plasma membrane. This allows for an increase in cellular glucose entry (Figure 1.4). The cascading phosphorylation by IRS-1 simultaneously promotes hepatic glycogen synthesis or lipid synthesis in adipocytes. *Ir* KO mice develop HI, thought to be a result of insulin signalling from the insulin-like growth factor-1 receptor (IGF-1R) (Accili et al., 1996, Joshi et al., 1996).

Joshi et al., 1996). On the other hand, *Ins* null mice develop DM (Duvillié et al., 1997). An eventual loss of β-cell volume and function are seen in T2DM. Thus, restoration or maintenance of β-cell health and function with new treatments and knowledge are actively pursued.

Unlike the peripheral tissues, the brain uses glucose in an insulin-independent manner (Seaquist et al., 2001). However, IRs have been identified in the hypothalamus and studies have recognised the importance of brain insulin signalling and function in maintaining glucose balance (Szabo and Szabo, 1975). Central administration of exogenous insulin reduces glucose synthesis from the liver, however, inhibition of IR signalling leads to increased hepatic glucose production in the presence of insulin resistance (Obici et al., 2002). Furthermore, specific ablation of IRs in mice from discrete hypothalamic neurons causes glucose intolerance and insulin resistance. However, these findings are confounded by the development of obesity in these mice (Bruning et al., 2000).

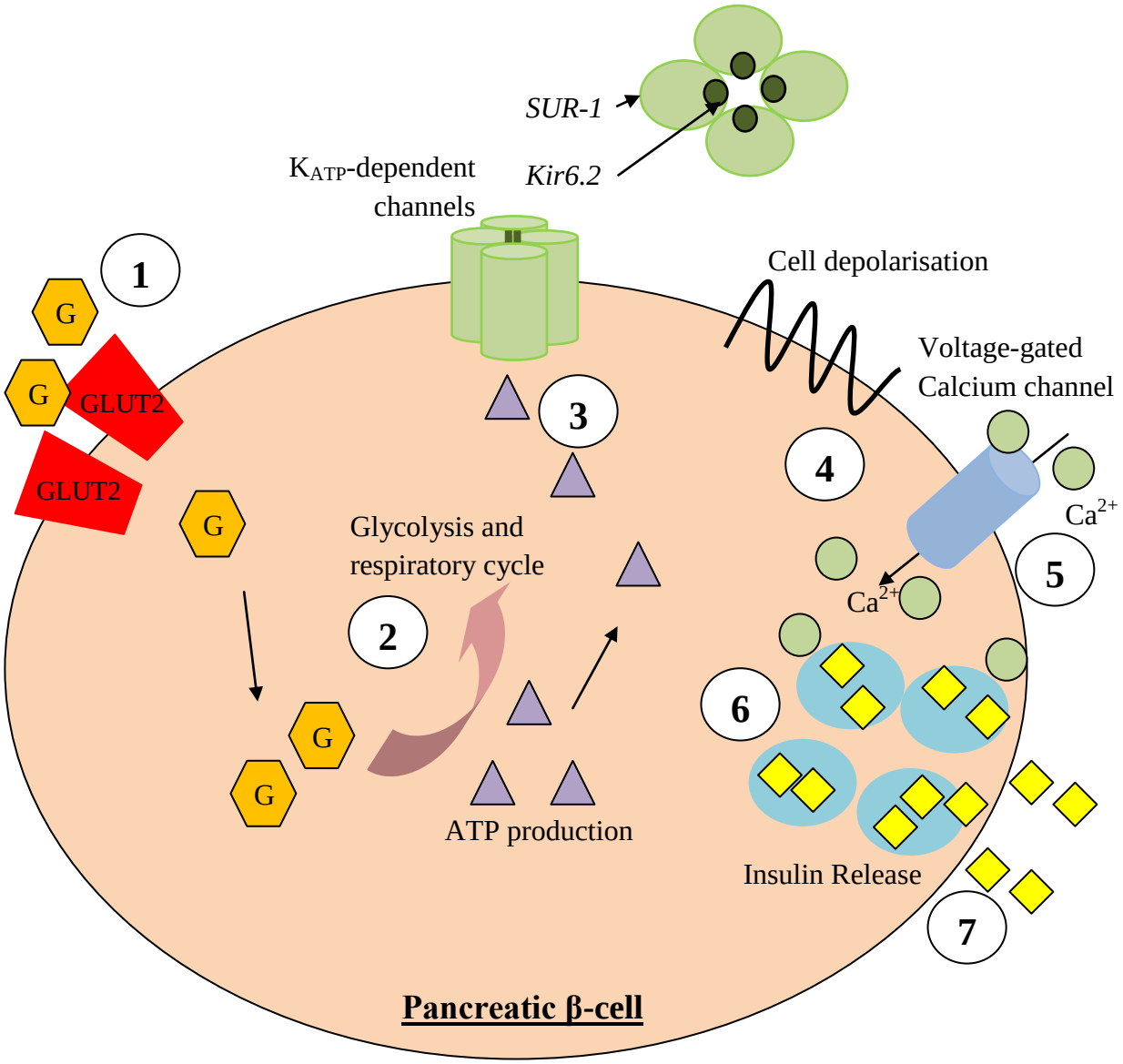

Figure 1.3: Diagrammatic representation of β-cell function. 1) Post-prandial glucose is taken into the β-cells via the GLUT2 glucose transporters. 2) Glucose is oxidised and the high-energy molecule, ATP is produced. 3) ATP travels to the K_{ATP} – dependent channels and 4) prevents the efflux of potassium which in turn causes the membrane to depolarise. 5) This trigger the opening of voltage-gated calcium (Ca^{2+}) channels (VGCC) and 6) calcium inflow 7) stimulates insulin exocytosis. *K_{ATP} – dependent channels: SUR-1 (sulphonylurea receptor-1) and Kir6.2 (the inward rectifying potassium ion channel).*

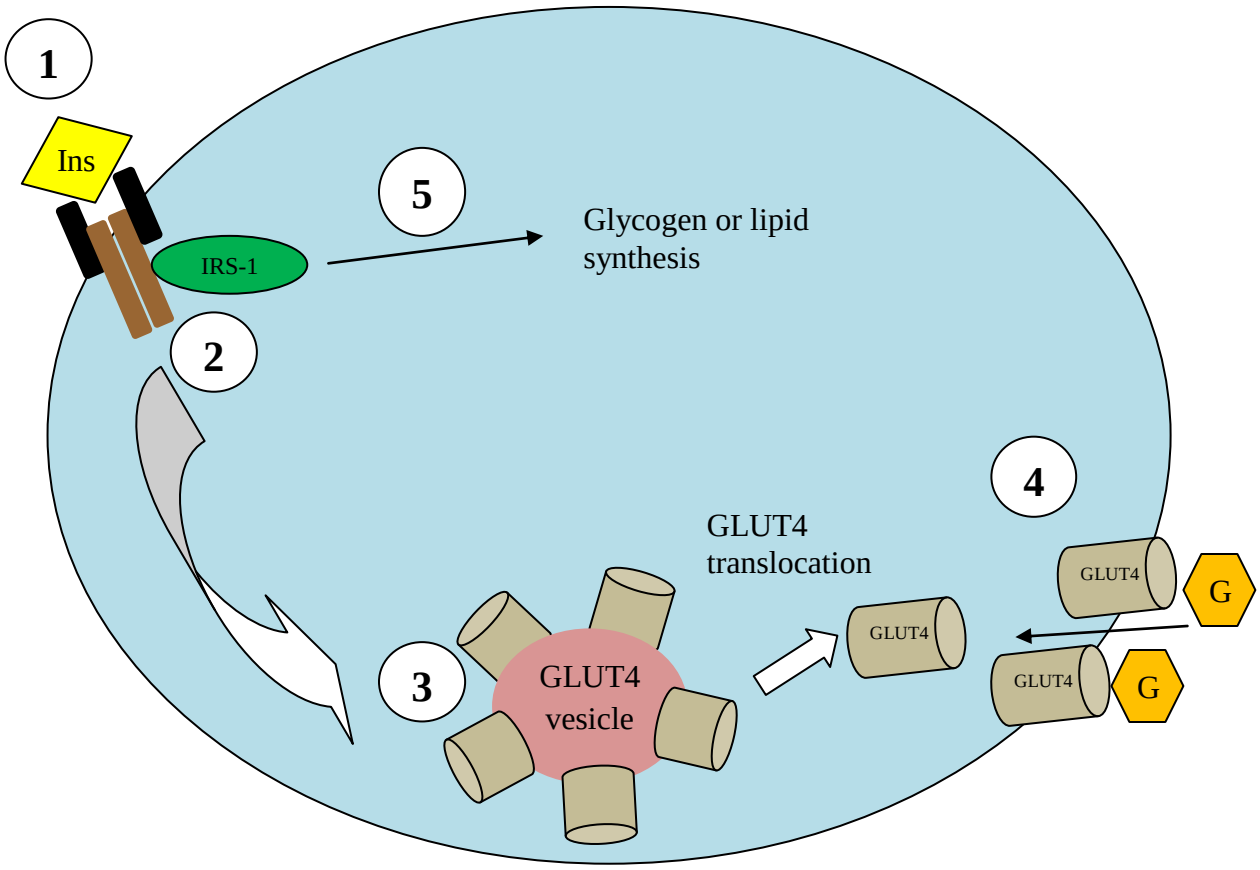

Figure 1.4: Diagrammatic representation of the proposed insulin action on responsive tissues. 1) Insulin binds to its receptor (IR) on responsive tissues and 2) activates IRS-1. 3) IRS-1 binds to and phosphorylates GLUT4 vesicles and leads to translocation. 4) Eventually there is an increase in the GLUT4 affinity for glucose. 5) Additionally, the IRS-1 supports glycogen or lipid synthesis.

1.4.2. Glucagon

During low energy states, the liver extracts insulin from the blood and down-regulates IR expression. At the same time, there is activation for the synthesis of glucagon, a pancreatic hormone produced from the *proglucagon* precursor via PC-2 activity into a 29 amino acid protein. Glucagon was initially discovered in the 1920s and found primarily in islet α-cells (Gaede et al., 1950). The hormone acts on the glucagon receptor (GCGR) and activates the secondary messengers; cyclic adenosine monophosphate (cAMP) and protein kinase A (PKA) (Hue, 1982). It also functions to tonically promote insulin release. However, the counter-regulation of glucagon secretion is lost in T2DM, promoting fasting and post-prandial hyperglucagonaemia which additively affects hyperglycaemia (Larsson and Ahren, 2000). In turn, glucagon activates hepatic glucose production through the glycogenolysis and gluconeogenesis pathways, whilst simultaneously inhibiting the glycogenesis and glycolysis pathways (Jiang and Zhang, 2003).

GCGR disruption by antagonism and antisera reduces hyperglycaemia in rodent models of diabetes (Johnson et al., 1982, Unson et al., 1996). *Gcgr* KO mice have an increase in glucose tolerance, and are resistant to streptozotocin- (STZ-) induced diabetes, *in vivo.* This suggests a decrease in glucagon action may act as potential therapy for T2DM (Gelling et al., 2003). Subsequently, Ali et al. showed $Gcgr^{-/-}$ have an decrease in fasting glucose and islet cell hyperplasia but glucose tolerance was blunted (Ali et al., 2011).

1.4.3. Somatostatin

A third islet cell subtype; the δ-cell expresses somatostatin. Six somatostatin genes exist in the vertebrates, whereas only one has been identified in the human. Somatostatin has also been found expressed in the stomach, here it functions to reduce gastric acid secretion via parietal cells (Gao and Hu, 2006). It is also known as growth hormone-inhibiting hormone (GHIH) or somatotropin release-inhibiting factor (SRIF) and has a role in other non-metabolic endocrine functions (Park et al., 2000). Somatostatin exists as two equipotent isoforms: as a 14 amino acid protein

(SS-14) or as a 28 amino acid product (SS-28) from a 92 amino acid precursor (Schally et al., 1980). Somatostatin inhibits glucagon and insulin release. It has been shown that *Sst* KO isolated islets have an increase in their first phase insulin response thought to be via lack of inhibitory action at K_{ATP} channels. A *Sst*$^{-/-}$ mouse was generated and phenotyped *in vivo* (Cordoba-Chacon et al., 2013). This mouse lost its first phase of insulin secretion but the second phase was exaggerated in the KO group. Moreover, *Sst* deletion also resulted in an increase in both insulin and glucagon secretion, *in vitro* and *in vivo* but failed to suppress glucose-mediated suppression of glucagon release (Hauge-Evans et al., 2009).

Somatostatin mediates its glucoregulatory effects via its G protein-coupled receptors (GPCR); somatostatin receptors (SSTR1-5). Transgenic mice for the different somatostatin receptor-subtypes have provided a deeper understanding of their function in glucose homeostasis. All SSTRs with the exception of SSTR3 couple to voltage-gated potassium channels (Youos, 2011). Somatostatin activates the potassium channels and promotes hyperpolarisation and inhibition of Ca^{2+} -mediated exocytosis (Sharp, 1996). Both SSTR2 and 4 are more potent at increasing the potassium currents (Yang et al., 2005).

SSTR 1-5 are located on α- and β-cells. Exogenous somatostatin and its analogues inhibit nutrient-stimulated insulin and glucagon secretion, both *in vitro* and *in vivo*. SSTR2 is found expressed on α-cells (Cejvan et al., 2003), whilst SSTR1 and 5 are both found on β-cells (Youos, 2011). *Sstr*2 null mice have an increase in nutrient-stimulated glucagon secretion without altering insulin release. *Sstr*5 KO mice have an increased level of islet insulin content, a reduction in blood glucose and plasma insulin levels yet have more glucagon compared to control mice (Strowski et al., 2003). These mice also developed hyperleptinaemia but are resistant to high-fat diet (HFD)- induced insulin resistance. Subsequently, Ramirez et al. developed another *Sstr*5 KO mouse, and the male transgenic group showed increases in SSTR1-3 immunoreactivity (ir), pancreatic somatostatin like-ir and gene expression and a reduction in islet insulin content (Ramirez et al., 2004).

1.5. The role of gastrointestinal hormones in energy control and glucose homeostasis

Our understanding of gut hormones and their role in regulating energy and glucose homeostasis has dramatically increased over the past few years. Consequently, strategies aimed at modulating circulating gut hormone concentrations or targeting their receptors is being developed as pharmacotherapies to treat obesity and/or DM.

1.5.1. Ghrelin

Ghrelin is a 28 amino acid peptide secreted from the gastric fundus' P/D1 cells and can also be found in the ε-cells of the islets (Arnes et al., 2012). This orexigenic hormone is released in response to hunger. Levels peak prior to a meal and are at its lowest post-prandially. It was discovered in 1999 by Kojima and co-workers. Ghrelin is transcribed from a 177 amino acid precursor to act on its GPCR; growth hormone secretagogue receptor (GHSR) (Kojima et al., 1999). Primarily, the peptide is synthesised as a unacylated protein and becomes bioactive once acylated by ghrelin O-acyltransferase (GOAT) (Zhao et al., 2010). To date, this is the only identifiable peripheral orexigen. Ghrelin has also been found to have a role in proliferation and anti-apoptotic effects on pancreatic β-cells (Granata et al., 2007). Studies have also suggested that body weight and ghrelin are negatively associated. Hence, obese adults have a blunted ghrelin response in comparison to lean controls (Stock et al., 2005).

Development of mutant mice have allowed for an understanding of an *in vivo* role for ghrelin in energy and glucose homeostasis. $Ghr^{-/-}$ mice showed no difference in appetite or body weight when compared to $Ghr^{+/+}$ mice, suggesting that ghrelin may not be involved in energy homeostasis (De Smet et al., 2006). Sun and co-workers developed mutant mice with disruption in ghrelin and GHSR signalling. Using these mice they showed that the primary role of ghrelin in the adult mouse might not be involved in energy control but instead be to balance glucose sensing (Sun et al., 2004). This was further supported by the *Goat* null mouse phenotype (Zhao et al., 2010). However, theories have been proposed to suggest ghrelin may have other

receptor targets other than GHSR and/or GHSR may have another endogenous ligand (Uchida et al., 2013). Thus, the variability of the different phenotypes from the different transgenic models makes it difficult to confirm ghrelin's regulatory pathway. Though these studies may be inconsistent, all this data suggests collectively a role for ghrelin's regulatory pathway in energy and glucose homeostasis does exist.

1.5.2. Glucose-dependent insulinotropic peptide (GIP)

After the stomach, post-prandial nutrients come into contact with and stimulate duodenal K-cells to release the first incretin hormone; glucose-dependent insulinotropic peptide (GIP). The incretin effect is the augmented response produced by enteral glucose stimulation versus the comparable glucose load placed by an intravenous administration to promote insulin release (Creutzfeldt, 1979). GIP is a 42 amino acid peptide encoded by the *GIP* gene from a 153 amino acid precursor. Once released into circulation, it is rapidly deactivated by an aminopeptidase; dipeptidyl peptidase-4 (DPP-4) (Drucker and Nauck, 2006). DPP-4 is an enzyme that removes the dipeptide from the terminal of any peptide containing either an alanine or proline at position 2. Hence, GIPs half-life is short; 7 minutes in healthy individuals and becomes reduced to less than 5 minutes in diabetic patients (Deacon et al., 2000). By comparison rats have 2 minutes of GIP bioactivity.

Bioactive GIP has a vital role in potentiating GSIS (Drucker, 2007b). GIP regulates this effect by acting on its receptor (GIPR) to increase islet β-cell cAMP levels whilst inhibiting the K_{ATP} channels. Collectively, these effects mediate the release of insulin. GIP triggers an increase in anti-apoptotic protein levels, *in vitro* (Trumper et al., 2001). Many studies have examined the role of GIP action in energy and glucose homeostasis (Irwin and Flatt, 2009). These studies have highlighted the importance of GIP action and have shown when endogenous GIP is redundant; the incretin effect is lost (Tseng et al., 1999, Miyawaki et al., 1999, Baggio et al., 2000). GIP promotes an increase in glucagon levels and dose-dependently stimulates a rise in somatostatin (Szecowka et al., 1982). Additionally, GIP appears to function as a promoter of lipoprotein lipase activity in adipocytes and is potently stimulated by fat. This has

been demonstrated in *Gipr* KO mice, which have a decrease in fat stores and are resistant to diet-induced obesity (DIO), but have increased insulin sensitivity in comparison to their controls (Miyawaki et al., 1999).

GIPR antagonists administered in *ob/ob* mice have been shown to (1) cause a reduction in weight gain with an improvement in glycaemia as well as (2) an increase in insulin release and sensitivity independent of food intake and weight changes in WT mice (Green et al., 2004). Taken together, the collated data suggests endogenous GIP acts in the adipocytes to increase energy storage as well as inhibit insulin action. On the other hand, GIPR activation on the β-cells promotes an improvement in insulin release. Consequently, it remains difficult to suggest whether stimulation or blockade of GIP signalling could be a method to combat diabesity.

1.5.3. Glucagon-like peptide-1 (GLP-1)

The second incretin hormone to be released post-prandially is glucagon-like peptide-1 (GLP-1), a peptide produced by the lower gut (Lamont et al., 2012). Its precursor; the proglucagon gene is expressed in the GI tract, pancreas and CNS (Ellingsgaard et al., 2011). In the pancreas, processing yields glucagon, and gut post-translational cleavage leads to GLP-1, GLP-2, with the remaining region being cleaved to other inactive fragments and oxyntomodulin (OXM) (Drucker, 2002) (Figure 1.5). GLP-1 circulates as either GLP-1 7-36 amide or GLP-1 7-37, with the predominant form in humans being GLP-1 7-36 amide. GLP-1 is released and most abundantly found in circulation post meal. However, its biological activity is less than 2 minutes due to degradation by DPP-4 (Hansen et al., 1999). GLP-1s function includes β-cell proliferation, increasing insulin synthesis and secretion both via and independently of cAMP and PKA activation. GLP-1 also increases β-cell function by stimulating an increase in Kir6.2 and SUR-1 expression via its GLP-1R (McClenaghan et al., 2006). Moreover, it also prevents the down-regulation of K_{ATP} channels in the presence of high levels of glucose (Drucker, 2007a). GLP-1 antisera, GLP-1R antagonism and *Glp-1r* KO mice have all shown the importance of GLP-1s glucoregulatory function (Baggio and Drucker, 2007). All these studies have

collectively suggested impaired endogenous GLP-1 signalling causes defective endogenous glucose tolerance.

Flamez and co-workers have also shown glycaemia disruptions occur in *Glp-1r*$^{-/-}$ mice, as well as an enhanced rise in cAMP and Ca^{2+} suggested to be due to an increase in GIP sensitivity (Flamez et al., 1999). Another *Glp-1r* KO mouse displayed fasting hyperglycaemia and abnormal glucose tolerance after an oral and i.p. glucose challenge (Scrocchi et al., 1996). This work confirms that GLP-1 action on GSIS can be mediated independently of the route glucose enters the system.

In addition, GLP-1 appears to have a tonic inhibitory effect on islet α-cells at basal levels (Schirra et al., 1998). *Gcgr*$^{-/-}$ have an increase in plasma GLP-1 levels (Gelling et al., 2003). A previous study found glucagon to potentially have affinity for the GLP-1R on β-cells (Moens et al., 1998). Furthermore, glucagon has also been shown to have capacity as a substrate for DPP-4, since like GLP-1, it is a post-translational product of proglucagon (Hinke et al., 2000, Pospisilik et al., 2001). Whether DPP-4 regulates endogenous glucagon remains unknown. Furthermore, Ali and co-workers constructed a double *Gcgr/Glp-1r* KO mouse which displayed an increase in GIP sensitivity (Ali et al., 2011). Further work by another group using GIPR antagonism in mice with deletion in the *Glp-1r* gene showed an increase in blood glucose and reduction in GSIS after an glucose challenge, *in vivo* It was postulated that exendin (9-39) may have the potential to antagonise the GIPR and thus disrupt GIP action (Wheeler et al., 1995). However, this was disproved by Baggio and group, who demonstrated that exendin (9-39) lost its effect on glucose excursions in the *Glp-1r* KO mice (Baggio et al., 2000). This also confirmed the antagonist's specificity for the GLP-1R.

Interestingly, GLP-1/R insulinotropic signalling is preserved in T2DM. Given these, current treatment of T2DM includes the use of GLP-1 analogues. These exogenous synthetics effectively lower glucose in T2DM patients, although these effects are dependent on glucose. Hence, there are limited hypoglycaemic events (Reid, 2012). Exogenous GLP-1 administration at physiological levels fails to produce a change in feeding behaviour, only when given at supra-physiological levels does it evoke an

anorectic response in humans. The GLP-1 analogues provide the incremental increase in GLP-1 levels and promote weight-loss in patients with T2DM. GLP-1 has a crucial role in neogenesis and this has been extensively studied. STZ-induced pancreatic destruction causes an up-regulation of the *Glp-1* gene (Nie et al., 2000). Furthermore, the neogenic properties of GLP-1 can be seen in the improvement of islet morphology in rodents treated with GLP-1R agonists. Conversely, DPP-4 inhibition appears to have no effect on islet morphology in DM models. This suggests that GLP-1R signalling may be therapeutically better at controlling glycaemia and improving islet health.

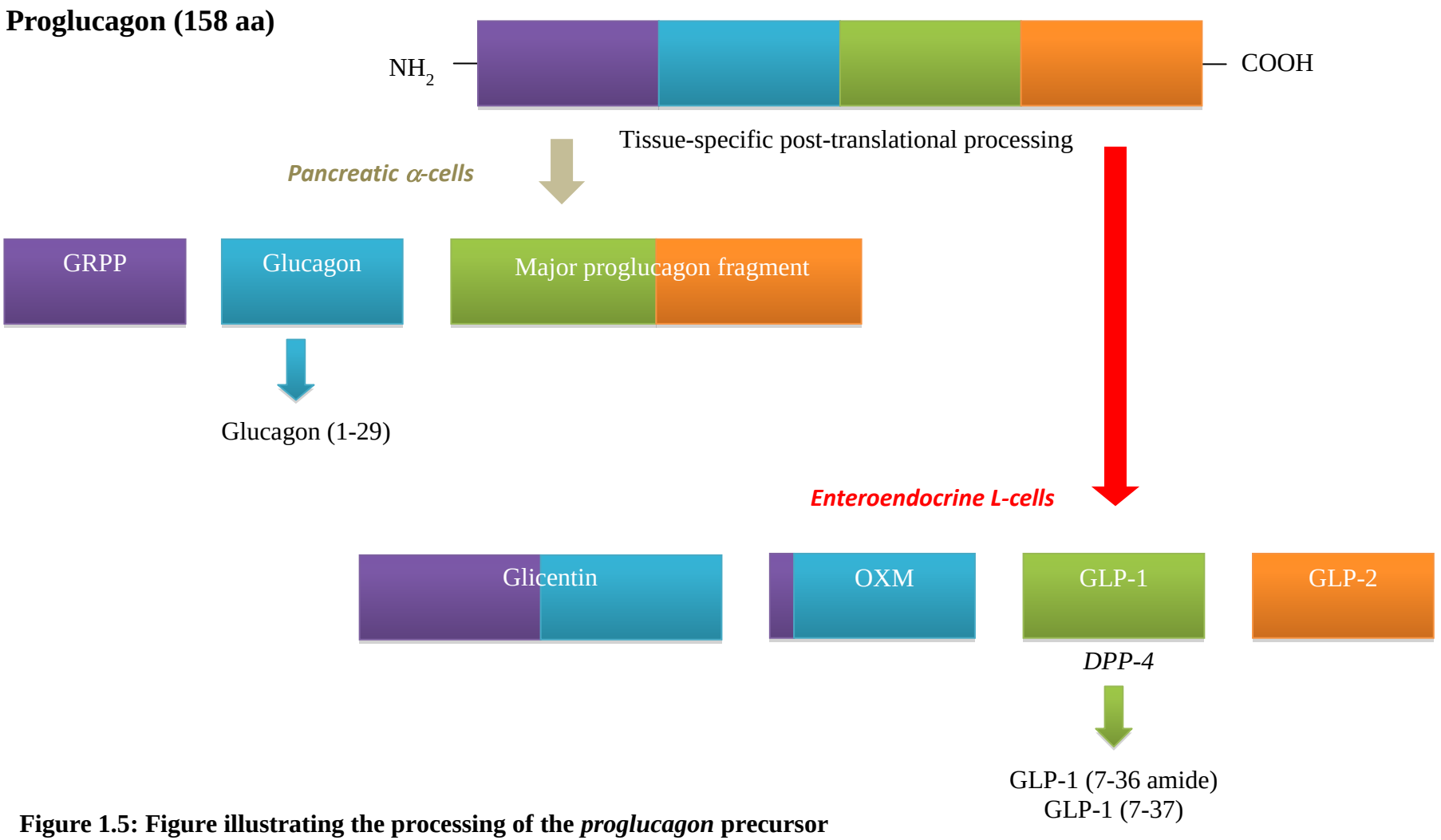

Figure 1.5: Figure illustrating the processing of the *proglucagon* precursor to its tissue-specific post-translational processing products. (Drucker, 2002).

1.5.4. Peptide YY (PYY)

Peptide YY (PYY) is a linear 36 amino acid peptide, which contains a tyrosine residue on either side of the terminals. The tyrosine is abbreviated to the letter Y, hence the name peptide YY. Initial isolation of this peptide occurred from porcine small intestinal extracts (Tatemoto and Mutt, 1980) which later led to the discovery of NPY and pancreatic polypeptide (PP) from the brains and pancreas, respectively (Tatemoto et al., 1982). Tatemoto et al. also found that the sequences and structure between these three peptides were homologous and therefore termed them as the Polypeptide family (Figure 1.6).

The *PreproPYY* gene is co-expressed in the pancreatic α-cells and in particular the ileal L-cells with proglucagon products glucagon and GLP-1 respectively (Kreymann et al., 1991). Once processed, the mature PYY 1-36 is formed. Post-prandially, this form of PYY is converted to the predominant circulating PYY form (3-36) that has known appetite-inhibiting effects (Batterham et al., 2002, Batterham and Bloom, 2003, Batterham et al., 2003). The removal of the first two amino acids from the N-terminus of PYY 1-36 (proline-tyrosine) is catalysed by the same DPP-4 enzyme that degrades the incretin hormones (Figure 1.7). Unlike the incretins, the degradation of PYY changes the conformational structure of the peptide interfering with receptor affinity and thus, changing the biological function of the peptide.

Figure 1.6: Comparison of sequence homology between PYY, NPY and PP. Different colours represent individual amino acids with homology between peptides linked by bars.

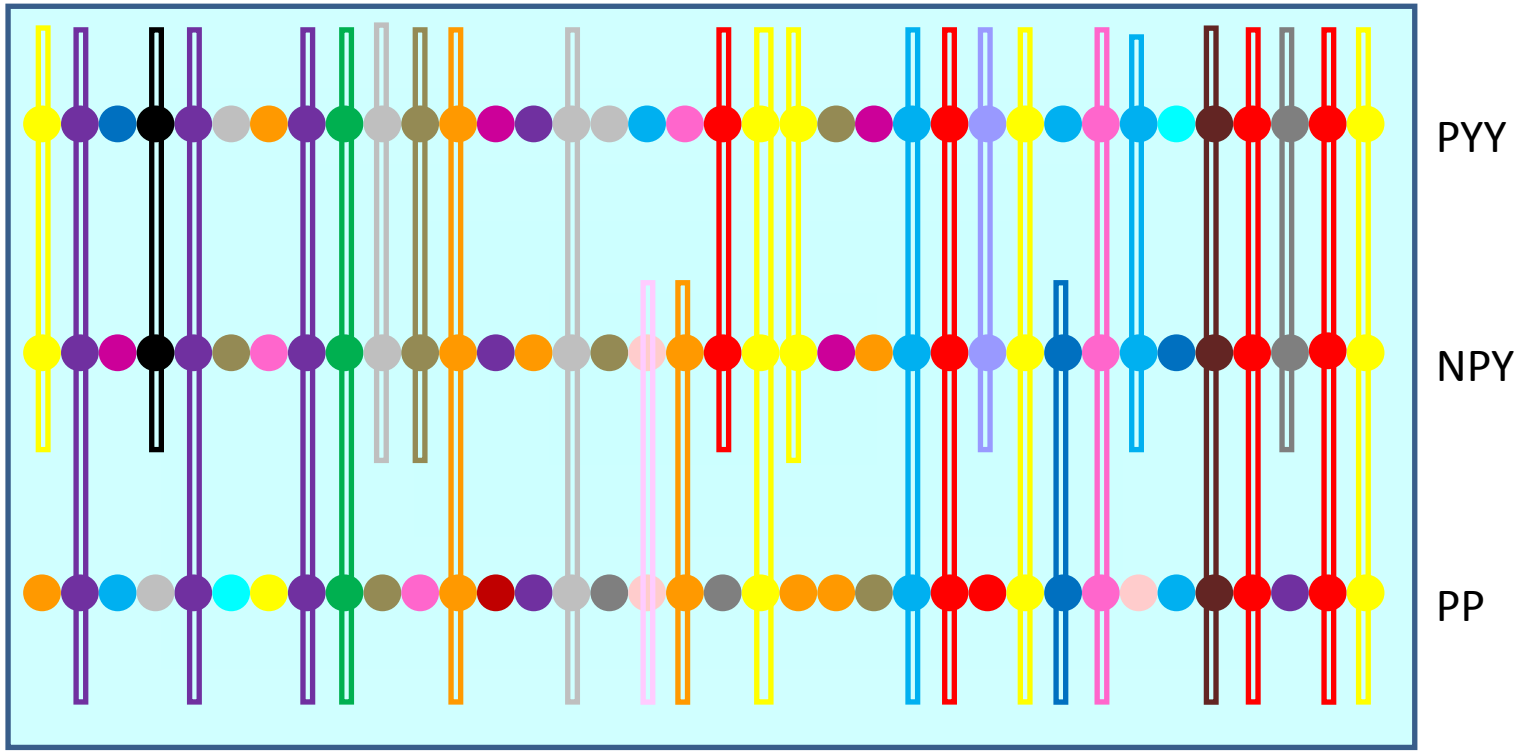

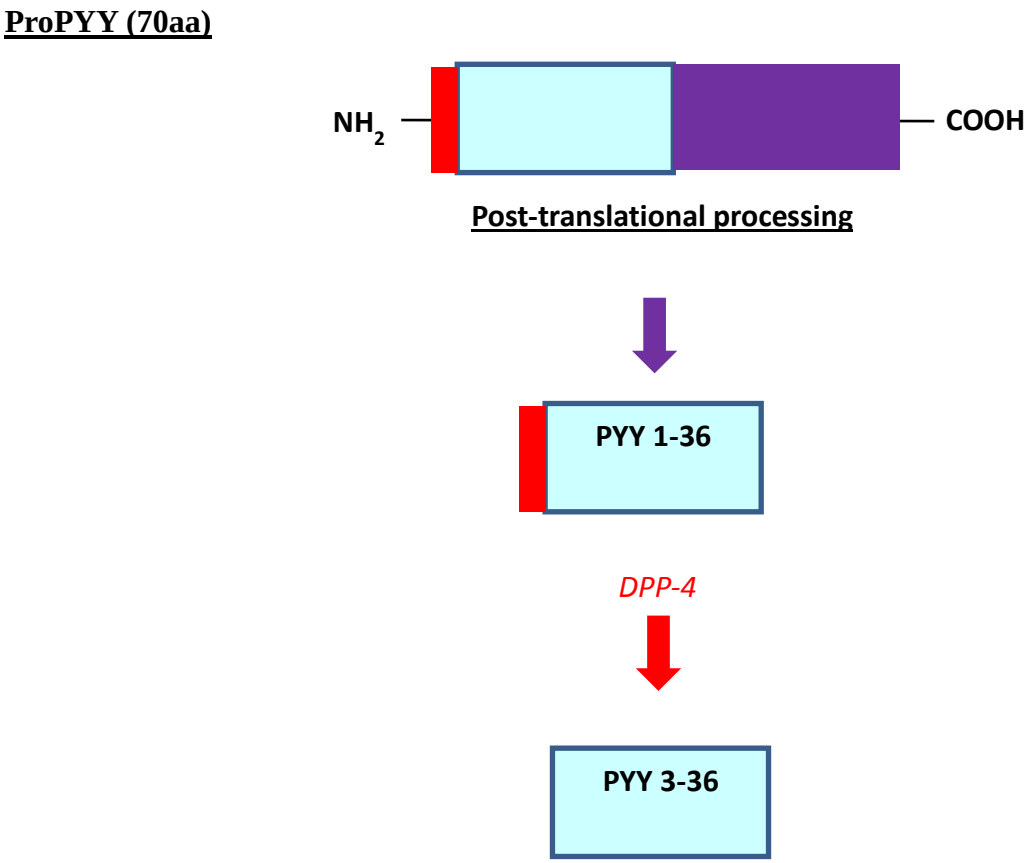

Figure 1.7: Figure illustrating the processing of the *proPYY* precursor to different bioactive isoforms of PYY. (Keire et al., 2002, Michael Conlon, 2002).

The target receptors for the polypeptide family belong to the GPCR superfamily and are known as the Y-receptors. The Y-receptors to date, have been identified as Y1R, Y2R, Y3R, Y4R, Y5R and Y6R, however, only Y1R, Y2R, Y4R, and Y5R are thought to regulate body weight and are expressed on various cells and organs (Michel et al., 1998). Y-receptors display varying affinities to PYY, NPY and PP (Ballantyne, 2006b). The Y1R and Y4R receptor bind to the C- and N-terminals on the peptides, whereas, Y2R and to a lesser degree Y5R only bind to the C-terminus, hence the PYY 3-36 is an Y2R > Y5R receptor specific ligand. Whereas, PYY 1-36 which has both terminals intact, is a ligand for Y1R & Y5R > Y4R. PP on the other hand is a Y4R-specific and preferred ligand and NPY acts at Y1R and Y5R (Ballantyne, 2006b).

Transgenic models targeting the YRs have provided useful information and the tools to study the individual pathways that regulate energy and glucose homeostasis. Many transgenic models have been developed to assess the implications of YR subtypes on energy balance. Global *Y1r* KO mice appear to develop late-onset obesity and HI in the absence of hyperphagia (Burcelin et al., 2001). Germ-line *Y2r* KO and global *Y4r* null mice both display a decrease in body weight and overall adiposity (Sainsbury et al., 2002a, Sainsbury et al., 2002b). However, *Y5r* KO mice appear to develop mild obesity with increases in food intake and body fat (Marsh et al., 1998).

PYY is mainly expressed in endocrine L-cells of the lower GI tract (terminal ileum and colon) as well as the stomach, intestine, and pancreas (Boey et al., 2008). The peptide can also be found in the brain including the brainstem (Glavas et al., 2008), and is known to mediates its effects on feeding behaviour in the hedonic centres (OFC) (Batterham et al., 2007), and various hypothalamic nuclei. PYY 3-36 levels post-prandially rise (to 67% of total PYY) and fall (to 37% of total) during fasting. Grandt and co-workers identified 60% of total murine circulating PYY as the full-length peptide, with the remaining accounting for the truncated form (Grandt et al., 1992). On the other hand, the ratio of human PYY 1-36: 3-36 was found to be relatively equal. The distribution of PYY varies greatly throughout the GI tract (Ballantyne, 2006a). The stomach has levels <3.4 pmol/g, with the duodenum and proximal jejunum expressing

<17.1 pmol/g and 65.4 pmol/g in the distal jejunum. The most abundant area appeared to be the terminal ileum (100 pmol/g). PYY has only been detected in the mucosal layer of the GI tract.

PYY has been well-documented for its role in the regulation of feeding (Karra et al., 2009). PYY 1-36 is known to cause an increase in food intake, primarily occurring at the Y1R and PYY 3-36 is known to produce satiety and increases in energy expenditure at the Y2R. PYY inhibits a number of functions, including insulin secretion, gastric secretion and emptying, GI motility, pancreatic and gut secretion, stimulates water and salt absorption into the colon and promotes vasoconstriction to the vessels of the GI tract and pancreas (Karra et al., 2009, Liu et al., 1997, Karcz-Socha et al., 2011).

In humans, protein consumption is the most potent macronutrient simulating PYY release & satiety in both obese and normal-weight individuals. In mice, increased dietary protein caused a reduction in adiposity, and food intake with an increase in plasma PYY (Batterham et al., 2006). Circulating PYY has a key satiety role in feeding behaviour as discussed above and has been well characterised for its involvement in energy balance (Batterham and Bloom, 2003, Batterham et al., 2002). On the other hand, pancreatic islet PYY appears to demonstrate a fundamental role in glucose homeostasis; however to what extent, still remains unknown (Boey et al., 2007, Boey et al., 2006b).

1.6. Hyperinsulinaemic hypoglycaemia (HH)

Primary importance of gut hormone action in maintaining glucose balance and alterations in their physiology in the T2DM state has been of great interest to many biochemists. Indeed, there are different approaches to treatment including GLP-1R agonists and DPP-4 inhibitors which exert their effects through the incretins and PYY. However, more recently, the implication of these peptides in hyperinsulinaemic hypoglycaemia (HH) is harbouring interest. HH is a condition caused by the dysregulation of β-cell secretion of insulin producing a hypoglycaemic state (Arya et al., 2013).

1.6.1. Weight loss surgery-induced HH

Islet adaptation to insulin resistance is critical to prevent the onset of T2DM. At present there is a vast array of drugs available to treat diabetes including insulin sensitizers (bigunaides) that promote an increase in tissue glucose uptake from the circulation as well as insulin secretagogues (sulphonylureas) which regulate insulin release from the islet β-cells. However these drugs are known to induce hypoglycaemic events, hence the use of DPP-4 inhibitors (gliptins) are becoming the drug of choice when treating T2DM as it works in line with normal physiology. Since gut GLP-1 release is only promoted by enteral stimulation and an autocrine negative feedback exists by GLP-1 on L-cells (le Roux and Bloom, 2005, Näslund et al., 1999), hence, serious hypoglycaemic events are not anticipated or noted.

Apart from the glycaemia control, the drug effects on body weight and lipid profiling have shown promise. However, limited drugs are available for the treatment of obesity and are ineffective in bringing individuals to a near-normal weight. So, more obese patients are opting for bariatric surgery for quick and effective results (Chandarana and Batterham, 2012). One such procedure is the gastric bypass surgery (GBP) which is regarded as the ‘gold standard’ weight-loss procedure in particular for those with

T2DM. It is effective in decreasing 80% of excess weight and resolves insulin resistance immediately post-surgery and prior to significant weight reduction. However, the reason for such drastic changes is still questioned. GBP reduces the stomach volume and is anastomosed to the mid-gut (jejenum) bypassing the *in situ* proximal GI tract. This results in decreased gastric content and limits food intake as well as absorption of nutrients to facilitate weight loss. A few clinical studies have shown that the GBP leads to an increase in post-prandial GLP-1 and PYY levels post-surgery and prior to noted weight loss (Peterli et al., 2009, Olivan et al., 2009). To explain for such changes in gut hormones post GBP, two theories have been proposed (Rubino et al., 2006). The first hypothesises that the bypass of the upper gut eliminates an 'anti-incretin' component which promotes an improvement in glycaemic control. Alternatively the second theory suggests that an increase in undigested nutrients stimulates the distal enteroendocrine L-cells and promotes a surge in GLP-1 and PYY levels. Further preclinical work using rodent models of GBP have allowed for the understanding of gut hormones in energy and glucose metabolism (Chambers et al., 2011). GBP performed in DIO rats improved glucose tolerance and insulin sensitivity. However, exendin (9-39) administration in these rats dampened the GBP-mediated improvement in glucose tolerance. Moreover, obese *Pyy* KO mice that underwent the GBP surgery did not display a significant reduction in body weight (Chandarana et al., 2011). These studies together support a key role of gut hormones in mediating weight and glycaemic balance.

Despite these encouraging effects of GBP on obesity-induced co-morbidities and mortality, the frequency of HH cases as a complication of such a procedure is mounting (Service et al., 2005, Patti et al., 2005). At the same time, it was suggested that if these incidents were investigated in more detail, a novel understanding could be sought for the treatment of T2DM (Cummings, 2005).

Post-prandial HH in GBP-induced nesidioblastosis suggests an enteral stimulus for the glucose impairment (Service et al., 2005). Two theories for this phenomenon exist, the first suggests GBP-induced HH was because of diabesity (i.e. obesity-induced HI) and the second line of thought is that the GBP foregut and/or hindgut peptides cause changes

in the function of the enteroinsular axis (Marsk et al., 2010). However, to date no studies have researched this further. A GBP-HH case report supports the notion that HH is not a result of islet dysfunction or an obesity-induced effect since most of the pancreas had been removed and the GBP was not reported to be reversed (Qintar et al., 2012). Furthermore, in the absence of stimulation in normal WT mice, a pancreatectomy model (Ppx) which has 90% removal of the pancreas has shown regeneration of pancreatic tissue (De León et al., 2003). This effect was thought to be mediated by GLP-1. Moreover, studies using GLP-1 and its analogue (exendin-4) induced a differentiation of pancreatic exocrine tumours to endocrine glucagon- and insulin-producing cells, *in vitro* (Zhou et al., 1999). Whereas, GLP-1R antagonism of *Sur-1* null islets promoted hyperglycaemia in the absence of glucose *in vitro* and independent of body weight changes *in vivo* (De Leon et al., 2008) which is what is required in patients who have undergone weight-loss surgery. GIPR antagonism has also shown potential in mediating suppression in HH, *in vitro* and *in vivo* (Ravn et al., 2013). It was historically reported that GIP dose-dependently increases somatostatin secretion, *in vitro* (Szecowka et al., 1982). On the other hand, a case was reported in which it was described that SST mimetics suppress incretins and HH. However, the SSTR subtype that promotes these effects remains unknown (Sato et al., 2013). Overall, these reports indicate towards a potential of incretin receptor antagonism as candidates for therapy in GBP-HH persons. Therefore, investigations into the physiological involvement of gut hormones in HH will provide novel insights in the regulation of the enteroinsular axis.

Other forms of HH exist, which have been researched for many years and can provide the unique model to study this disease in the absence of confounding factors such as obesity. One such condition is the congenital form of HH.

1.6.2. Congenital forms of HH

Congenital hyperinsulinism (CHI) is the most common cause of transient and permanent hypoglycaemia in neonates and because of this, the disorder could potentially be life threatening causing neurological damage and requires quick and effective treatment and management (Hussain, 2011) (Table 1.2). This disorder is rare and has an incidence of around 1:50,000 births in the general population (Senniappan et al., 2013). Hypoglycaemia in infants is characterised as a blood glucose concentration < 3.5 mM. Infants require constant feeding to stabilise the hypoglycaemia. Congenital genetic dysregulation of insulin function represents the most frequent type of permanent hypoglycaemia. Currently eight gene mutations have been identified to be associated with CHI. These genes encode for glucokinase (GCK), glutamate dehydrogenase (GLUD1), 3-hydroxylacyl-CoA dehydrogenase (HADH), hepatocyte nuclear factor-4 α (HNF4α), monocarboxylate transproter-1 (MCT-1), UCP-2 and the two subunits: SUR-1 and Kir6.2; that make up the K_{ATP} channels (Table 1.3). These have all been described at length for their implications in HH (De Leon and Stanley, 2007).

Defects in the K_{ATP} channels are one of the most common causes of CHI (K_{ATP}HI) (Hussain, 2011). Therefore, this thesis will focus on K_{ATP}HI. K_{ATP} channels are comprised of two subunits; the Kir6.2 ion channels and SUR-1 (Inagaki et al., 1995). Both these subunits are sensitive to the ADP/ATP nucleotide ratio and work together to promote cell depolarisation and eventually insulin secretion. Mutations in the *KCNJ11/ABCC8* genes are known to cause defects in trafficking of these subunits to the plasma membrane, thus causing K_{ATP}HI (De Leon and Stanley, 2007).

Table 1.2: Aetiology of hypoglycaemia in neonates. (De Leon and Stanley, 2007).

Transient hypoglycaemia:

- Impaired gluconeogenesis and ketogenesis in neonate
- Maternal factors: maternal DM, glucose administration during labour or birth or prescription to hypoglycaemic drugs

Prolonged hypoglycaemia:

- Perinatal stress-induced HI
- Beckwith-Weidemann syndrome
- Hypopituitarism

Permanent hypoglycaemia:

- CHI: genetic mutations in *GCK*, *GLUD1*, *HADH*, *HNF4α*, *SLC16A1*, *UCP2*, *ABCC8* and *KCNJ11*
- Impaired counter-regulatory hormones: hypopituitarism, adrenal insufficiency
- Gluconeogenesis or glycogenolysis enzyme defects
- Fatty oxidation disorders

Table 1.3: Key genes involved CHI. (Senniappan et al., 2013).

***Gene* (mutation type)**	**Protein**	**Reference**
1. *GCK* (Dominant)	Glucokinase	(Christesen et al., 2008)
2. GLUD1 (Dominant)	Glutamate dehydrogenase	(Xu et al., 2013)
3. *HADH* (Dominant)	3-hydroxylacyl-Co A dehydrogenase	(Kapoor et al., 2010)
4. *HNF4α* (Dominant)	Hepatocyte nuclear factor-4 α	(Kapoor et al., 2010)
5. UCP2 (Dominant)	Uncoupling protein-2	(González-Barroso et al., 2008)
6. SLC16A1 (Dominant)	Monocarboxylate transproter-1	(Pullen et al., 2012)
7. *ABCC8* and 8. *KCNJ11* (Dominant)	K_{ATP} channels two subunits: SUR-1 and Kir6.2	(James et al., 2009)

Histologically, there are two types of K_{ATP}HI; focal (F-CHI) and diffuse disease (D-CHI). F-CHI is sporadically inherited but D-CHI can be autosomally recessive or dominantly inherited (Senniappan et al., 2013). Due to these factors, management of the two types of K_{ATP}HI are very different. F-CHI only requires a lesionectomy (potentially curing the patient), whereas, D-CHI require medical therapy often with diazoxide; a K_{ATP} channel activator. However, some D-CHI patients are diazoxide-unresponsive; they are treated with alternative drugs including glucagon as well as somatostatin analogues (octreotide and lanreotide) to counteract the unregulated HH. If all these avenues fail, a near-total pancreatectomy is performed. This usually risks DM and possible pancreatic exocrine insufficiency (Senniappan et al., 2013). Hence, it is very important to understand the mechanisms that cause the dysregulation of insulin function so that patient care and management is most effective. Such invasive

treatments are limited to the failure of drug therapy so more research is actively required.

Though no reports have been published in determining the circulating levels of somatostatin and little is known of glucagon in HH individuals, these appear to play a clear role in reducing the surge in insulin and its action since they are commonly used in the management of HH. More research is required to ensure the action and signalling of these drugs is not limited.

The mouse model for K_{ATP} mutation is the *Sur-1* null mouse which presents with mild CHI. *Sur-1* deletion causes a defective glucagon secretory response, *in vivo* (Shiota et al., 2002). Clinical presentations of CHI are also known to be induced by protein ingestion and amino acid-stimulated insulin release (Fourtner et al., 2006). More recently, the role of gut hormones in HH has become of interest to K_{ATP}HI researchers due to the implications seen in bariatric surgery. It was demonstrated in both WT and *Sur-1* KO mice that the GLP-1R antagonist; exendin (9-39) induces a decrease in plasma insulin levels coupled with a rise in blood glucose (De Leon et al., 2008). This finding was subsequently confirmed in the *Glp-1r* KO mice. Furthermore, this group reported an improvement in glucose tolerance in K_{ATP}HI persons after exendin (9-39) administration in the absence of changing plasma GLP-1 concentrations (Calabria et al., 2012). Hence, suppression of the incretins signalling/function appears to be important in reducing HH. At present it remains unknown as to the mechanism of such observations. Moreover, there are currently no reports on the effects of PYY which is known to mediate GLP-1 action in the liver (Chandarana et al., 2013).

1.7. Rationale of study

A biochemical correlation between obesity and T2DM exists. Gut hormone-targeted therapy appears to be the way forward when trying to develop effective treatments for diabesity. However, many studies have been contradictory. GIP is known to promote fat storage and glucagon secretion as well improve glucose tolerance. On the other hand, GLP-1 produces an increase in circulating insulin and improves glycaemic control in DM patients (Drucker, 2007b). However due to its rapid inactivation by the ubiquitously expressed enzyme DPP-4 current therapy for T2DM includes the use of DPP-4 inhibitors to block the enzymes inhibitory action on both incretins. It remains unknown if DPP-4 inhibition leads to an increase in adiposity by GIP action. Additionally, this enzyme also interacts with PYY. The DPP-4 inhibition would stimulate changes to the PYY isoform, hence a change in physiological function on energy and glucose balance.

The current available data illustrates the importance of PYY in glucose and energy homeostasis and implicates intra-islet PYY as a physiological regulator in this balance. This is supported by findings including the inhibition of insulin secretion in mouse islets by exogenous PYY 1-36 (Chandarana et al., 2013, Chandarana, 2009). In addition, blocking of PYY with antisera (Karlsson and Ahren, 1996), global *Pyy* KO (Boey et al., 2006b) or global *Y1r* KO (Burcelin et al., 2001) in mice have all shown a potentiation of insulin release . However, the obese phenotype of the *Pyy* KO mouse doesn't agree with HI (Batterham et al., 2006). Together, all this data suggests intra-islet PYY 1-36 action at the Y1R may cause the inhibition of GSIS. DPP-4 changes the biological activity of PYY by converting it to a Y2R-specific ligand and thus, promotes a reduction in inhibition on insulin release, post-prandially (Figure 1.8).

Naslund and group have shown that GLP-1 has a negative feedback on PYY (Näslund et al., 1999). Recently a published article has reported that PYY 3-36 via Y2Rs mediate the GLP-1 glucoregulatory action in the hepatoportal system (Chandarana et al., 2013). Hence the use of DPP-4 inhibitors could be potentially counter-regulatory with regard to glucose control. On one hand, DPP-4 inhibition

would promote a prolonging of active GLP-1 action on the enteroinsular axis and on the other, PYY 3-36 would be inactivated and thus inhibit the enteroheptic action of GLP-1. Therefore it would appear DPP-4 inhibition switches GLP-1s site of action but the consequences of such a change remains elusive. Additionally, there would be an increase in intra-islet PYY 1-36 which could induce a suppression of GSIS (Burcelin et al., 2001, Boey et al., 2006b) and also have the potential to promote hunger (Burcelin et al., 2001). The duality of DPP-4 activity in the inhibition and activation of the different gut hormones and its consequential effects on energy and glucose homeostasis are important towards an understanding of tackling obesity and glucose dysregulation.

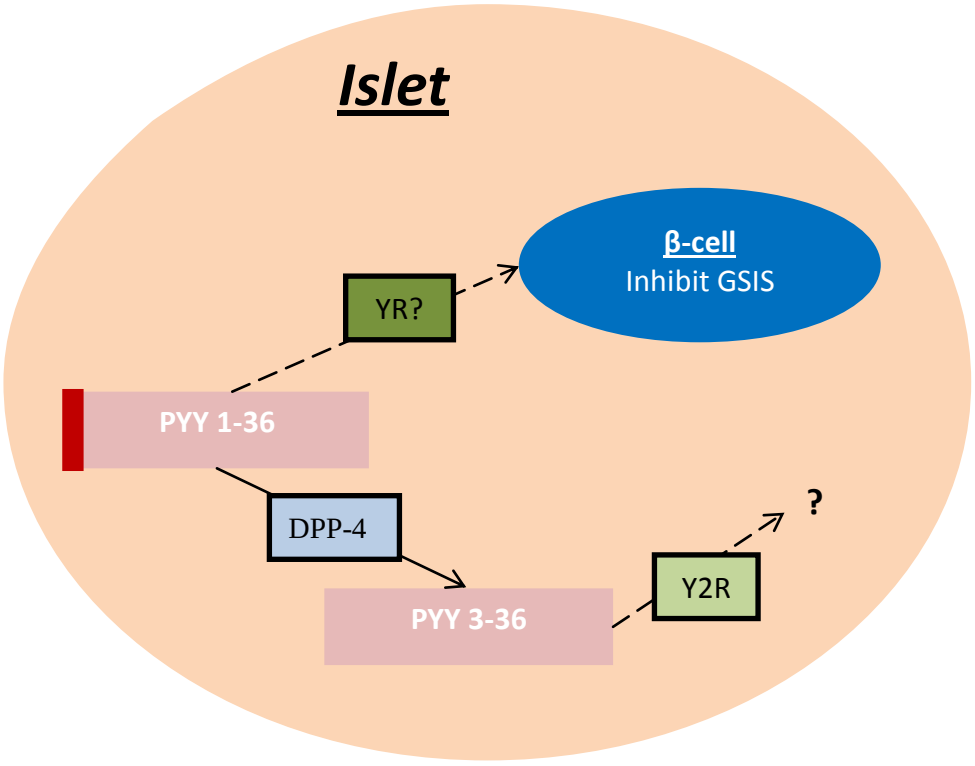

Figure 1.8: Possible regulatory pathways of intra-islet PYY. Intra-islet PYY 1-36 inhibits glucose-stimulated insulin secretion via an unknown YR. DPP-4 changes the biological activity of PYY by converting it to a Y2R-specific ligand and therefore promotes an unknown effect on glucose homeostasis.

As described at length, obese and T2DM individuals are known to have a blunted level of PYY (Batterham et al., 2003, le Roux et al., 2006). Moreover, low levels of circulating PYY has been implicated in the predisposition of obesity and T2DM (Boey et al., 2006a). Incretin hormones are also known to have a role glucose homeostasis (Drucker, 2007b). GIP and GLP-1 are implicated in the pathogenesis of obesity and diabetes. GIP responses are attenuated in T2DM. On the other hand, GLP-1 activity is preserved in T2DM and thus is has been thoroughly researched for its potential as a therapeutic target.

The GBP surgery is primarily the weight loss surgical option for T2DM obese individuals. This invasive procedure re-routes the GI tract, so that the area from where GIP is synthesised and secreted is bypassed and food is passed further into the lower gut where GLP-1 and PYY are co-released. Results from the procedure include the resolution of T2DM and improved glycaemia to a healthy range even prior to body weight changes (Chandarana and Batterham, 2012). Whilst the mechanism of action still remains ambiguous it has been hypothesised to be due to GLP-1 and PYY hyperfunction (hindgut theory). However, there has been a surge in the number of nesidioblastoma diagnoses as a result of GBP which induce HH (Service et al., 2005) assumed to be due to the hyperfunction of GLP-1. Support for this theory is the *Sur-1*$^{-/-}$ mice which when given exendin (9-39) displays hyperglycaemia (De Leon et al., 2008). This phenotype is similar to the *Glp-1r* KO mice (Baggio et al., 2000). Jointly, all this data suggests that suppression of GLP-1R signalling may be a therapeutic target for the treatment of HH (Figure 1.9). Finally, the knowledge of how GBP-induces HH will allow for the pre-surgical identification of bariatric patients that are at risk of this complication, thus improving the doctors ability to make an educated decision about the patients surgical options. As well as understand how the implicated pathways can be manipulated in insulin resistance and hyperglycaemia.

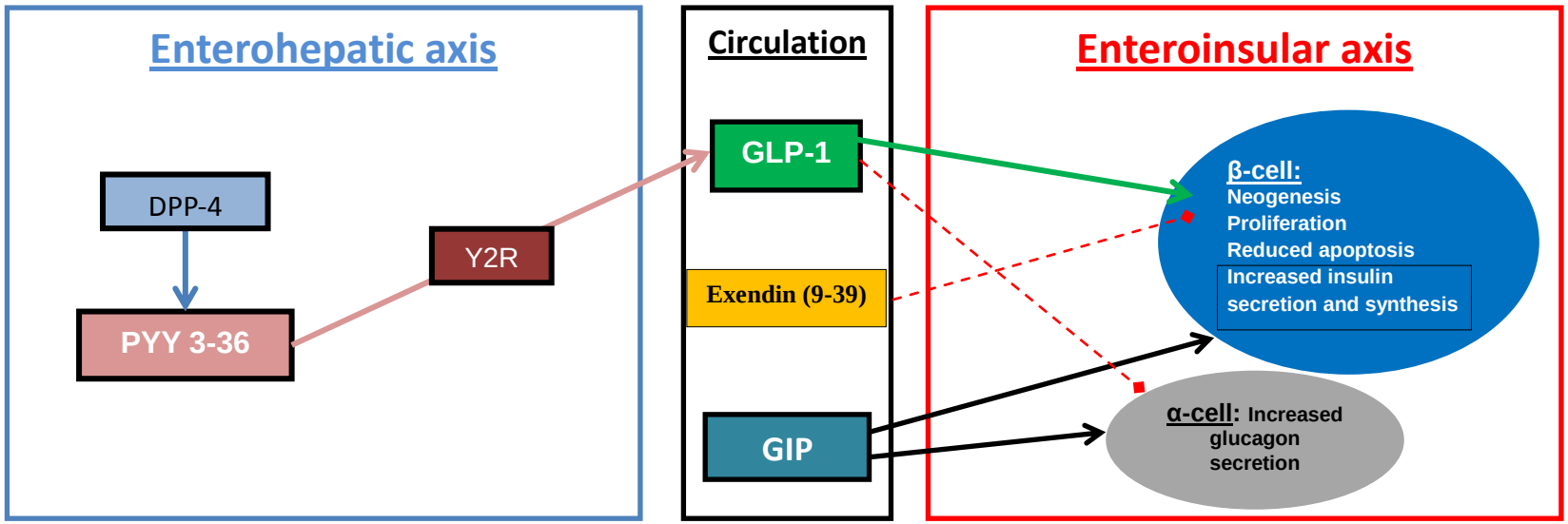

Figure 1.9: Schematic representation of reported pathways that potentially promote islet β-cell regeneration and secretion. DPP-4 stimulates the production of GLP-1 action via PYY and its Y2R. GLP-1 acts on its receptor to promote β-cell neogenesis, proliferation, increases in insulin synthesis and secretion and prevents β-cell apoptosis and glucagon release. The GLP-1R compound; exendin (9-39) antagonises this regulatory pathway. Post-prandially, GIP acts on the GIPR to promote insulin and glucagon secretion (Baggio et al., 2000, Chandarana et al., 2013).

The work of this thesis discusses the data generated and reviews the interpretation of these findings in relation to published studies. Overall it aims to improve our understanding of gut hormones in the role and regulation of energy and glucose homeostasis.

1.8. Objectives of thesis

- To characterise the intra-islet PYY system,
- To investigate the *in vivo* role of intra-islet PYY on energy and glucose homeostasis,
- To characterise the role of gut hormones in HH.

Chapter 2

Methodology

2. Methodology

2.1. Materials

Supplies such as pipette tips, various solvents and reagents were obtained from Sigma Aldrich (Sigma Aldrich, Dorset, UK), Invitrogen (Invitrogen, Paisley, UK) or VWR (VWR, Lutterworth, UK) unless stated otherwise.

2.2. Patients

2.2.1. Ethics

Ethical approval was obtained from National Research Ethics (NRES) Committee (Reference: 05/Q0508/84). Institutional approval was obtained from Great Ormond Street Hospital for Children NHS Foundation Trust, the Research and Development Office. Study information and patient leaflets were provided to the family and a detailed discussion was held prior to obtaining informed consent.

2.2.2. Patient recruitment

Great Ormond Street Hospital (GOSH) is a referral centre for the diagnosis and management of children who present with all complexities of HI. Once the patient arrives, they are diagnosed by blood sample collection during hypoglycaemia and simultaneous measurement of glucose and insulin. Patients are managed on medication and sometimes, surgery. Distinguishing between the histological-type of K_{ATP}HI disease makes the management of the patient easier. K_{ATP}HI patients, who do not respond to medications, undergo a PET scan to determine whether they have a focal lesion, in the absence of this diagnosis, it is assumed the patient has diffuse disease. Thereafter, surgery for focal (removal of lesion) or diffuse (near total pancreatectomy) takes place. All patients that undergo pancreatectomy have their biopsies checked by GOSH pathologists to confirm the type of K_{ATP}HI and to confirm that all pathological tissue has been removed. K_{ATP}HI patients are recruited into the study in a prospective manner. All

subjects are recruited prior to histological diagnosis. Thereafter, they were removed from the study if they were not in line of the criteria. Exclusion criteria for this are use of anti-reflux medications and oral feed-dependency with the inability to achieve a minimum 3-hour fast to baseline reading for the hypoglycaemia screening.

2.2.3. Patient blood collection

Blood is collected from the K_{ATP}HI patient prior to- and the end of a hypoglycaemia screen through a cannula by a specialist CHI nurse/doctor. Patients are fasted for a minimum of 3 hours and medication weaned off 48 hours prior to study. During the hypoglycaemia screen, the patient's i.v. dextrose (20-40%) is slowly decreased and blood sample taken by a qualified HI specialist nurse. Blood was collected into chilled syringes and immediately transferred to ethylenediaminetetraacetic acid (EDTA) vaccutainers (BD, Oxford, UK) containing DPP-4 inhibitor (10 µl/ml blood: Millipore, Watford, UK) and aprotinin (Trasylol 5000 KIU/ml blood: Bayer, Newbury, UK). Blood samples were collected and processed according to the manufacturers' instructions for the measurement of hormones using commercially available assays.

2.2.4. Patient tissue collection

After consent from K_{ATP}HI patient's guardians, pancreatectomised tissue was either taken for quantitative expression analysis or for histological examination by the GOSH Histopathology Lab. For gene expression studies, tissue was placed in 5 ml RNAse inhibitor (RNAlater, Invitrogen, UK) until extraction of RNA. For histological analysis, pancreatic tissue were placed in 70% formalin and fixed according to section 2.7.

2.3. Animals

All animals were housed in the registered biological services unit (BSU) facility University College London with breeding, handling and experimental procedures being in accordance with Home Office Animals Scientific Procedures Act (1986) and the UCL Animal Users Ethics Committee (Project Licence No.70/7151 and 70/6648). The

animals were kept in a specific-pathogen free (SPF) barrier facility and maintained under a controlled environment (temperature 21 +/-1°C, 12 hour light/dark cycle, lights on at 07.00) with free access to water and food (RM1 diet SDS UK Ltd) unless stated otherwise.

2.3.1. C57BL/6 mice

C57BL/6 mice were obtained from Charles River (Charles River, USA) and acclimatised for one week prior to any experimentation. Mice were housed appropriately for each specific study carried out at the ages stated for each experiment.

2.3.2 *Pyy* mice

Previously published *Pyy* KO (*Pyy* $^{-/-}$), *Pyy* lox $^{+/+}$ (*Pyy* floxed) and *Pyy* WT (*Pyy* $^{+/+}$) mice were used for appropriate studies (Batterham et al., 2006). Breeding and genotyping of the animals were carried out in-house. *Pyy* null mice have no expression of PYY mRNA and protein. These mice have also been reported to be hyperphagic and obese. The floxed *Pyy* mice showed no difference in PYY levels and expression, body weight or feeding behaviour when compared to the *Pyy* WT mice (Batterham et al., 2006).

2.3.3 *PdxPyy* mice

PdxCre (pancreatic duodenal homeobox-1 promoter driven *cre* recombinase) transgenic mice were generated and generously donated as a gift by Professor Pedro Herrera (Herrera, 2000). *PdxCre* mice and the *Pyy* heterozygous floxed mice were crossed to produce the *PdxPyy* KO (*Pdxcre*$^{+}$ *Pyy* lox $^{-/-}$) and their control littermate mice; *PdxPyy* WT (*Pdxcre*$^{+}$ *Pyy* $^{+/+}$).

2.3.4 *YfpPyyCre* mice

ROSA26YFP-reporter mice were crossed with *PyyCre (*promoter driven cre recombinase) mice generating *PyyYfp transgenic* mice. These mice express yellow fluorescent protein (YFP) within PYY-expressing cells within the gut, pancreatic-islets as well as other *Pyy*-expressing cells (Gelegen et al., 2012).

2.4. Genotyping

2.4.1 Ear clipping

At weaning (postnatal day 21-28), 2 mm ear or tail biopsies were taken from mice using ear clips or scissors (Kent Scientific, Connecticut, USA) in order to confirm the genotype of mice. DNA was subsequently extracted as described in section 2.4.2 to determine the genotype of each mouse using polymerase chain reaction (PCR) as described in section 2.4.3.

2.4.2 DNA extraction

150 µl of tail lysis buffer was added to each tissue sample. The sample was incubated at 100 °C for 10 minutes in a heat block and cooled before 5 µl of proteinase K (20 mg/ml) was added, pulse spun and incubated at 55 °C for approximately 2 hours. The samples were then heated for 10 minutes at 100 °C and finally spun at 13,000 rpm for 5 minutes to settle debris. 1 µl supernatant was then used as template DNA for PCR amplification as described in section 2.4.3.

2.4.3 Polymerase chain reaction (PCR)

Genotyping PCR was performed using 1 µl of DNA template. PCR primers (Eurogentec, Southampton, UK) and conditions are shown in Table 2.1. Pdx genotyping was done with LoxP and Pdx PCR to detect the *floxed* and/or the *WT* gene in the presence or absence of the *PdxCre* gene. The *Pyy* mice were genotyped with the *LoxP* and *Pyy GN* PCR to detect the *WT* or *KO* amplicons, respectively. PCR products were

visualized using a UV transilluminator (Bio-Rad Laboratories Ltd) following electrophoresis at 95 mV for 100 minutes. The gel was prepared as a 2 % w/v agarose gel using 1x Tris-acetate- EDTA (TAE) and stained with 0.02 % v/v ethidium bromide.

Table 2.1: Genotyping primers and PCR conditions. F: Forward primer, R: Reverse Primer, *LoxP: Floxed* gene, *GN or KO:* gene deletion, *Pdx: PdxCre* gene, *WT: wild-type* gene.

PCR	**Allele**	**Primer sequence**	**Product size (bp)**	**T_m (^oC)**	**Cycles**	**Extension (seconds)**
LoxP	*WT*	F: 5' GACCTCGGTGTTTAATGGG 3' R: 5' GAGTTTAAGGTCCAGGAG 3'	326	60	30	30
	Floxed		350			
Pdx	*Pdx*	F: 5' CGGTGAACGTGCAAAACAGG 3' R: 5' AGGACACATTGTGCCAAAGG 3'	750	60	30	30
	IL2 (control)	F: 5' TAGGCCACAGAATTGAAAGATCT 3' R: 5' GTAGGTGGAAATTCTAGCATCATCC 3'	324			
Pyy GN	*KO*	F: 5' GACCTCGGTGTTTAATGGG 3' R: 5' ATCTCCTGTCCCTTGTAGCC 3'	300	60	30	30
YFP	*YFP*	F: 5' AAAGTCGCTCTGAGTTGTTAT 3' F: 5' GCGAAGAGTTTGTCCTCAACC 3' R: 5' GGAGCGGGAGAAATGGATATG 3'	250	60	40	30
	WT		550			
Cre	*Cre*	F: 5' GCGGTCTGGCAGTAAAAACTATC 3' R: 5' GTAAAACAGCATTGCTGTCACTT 3'	100	60	30	30

2.5 Gene expression measurements

To minimize destruction of RNA by environmental RNases, all equipment was cleaned with an RNase inhibitor (RNaseZap; Ambion, Huntingdon, UK) and only nuclease-free filter pipette tips were used during RNA isolation. Instruments were autoclaved before use.

2.5.1. Islet isolation

Mice were killed by cervical dislocation and a laparotomy was performed. The pancreas was perfused with 2 ml of ice-cold pancreatic digestion solution and immediately dissected out and placed in a 15 ml falcon tube containing 2.5 ml of ice-cold pancreatic digestion solution. After 16 minutes of incubation at 37 °C in a water bath, the sample was placed on ice and 20 ml of ice-cold quenching buffer was added and the tube was shaken vigorously to dissociate exocrine tissue from the islets. The digest was poured through a 500 µm mesh well in and then centrifuged at 200 rcf for 1 minute at 4 °C. The supernatant was discarded and the pellet was resuspended in 20 ml of quenching buffer. The centrifugation step was repeated two more times, and after the last spin the pellet was resuspended in 30 ml of Ficoll-Paque and the sample vortexed. 10 ml of ice-cold quenching buffer was added followed by centrifugation at 1100 rcf for 22 minutes at 10 °C. The islets in the Ficoll layer were collected and passed through a 40 µm cell strainer and were washed with ice-cold 1x PBS (phosphate buffered saline) and RNA immediately extracted from freshly isolated islets (as described in section 2.5.2.).

2.5.2. Islet RNA extraction

Due to the low yield of RNA that can be extracted from islets isolated from mice (Chapter 4, Table 4.1), a different method was utilized. Islets were collected following isolation described previously and centrifuged for 1 minute at 13,000 rpm at 4 °C. The supernatant was removed from the islet pellet and RNA was extracted using the RNeasy mini kit (Qiagen, Crawley, UK). 350 µls of the homogenising buffer supplied with the kit was added to the islet pellet and passed through a 20-gauge syringe and then a 33-

gauge needle, 10 times each. 350 µl of 70 % ethanol was added to the lysate and mixed by pipetting. This mixture was transferred to a spin column attached to a 2 ml collection tube and centrifuged at 10,000 rpm for 15 seconds at 4 °C. The flow through was discarded and the spin column washed with buffers provided in the kit. The spin column was placed in a clean eppendorff and 30 µl of nuclease-free water (NFW) (Ambion, Huntingdon, UK) was added to the column to elute RNA. The final RNA sample was either placed on ice for further analysis or stored at –80 °C for long-term storage.

2.5.3. Whole tissue RNA extraction

According to manufacturer's instructions, whole tissue RNA extraction was performed using TRIzol reagent. Tissues were homogenized in 1 ml TRIzol followed by the addition of 200 µl of chloroform. The mixture was vortexed and incubated at room temperature for 5 minutes before being centrifuged at 13,000 rpm for 15 minutes at 4 °C. The RNA-containing aqueous phase was transferred to a new eppendorff tube and 500 µl of chilled isopropanol was added and the sample vortexed. The tubes were incubated at room temperature for 20 minutes, and then centrifuged at 13,000 rpm for a further 30 minutes at 4 °C. The supernatant was aspirated and discarded without disturbing the RNA pellet and 500 µl of 70 % ice-cold ethanol was added to the tubes, vortexed and centrifuged at 8000 rpm for 5 minutes at 4 °C. The supernatant was discarded and pellet air-dried for 5-10 minutes. The RNA pellet was resuspended in NFW and incubated for 10-15 minutes at 55-60 °C. The final RNA sample was either placed on ice for further analysis or stored at –80 °C for long-term storage.

2.5.4. RNA purification

Additional precautions were taken to purify RNA, by removing DNA contaminants using a DNA-free kit (Ambion, UK). 10 µl of DNase chelating reagent was added and vortexed over 2 minutes. This was followed by centrifugation of the samples at 13,000 rpm at 4 °C. The supernatant was removed without disturbing the DNA pellet. These DNA-free samples were then used to measure the RNA integrity number (RIN) using

the Agilent 2100 bioanalyzer (Figure 2.1). 1 μl of RNA was loaded into a RNA Nano LabChip where the degradation products and the RNA quality were determined. An algorithm assigns a number from 1 to 10, with 10 extrapolating intact RNA. A RIN value of >8 was deemed statistically significant (validated in-house), hence only samples with a RIN of more than 8 were used (See Chapter 4: Table 4.1).

Figure 2.1: RNA integrity number measurement by the Agilent bioanalyser. Intact RNA is indicated by two bands on (A) and two peaks on the electropherogram (B). The blue and red arrows show the 18s and 28s (ribosomal) RNAs, respectively. FU- fluorescence units, s-size.

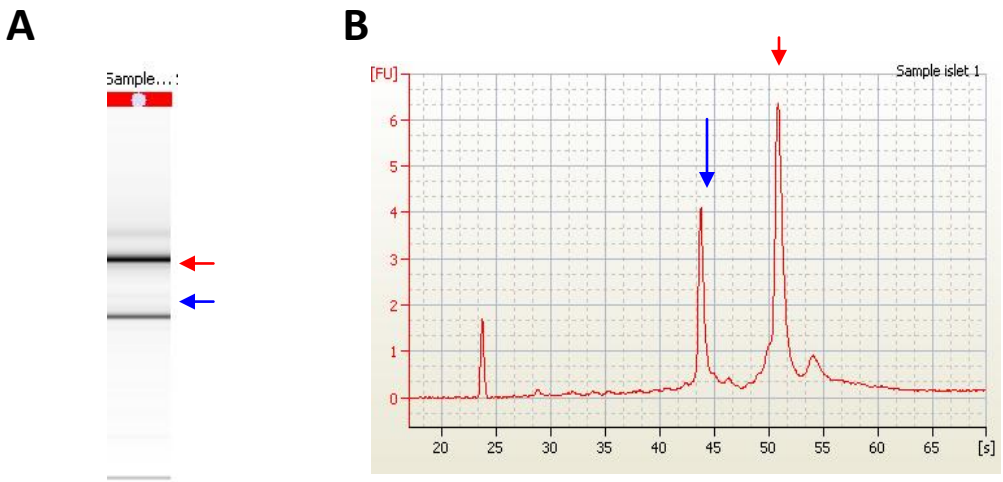

rRNA Ratio [28s/18s]: 2.040185

RNA Integrity Number (RIN): 9.8 AU

Concentration of RNA: 89 ng/µl

2.5.5 Quantification of RNA

1 µl from total RNA was quantified using the NanoDrop Bioanalyzer ND1000 (NanoDrop; Labtech, Ringmer, UK). DNA contaminants are measured by the ratio of A260/A280. A ratio value of 2 equates to pure RNA, hence, a value of 1.80-2.20 was found to be suitable for synthesis of cDNA.

2.5.6. cDNA synthesis

Following isolation, reverse transcription of RNA template to make cDNA was done using a TaqMan Retrotranscription kit (Applied Biosystems, Warrington, UK). Each reaction was set up as follows: 3.0 µl 10x reverse transcription buffer, 1.2 µl 25X dNTP (deoxyribonucleotide phosphate) mix, 3.0 µl random hexamers, 1.5 µl reverse transcriptase, 6.3 µl NFW, 15.0 µl (0.5 µg) RNA template. Samples were heated to 25 °C for 10 minutes, 37 °C for 120 minutes and then 85 °C for 5 minutes. The cDNA template was kept at 4 °C until further analysis.

2.5.7 Quantitative Real-Time PCR (qRTPCR)

Gene expression measurements were performed in duplicates unless otherwise stated. Each reaction replicate contained 1 µl of cDNA template (0.5 µg), 5 µl TaqMan PCR master mix, 2 µl of 20X primer of each respective proprietary FAM/TAMRA probe (Table 2.2) and 2 µl NFW. Tubes are vortexed and pulse spun at 13,000 rpm before loading 10 µl into respective wells of a 384-well clear optical reaction plate and sealed with an optical adhesive cover (Applied Biosystems, Warrington, UK) and centrifuged at 1,000 rpm for 1 minute before loading into the ABI Prism 7900 HT Thermocycler.

qRTPCR cycle:

Temperature	**Time**	
50 °C,	2 minutes	
95 °C	10 minutes	
95 °C	15 seconds	cycle 40
60 °C	1 minute	
72 °C	5 minutes	

In order to normalise mRNA levels, genes of interest were evaluated in proportion to a stable, unchanging housekeeping gene. The Ct value for each sample was automatically computed using SDS software (Applied Biosystems, Warrington, UK). The ΔCt value of each target was compared to the ΔCt value of the housekeeper to normalise the gene expression and show direct difference between groups in arbitrary units (AU).

Gene	Symbol	Product number	Amplicon Size (bp)
Peptide YY	*Pyy*	Mm00520715-m1	61
	PYY	Hs00373890_g1**	150
Glucose-dependent insulinotropic Peptide	*GIP*	Hs00175030_m1	78
Cholecystokinin	*Cck*	Mm00446170_m1	79
Ghrelin	*Ghr*	Mm00439093_m1	61
Glucagon Like Peptide-1*	*Glp-1*	Mm00553234_m1	63
Glucagon Like Peptide-1 receptor	*GLP-1R*	Hs00157705_m1	78
Dipeptidyl Peptidase -4	*DPP4*	Hs00175210_m1	90
Neuropeptide Y receptor Y1	*Npy1r*	Mm01348999_m1	121
	NPY1R	Hs007020150_s1**	120
Neuropeptide Y receptor Y2	*Npy2r*	Mm01218209_m1	86
	NPY2R	Hs01921296_s1**	143
Neuropeptide Y receptor Y4	*Npy4r*	Mm01220859_m1	109
	PPY1R	Hs00275980_s1**	95
Neuropeptide Y receptor Y5	*Npy5r*	Mm00443855_m1	148
	NPY5R	Hs01883189_s1**	149
Neuropeptide Y receptor Y6	*NPY6R*	Hs00246222_s1**	98
Insulin	*Ins2*	Mm00731595_gH**	99
Glucagon	*Gcg*	Mm01269055_m1	62
	GCG	Hs01026189_g1**	64
Somatostation	*Sst*	Mm00436671_m1	86
	SST	*Hs00356144*_m1	86
Ubiquitin C	*Ubc*	Mm02525934_g1**	176
Glyceraldehyde-3- phosphate dehydrogenase	*Gapdh*	Mm 99999915_g1**	109
Hypoxanthine guanine phosphoribosyl transferase	*Hprt*	Mm446968_m1	65
18s ribosomal RNA	*Rn18s*	Mm03928990_g1**	86
β Actin	*ACTB*	Hs99999903_m1	171

Table 2.2: Probes used for TaqMan gene expression analysis. Probes used for qRTPCR, gene symbol, product number and amplicon size. **Glp-1* referred to as *enteroglucagon* gene, **primer does not span intron/exon boundaries and detects gDNA. *Hs*-human gene and *Mm*-mouse gene.

2.6. *In vivo* metabolic studies

2.6.1. Acute feeding studies

16-hour fasted mice were given a pre-weighed amount of chow. At 1, 2, 4, 8, and 24 hours post fast, food remaining in the cage dispenser and mouse body weight were weighed using a GW 600 balance (ATP Instrumentations, Ltd., Ashby-De-la-Zouche, UK) recording to the nearest 0.1g.

2.6.2. Chronic feeding studies

Body weight and food intake were measured once a week between 09.30-11.00 hours from weaning until age stated.

2.6.3. Fasting blood glucose measurement

Mice were fasted for 16 hours and blood glucose levels were measured from the tail vein, after application of local anaesthesia (Cryogesic, UK) with a glucometer (Bayer, UK).

2.6.4. Intraperitoneal glucose tolerance test (IPGTT)

Mice were fasted for 16 hours and injected intraperitoneally (i.p.) with a bolus of 1 g/kg of glucose (relative to body weight (BW) w/v). Blood glucose was measured before and at t = 15, 30, 60, 90 and 120 minutes after injection.

2.6.5. Oral glucose tolerance test (OGTT)

Mice were treated as stated in 2.6.4 and glucose was administered by oral gavage.

2.6.6. Oral glucose-stimulated insulin secretion (OGSIS) measurement

During the OGTT, blood was collected in starstedt tubes at time points indicated. The blood was kept on ice until processing. To process, blood was spun at 10,000 rpm for 15 minutes at 4 ℃ and 10 µl of serum was collected in tubes before assessment of plasma insulin was determined by ELISA, described in section 2.8.2.

2.7. Pancreatic immunohistochemistry (IHC) and morphological analysis

2.7.1. Preparation of pancreata

I. Murine

Mice were killed by cervical dislocation and laparotomy performed. The pancreata were quickly dissected out, immediately spread and pinned to cork boards, which were rapidly placed into jars containing 10% neutral buffered formalin (NBF). Tissues were fixed in formalin for up to 24 hours, rinsed well with tap water and stored in 70% alcohol (all at room temperature).

II. Human

Patients diagnosed with K_{ATP}HI who are non-responsive to drug therapy are pancreatectomised. All tissues were checked by Histopathologists (GOSH, NHS Trust). The normal areas from focal K_{ATP}HI pancreatic tissue were used as controls. All tissues fixed in formalin for up to 24 hours, rinsed well with tap water and stored in 70 % alcohol (all at room temperature).

2.7.2. Tissue processing for paraffin embedding

Tissues were processed as described below. Steps 1 to 9 were performed at room temperature and 9-11 at 60 ºC. Each step was 30 minutes. After processing, the tissues were embedded in paraffin and cooled on ice.

1) 70 % ethanol
2) 80 % ethanol
3) 95 % ethanol I
4) 95 % ethanol II
5) 100% ethanol I
6) 100% ethanol II
7) Xylene I
8) Xylene II
9) Paraffin wax I
10) Paraffin wax II
11) Paraffin wax III

2.7.3. Sectioning and de-paraffinisation

Paraffin embedded tissues were sliced with a microtome using a Finesse 325 retraction microtome (Thermo Shandon, Loughborough, UK) and low-profile disposable Tissue-Tek AccuEdge blades (VWR, Lutterworth, UK) to obtain 5 μm sections. The sections were float mounted on to positively charged Swiss glass slides and dried at room temp overnight. Dried slides were baked at 60 ºC for 2 hours. Deparaffinisation of the sections was performed as described below:

1) Xylene I, 5 minutes
2) Xylene II, 5 minute
3) Xylene III 5 minutes
4) 100 % ethanol I, 1 minute
5) 100 % ethanol II, 1 minute
6) 95 % ethanol, 1 minute

7) 70 % ethanol, 1 minute
8) ddH_2O, 5 minutes

2.7.4. Immunostaining for fluorescent detection

Following deparaffinisation, sections were placed in a heat-induced antigen retrieval solution (Dako, UK) for 3 minutes. Followed by cooling of the slides in 1 X PBS at room temperature. Thereafter, the slides were incubated at room temperature for 30 min with appropriate blocking solution. Blocking solution was removed and the sections were placed in a hydration chamber and incubated overnight at 4 °C with a primary antibody (or antibody cocktail in co-localisation experiments, Table 2.3).

Next day the sections were washed with PBS for 5 minutes at room temperature. The sections were incubated at room temperature in darkness for 30 minutes with secondary antibody conjugated to an Alexa Fluor dye (1:200), and washed with PBS for 15 minutes. Lastly, the sections were mounted with 4', 6-diamidino-2-phenylindole (DAPI) mounting media (Vector Laboratories, UK) and visualised using either a fluorescent or a confocal microscope (Zeiss, UK).

2.7.5. Pancreatic immunofluorescent images and morphometric analysis

Immunostained pancreatic images were taken with a Zeiss LSM 710 inverted confocal microscope with x10, x20 (dry) or x40, x63 and x100 (oil) objective lens. For morphometric measurements, pancreatic sections were taken 50 µm apart and captured on an Olympus fluorescent microscope (Olympus, Southend-on-sea, UK). Fluorescent filters were used at 405 nm for DAPI, 488 nm for FITC and between 555-594 nm for TRITC at the magnification stated. Immunofluorescence was measured using ImageJ software and results were expressed as a percentage of total pancreatic area.

Primary:					
Antibody	***Supplier***	***Catalogue Number***	***Raised in***	***Cross-reactivity***	***Working Dilution***
Anti-PYY	Acris	EUD5201	Guinea Pig	H, R	1:750- R, 1:50-H
Anti- insulin	Dako	A0564	Guinea Pig	R	1:6000-R
Anti- insulin	Cell Signalling	4590S	Rabbit	H, R	1:100-R, 1:25-H
Anti- proinsulin	Novus bio	NBP1-50246	Rabbit	H, R	1:4000-R
Anti-glucagon	Abcam	A0565	Rabbit	H, R	1:50-H & R
Anti-somatostatin	Millipore	AB5494	Rabbit	H, R	1:500-R, 1:50-H
Biotinylated-DPP-4	R&D Systems	BAF954	Goat	R	1:10-R
Biotinylated-DPP-4	R&D Systems	AF1180	Goat	H	1:10-H
Anti-Y1R	Abcam	AB73897	Rabbit	R	1:2
Anti-Ki67	BOND	PA0118	Mouse	H, R	Ready-to-use
Secondary:					
Antibody	***Supplier***	***Catalogue Number***	***Raised in***	***Working Dilution***	
Goat anti-guinea pig Alexa Fluor Molecular Probes 488/555	Invitrogen, USA	A-11073 A-21435	Goat	1:200 1:200	
Goat anti-rabbit Alexa Fluor Molecular Probes 488/594	Invitrogen, USA	A-11034 A-11012	Goat	1:200 1:200	
Streptavidin Alexa Fluor Molecular Probe 488	Invitrogen, USA	S-11223	N/A	1:200	

Table 2.3: IHC antibodies. Table summarising the supplier, host species and working dilution of antibodies used for IHC. H-Human, R-Rodent.

2.7.6. Haematoxylin and eosin staining

Sectioning of pancreata tissue was carried out as previously described. A Leica autostainer was used to deparaffinise and stain the sections as described below, followed by mounting with vectashield mounting media (Vectashield, USA):

1) Xylene I, 3 minutes
2) Xylene II, 3 minutes
3) Xylene III, 3 minutes
4) 100 % ethanol I, 3 minutes
5) 100 % ethanol II, 3 minutes
6) 95 % ethanol, 2 minutes
7) 70 % ethanol, 2 minutes
8) ddH_2O I, 2 minutes
9) ddH_2O II, 2 minutes
10) Haematoxylin, 1 minute
11) ddH_2O, 2 minutes
12) Clarifier, 30 seconds
13) ddH_2O, 2 minutes
14) Blueing, 1 minute
15) ddH_2O, 2 minutes
16) 95 % ethanol, 1 minute
17) Eosin, 10 seconds
18) 100 % ethanol I, 1 minute
19) 100 % ethanol II, 1 minute
20) 100 % ethanol III, 2 minutes
21) Xylene I, 1 minute
22) Xylene II, 1 minute
23) Xylene III, 1 minute
24) Xylene IV, 1 minute

2.8. Assays

Assays were used to quantify the circulating concentration of peptides or hormones of interest from studies. Each assay was carried out in accordance with the manufacturer's guidelines in duplicates (Millipore, Watford, UK).

Kit	***Immunoassay type***	***Catalogue Number***
Human PYY (3-36) Specific RIA	RIA	PYY-67HK
Human Total GIP	ELISA	EZHGIP-54K
Multispecies Active GLP-1	ELISA	EGLP-35K
Rodent Insulin	ELISA	EZRMI-13K

Table 2.4: Immunoassays used for quantification of circulating hormones. Table summarising the assay kit, type and catalogue number for the quantification of circulating hormones of interest.

2.8.1. Radioimmunoassay (RIA)

The kit was used as per the manufacturer's guidelines with reactions being carried out in duplicates. 300 µls of assay buffer was added to tubes for non-specific binding (NSB), 200 µls added to the reference tubes (Bo), and the remaining tubes had 100 µls assay buffer added to them. 100 µl of either a standard or quality control samples supplied with the kit of known concentration and was also added to separately labelled tubes in duplicates. 100 µl of the unknown samples were added to the remaining tubes. 100 µl of the antibody was added, each tube was vortexed, covered and incubated 20 – 24 hours at 4 °C. Thereafter, 100 µl of the radioactively labelled (^{125}I) tracer was added to all tubes and two tubes labelled 'total count' (TC). Tubes were again vortexed, covered and incubated for a further 20 – 24 hours at 4 °C. Finally, 1ml of precipitating reagent was added to all tubes except TC tubes. The tubes were vortexed and incubated for 40 minutes at 4 °C. Later on, all tubes with the exception of TC tubes were centrifuged at 10,000 rpm for 40 minutes at 4 °C. The supernatant was decanted from these tubes immediately after centrifugation. The radioactivity remaining in each test tube was then quantified with a gamma emission counter (Packard Cobra, MN, USA).

2.8.2. Enzyme-linked immunoassay (ELISA)

The ELISA assays feature the capturing of a specific protein in samples by antibodies. Firstly, the sample is added to a microtitre plate which contain the antibodies and any unbound material is washed off. The detection conjugate is then added to the bound material, producing a chemical reaction which is either fluorescently or spectrophotometrically quantified. Results are interpolated from a reference curve which is generated in the same assay by known standard concentrations. All samples were performed in duplicates as per the manufacturer's instructions.

2.9. Statistical analysis of data

All data is presented as mean ± standard error of mean (SEM) unless otherwise stated. Statistical interpretation for body length, gonadal fat mass, gene expression and immunostaining analysis were assessed by unpaired Student's t-test. For 3 or more variables, one-way analysis of variance (ANOVA) was used. For studies assessed over time such as body weight, feeding studies, GTTs and GSIS, analysis was carried out by repeated- measures ANOVA (RM-ANOVA) followed by Fishers post-hoc multiple comparison test. Area under curve (AUC) was determined by the trapezoidal method and compared by unpaired Student's t-test. Differences in plasma hormones and metabolite concentrations of K_{ATP}HI subjects were assessed by paired Student's t-test. Correlation analyses were examined by Pearsons correlation. Raw data was organised and collected in Microsoft Excel and GraphPad Prism 6. Further analysis and preparation for graphical presentation was carried out in GraphPad Prism 6. For all results significance was set at $p < 0.05$.

Chapter 3

Characterisation of the intra-islet PYY system

3. Characterisation of the intra-islet PYY system

3.1. Introduction

The islets of Langerhans are composed as complex multicellular structures forming the endocrine portion of the pancreas. Insulin-producing β-cells make up the largest islet-cell subtype at around 70-80% of the islet (Elayat et al., 1995). Glucagon-producing α-cells account for 15-20% of the islet with somatostatin-producing δ-cells, PP-producing PP-cells and ghrelin-producing ε-cells accounting for the remaining minority. PYY is expressed in the pancreatic islets of Langerhans in rodents (Ekblad and Sundler, 2002) and humans (Ali-Rachedi et al., 1983). In particular PYY is expressed in the α-, δ- and PP-cells post-natally (Ali-Rachedi et al., 1983, Nieuwenhuizen et al., 1994, Jackerott et al., 1996, Myrsén-Axcrona et al., 1997), with some data also suggesting that co-localization occurs prenatally with β-cells (Upchurch et al., 1994). Furthermore, PYY is found to be the earliest detectable peptide to appear during ontogeny in the enteroendocrine cells (Upchurch et al., 1996) and islets (Upchurch et al., 1994). It appears to share lineage with all five islet-cell subtypes (Upchurch et al., 1994, Arnes et al., 2012), with the highest expression occurring in the embryonic pancreas, falling dramatically post-birth and continuing to reduce through adulthood (Upchurch et al., 1994). The physiological consequences of PYY as an early appearing bioactive peptide (during development in the intra-islet cells) are still not fully understood.

Isolated islets placed in media containing PYY have been shown to inhibit stimulated insulin secretion (Bottcher et al., 1989, Bottcher et al., 1993). DPP-4, a ubiquitously expressed enzyme cleaves PYY 1-36, a bioactive form (that acts on all YRs), to the Y2R-selective isoform; PYY 3-36. Nieuwenhuizen et. al., (Nieuwenhuizen et al., 1994) have also shown PYY's inhibitory effect on GSIS, *in vitro*, mediated by a reduction in cAMP. Chandarana et. al., (Chandarana, 2009) presented studies in which they showed that PYY 1-36 supplemented with DPP-4 inhibitor result in a significant increase in GSIS when compared to isolated islets placed in media containing PYY 1-36 alone. They additionally showed that PYY 3-36 in the presence or absence of DPP-4 inhibitor

did not cause a change to GSIS, *in vitro*. Thereafter, a study using transgenic mice ablated PYY in PYY-expressing tissues including the pancreatic islets (Sam et al., 2012). In this report, the resultant *Pyy* null mouse (PYY-DTR) was given PYY 3-36 to assess if the loss of islet content could be rescued, and found no difference in the pharmacologically-treated *versus* the vehicle-treated mice. Moreover, STZ-treated mice and the PYY-DTR mice were both given a PYY 1-36 analogue. Both mice strains displayed a reduction in β-cell death. *In vivo*, transgenic *Y1r* and *Pyy* null mice display an increase in insulin release (Burcelin et al., 2001, Boey et al., 2006b). Taken together, these reports suggest very distinct roles for these two molecular species of PYY on glucose homeostasis. This implies that islet PYY 1-36 inhibits GSIS possibly via the Y1R. However, studies so far have failed to confirm this and the physiological role and regulation of this population of islet PYY still remains largely unknown.

3.3. Hypothesis

'PYY 1-36 is the bioactive isoform within the intra-islet system'

3.4. Aims:

- To establish and optimise a murine islet isolation protocol for extraction of RNA for gene expression.
- To confirm the presence of islet *Pyy* and *Dpp-4* from isolated islets of C57BL/6 mice.
- To determine the *Yr* subtype gene expression in isolated islets from C57BL/6 mice.
- To evaluate the localisation and distribution of PYY, DPP-4 and Y1R in islet cell subtypes of the WT mouse using IHC.
- To evaluate the gene expression of *Ins, Gcg* and *Sst* in the *Pyy* mice.
- To evaluate the expression changes of α-, β- and δ-cell area in the *Pyy* and *PdxPyy* mice using IHC.

3.5. Study design:

An islet isolation protocol was established and optimised (Liao, 2012). In addition, the presence or absence of *Yr*-subtypes from C57BL/6 (WT) islets was determined. Thereafter, distribution of DPP-4 and PYY expression in the different islet cell subtypes and the expression of Y1R with insulin and DPP-4 was evaluated using IHC in C57BL/6 mice. Finally, changes in gene and protein expression of insulin, glucagon and somatostatin were measured in the *Pyy* and *PdxPyy* mice.

3.5. Results

3.5.1. Establishing and optimising an islet isolation protocol in mice

The pancreas is made up of the exocrine cells and endocrine islets. The islets contain signalling factors and hormones that are involved in glucose homeostasis. Hence, to assess the response of various conditions and factors on the islet PYY system, islets were isolated successfully and repetitively to ensure accuracy and reproducibility. Initially, to acquire islets, separation from the remaining pancreatic tissue was done by perfusion of a collagenase buffer via the common bile duct.

Figure 3.1 shows the anatomical positioning of various tissues with respect to the pancreas. The ampulla of Vater or hepatopancreatic ampulla (circle) is formed by the merging of the pancreatic duct and the common bile duct and is specifically located at the junction with the duodenum. Pancreatic secretions are carried from the pancreas and passed through these pathways into the gut (the enteroinsular axis). Using these networks, a collagenase buffer was administered along the common bile duct through the incision of the ampulla.

Once successful perfusion of the pancreas had taken place, fractions of various cells were centrifuged off until a floating layer of islets in a Ficoll gradient remained. A pellet containing mostly exocrine and undissociated islets formed at the bottom of the tube (Figure 3.2A). A fraction containing islets are passed through a 40 μm strainer and then plated before islets were isolated by handpicking (Figure 3.2B-D). The healthy islets are generally then either (1) incubated overnight and used for static incubation studies to assess the intra-islet physiology when incubated in a given test buffer and/or (2) taken to extract RNA immediately and perform qRTPCR to assess gene expression.

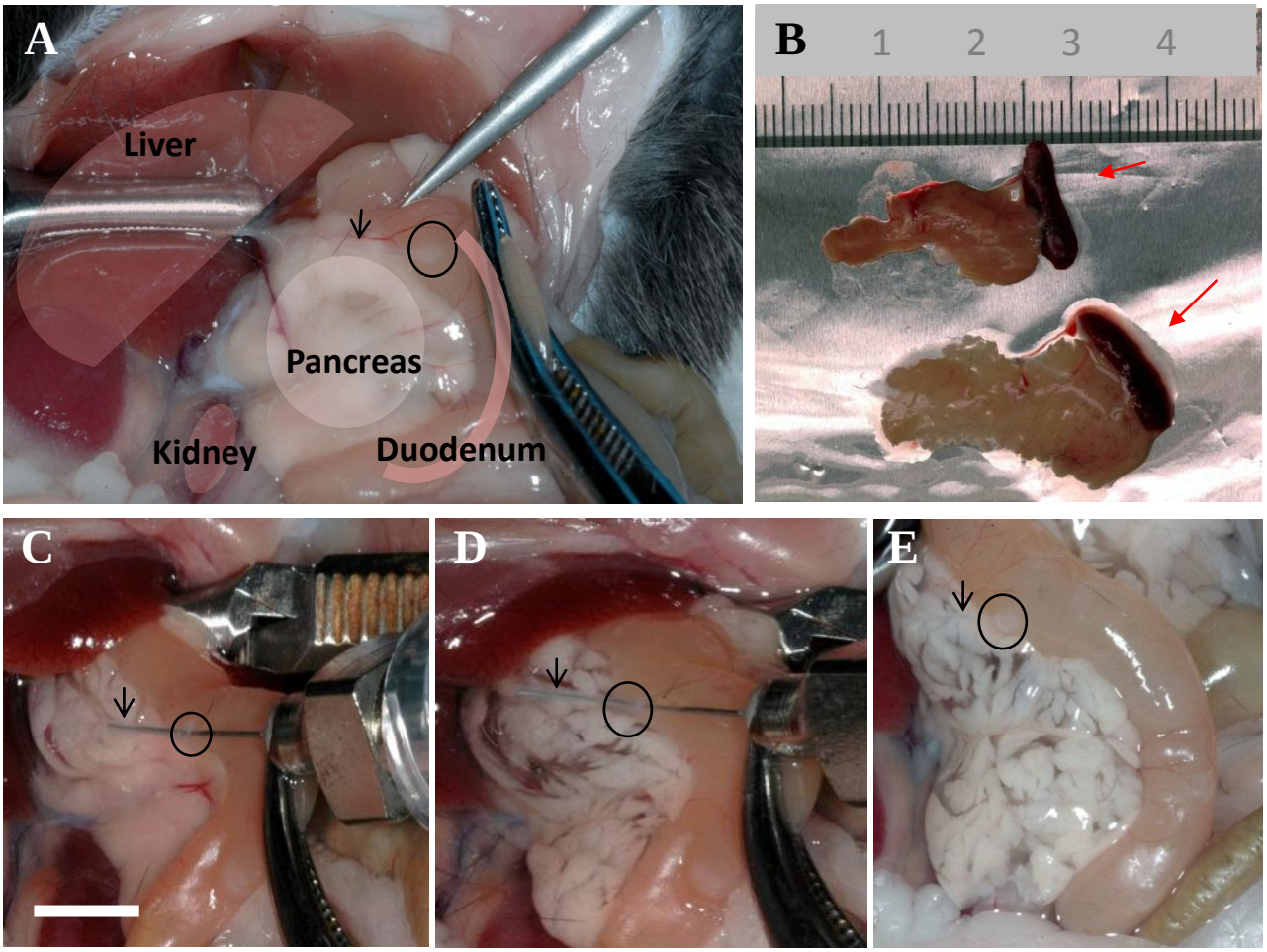

Figure 3.1: Successful pancreatic perfusion with collagenase buffer to yield isolated islets. (A) Anatomical view of abdominal tissue with respect to the pancreas. (B) Difference seen when successful perfusion occurs in the pancreas. Red arrow indicates spleen. (C-E) Images showing various stages of perfusion. Circle shows site of needle insertion: ampulla. Black arrow indicates the common bile duct. Representative line = 1 cm.

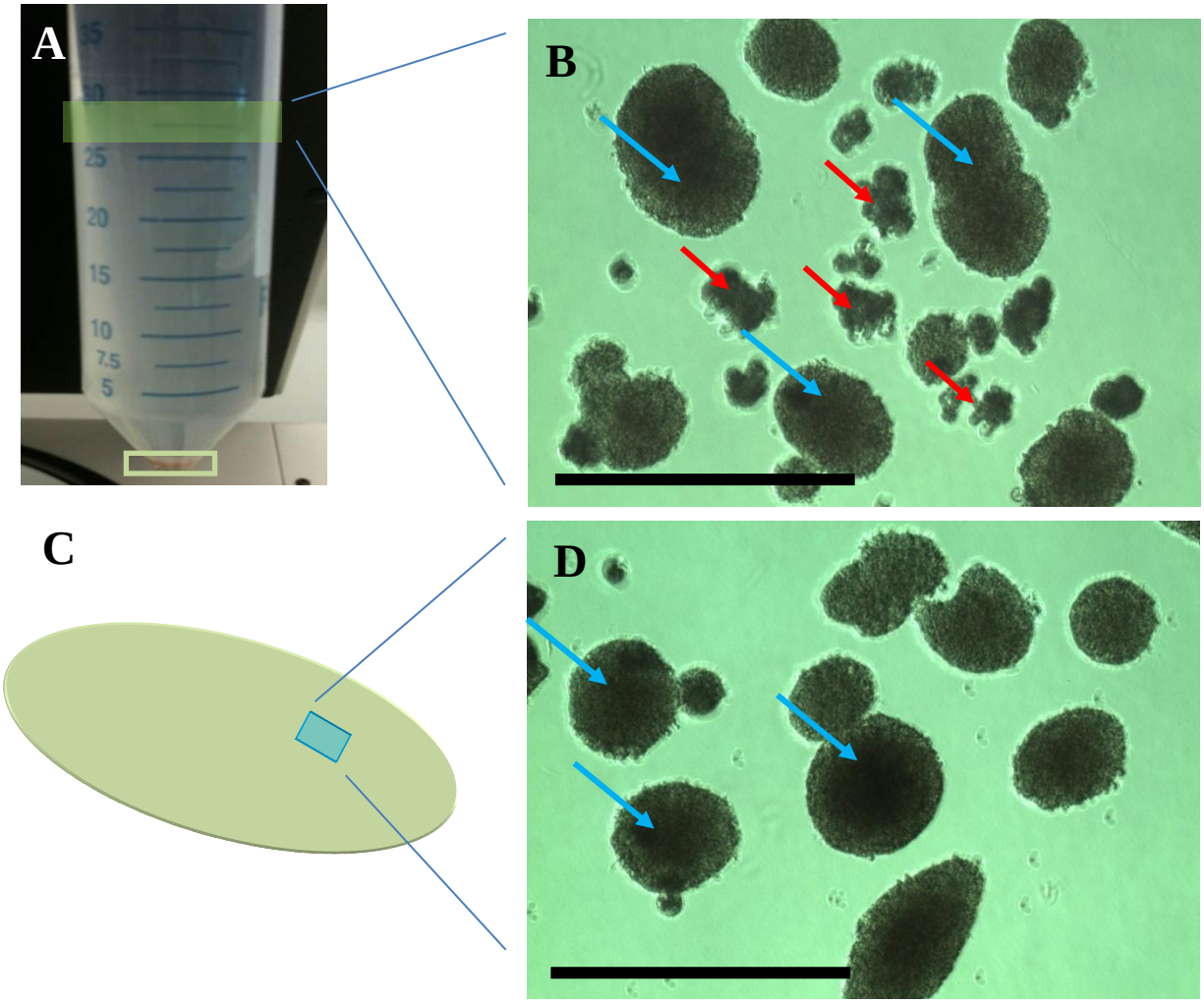

Figure 3.2: Islet isolation from collagenase perfused whole pancreata. (A) Isolated islets gather in the Ficoll gradient layer seen after centrifugation. (B) Cell fraction pipetted from layer after passing through 40µm cell strainer. (C-D) Handpicked isolated islets prior to RNA isolation. Red arrows indicate exocrine pancreas, lysed islets etc. Blue arrows indicate islets that are isolated and RNA extracted. Representative line = 200 µm.

3.5.2. Optimising the qRTPCR protocol to determine the *Yr* subtypes present in isolated pancreatic islets from C57BL/6 mice

Gene expression of *Pyy*, *Dpp-4* and *Yr* in the isolated islet was evaluated in C57BL/6 mice to direct our studies into determining the islet PYY isoforms and target receptors. As previously described, PYY 1-36 is an endogenous ligand for all YRs; however PYY 3-36 has specific Y2R affinity. Studies were performed with the assistance of Dr J. Way and Ms D. Danger.

3.5.2.1. RNA extraction:

To assess the protocol validity and enquire about the possible RNA yield from isolated islets, RNA was isolated from a pool of 2 mice. Extraction was successful using the RNeasy mini kit, and yield was both high (98 ng/µl) and almost completely intact (RIN-9.8 AU). Hence, it was considered that sufficient RNA could be extracted from individual mice. Thereafter, islets were individually isolated from another six mice and RNA extracted successfully (Table 3.1).

Date of RNA isolation	**Tissue**	**RNA conc. (ng/µl)**	**Absorbance (A260/A280)**	**RIN (AU)**
30/11/2011	Islets*	98.0	2.13	9.8
01/12/2011	(i) Islets	20.1	2.12	>8
	(ii) Islets	83.6	2.09	>8
	(iii) Islets	60.1	2.09	>8
	(iv) Islets	33.0	2.18	>8
	(v) Islets	20.5	2.13	>8
	(vi) Islets	23.7	2.17	>8

Table 3.1: RNA extraction of isolated islets from wild type mice using Qiagen RNeasy kit. Quantification and integrity of RNA was determined by Nanodrop photospectrometry and electropherogram. N = 8. *pool of 2 mice. *RIN: RNA integrity number.*

3.5.2.2. Reverse transcription:

cDNA was synthesised from the islet RNA. RT reactions performed were successful; however, since the RNA concentrations of the samples were sometimes low, we used 0.6 -1.0 mg of RNA template for RT to get a minimum of 10 ng/µl per sample of cDNA template required for the qRTPCR reactions.

3.5.2.3. qRTPCR

Expression levels for *Yr* subtypes were quantified by qRTPCR. Commercially available brain and intestine cDNA (Zyagen, USA) were used as positive control tissues for *Y1, Y2, Y4* and *Y5* receptors expression. All probes were confirmed to be expressed in control tissue, and this ensured the probes were active and qRTPCR protocol was successful (Chapter 2, Table 2.2).

Gapdh was strongly expressed in all tissues, with stable patterns of within-tissue expression, hence it was deemed suitable as a housekeeping gene. Ct values were recorded for the different probe sets after 40 PCR cycles. ΔCt was calculated which was used to normalise abundance of the gene of interest relative to the housekeeping gene (average abundance of target/average abundance of *Gapdh*). Values that remained undetected after the 40 cycles were deemed as unexpressed. Isolated islets were retrieved and RNA extracted by methods previously described. The qRTPCR probes were initially assessed using brain tissue cDNA.

3.5.2.4. Determining islet Yr subtype expression

Previous data have made suggestions of the YR subtype mediating intra-islet PYY's inhibition on insulin. But have thus far failed to confirm this.

Thereafter, we detected *Y1r* expression in cDNA from whole pancreas and isolated islets in the WT mice. On the other hand, *Y4r* mRNA was only found to be present in whole pancreas, but was absent in all islet samples after 40 PCR cycles. *Y2r* and *Y5r* expression were undetectable from both whole pancreas and isolated islets. *Y4r* expression (0.0071AU) was almost six-fold higher than *Y1r* expression (0.0012AU) in the whole pancreas of the WT mice (Figure 3.3A). In isolated islets, of all the YR-subtypes, *Y1r* gene expression was the only receptor that was detectable (Figure 3.3B).

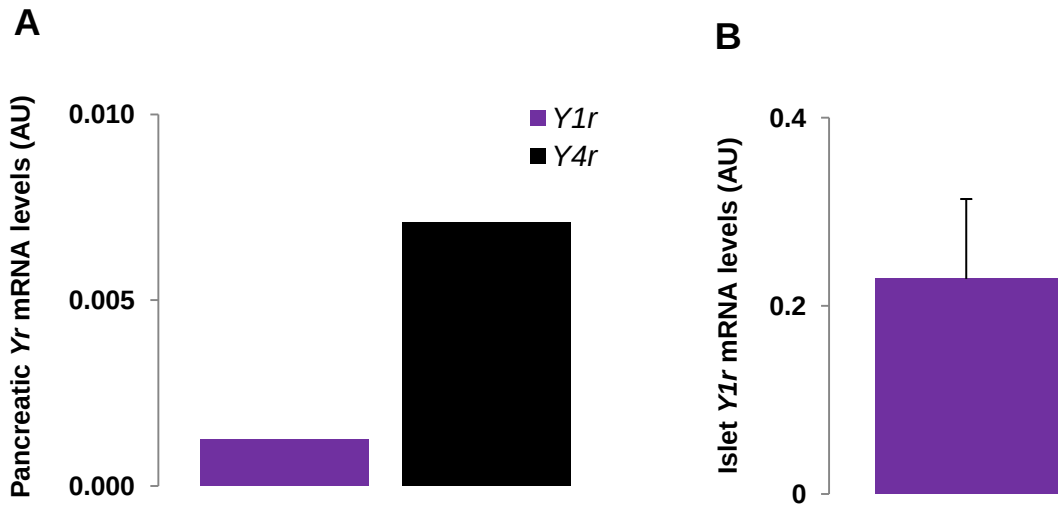

Figure 3.3: Differences in *Yr* expression of the whole pancreas and isolated islets. Expression of *Yr* in A) whole pancreas and B) the endocrine islets. *Y1r* expression (purple) in islets and pancreas, *Y4r* expression (black) in pancreas N = 8 for islet samples & n = 1 for pancreas from C57BL/6 mice. Data shown as mean of triplicates + SEM.

3.5.3. Evaluating the intra-islet localisation of PYY and DPP-4 in normal WT mouse pancreata using IHC

The pancreatic endocrine islets consist of five islet-cell subtypes. Insulin was used as a marker for β-cells, which are located in the core of the islets. Glucagon was used as an α-cell marker, and somatostatin as a δ-cell marker. Both of these cell subtypes are found on the mantle/periphery of the islets. Other cell types include the PP- cells, and the ε-cells. Of the five cell-subtypes, we assessed distribution of PYY, DPP-4 and Y1R expression in the α-, β- and δ-cells.

3.5.3.1. Confirmation of islet PYY expression using transgenic reporter mice

PYY protein expression was confirmed and validated in the *YfpPyy* mouse. YFP was predominantly expressed in the lower gut and islets consistent with the localisation of PYY (Figure 3.4).

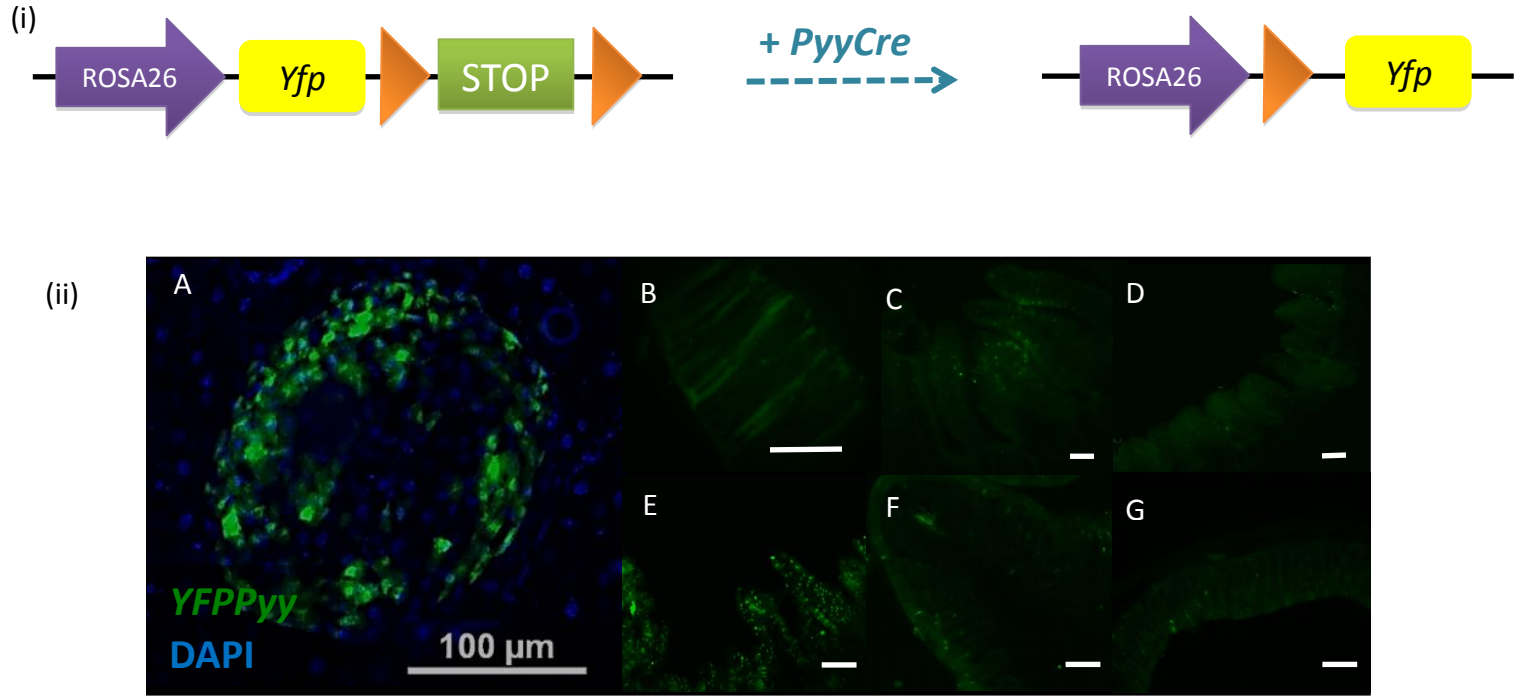

Figure 3.4: Validation of PYY protein expression using a transgenic reporter line. (i) The ROSA26 promoter drives the expression of the *yellow fluorescent reporter* gene (*Yfp*) located upstream of the floxed (orange triangles) stop cassette (green). Expression of the *PyyCre* within the same cell population produces a recombination that removes the stop cassette and thus, activates the expression of the ROSA26-driven *Yfp* gene. This allows for the identification of cells that express *Pyy* and in which *Cre* has functioned. (ii) Representative pancreas and gut sections showing *YfpPyy* in green (bars: 100 µm) within (A) Islets (B) stomach, (C) proximal duodenum, (D) jejenum, (E) distal ileum, (F) ascending colon and (G) descending colon. DAPI blue nuclear staining (Gelegen et al., 2012).

3.5.3.2. IHC antibody optimisation & controls

Using immunostaining, normal islet-cell subtype distribution was confirmed. Primary and secondary antibody dilution factors were determined for all antibodies (Chapter 2, Table 2.3). Staining distribution was assessed to evaluate correct staining of the antibodies. Insulin was found to stain the core of the islet, whereas the glucagon and somatostatin staining localised on the mantle of the islet. Thus, localisation of islet cell subtypes appeared to stain as expected (Figures 3.5). IHC imaging was conducted with the assistance of Dr E. Kleymenova.

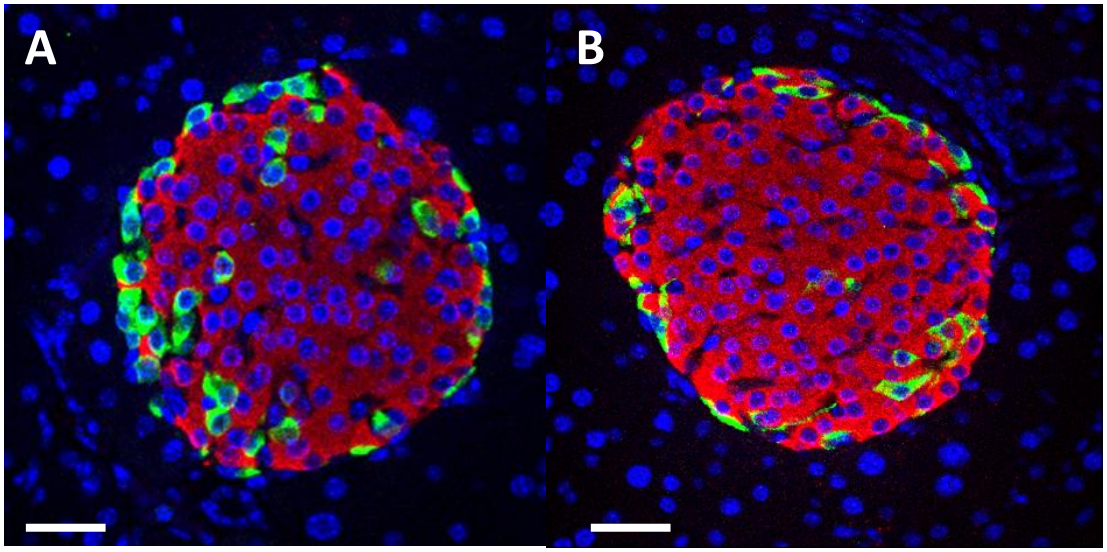

Figure 3.5: Confirmation of normal islet cell staining in WT mice. Representative image showing islet immunostaining in WT mice (A) using glucagon as an α-cell marker (green) and insulin as a marker for β-cells (red). (B) β-cell marker insulin (red) was co-stained with somatostatin as marker for islet δ-cells (green). Nuclei are labelled with DAPI (blue). Magnification x 20. N = 8 mice per group, 6 sections per mouse. Reference line: 20 µm.

3.5.3.3. Assessing PYY antibody cross-reactivity with homologous sequences

It has previously been reported that PYY antibodies are non-specific and cross-react with NPY (Glavas et al., 2008). To validate the PYY antibody, we used our transgenic *Pyy* KO mice that have the global *Pyy* gene deleted with complete absence of the PYY protein (Batterham et al., 2006). The *Pyy* KO showed no staining for islet PYY; hence we conclude that the antibody did not cross-react with NPY (Whim, 2011) or any other homologous sequence within the pancreas (Figure 3.6).

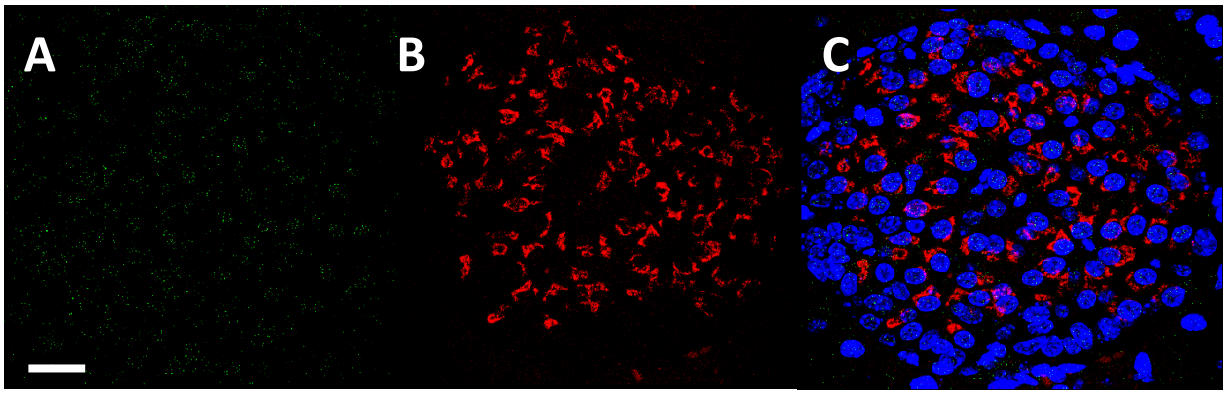

Figure 3.6: Absence of PYY staining in *Pyy* KO mice. Representative image showing islet immunostaining for (A) PYY (green) and (B) Proinsulin (red) in the *Pyy* KO mice. Nuclei are labelled with DAPI (blue). Magnification x 40. N = 8 mice per group, 6 sections per mouse. Reference line: 20 µm.

3.5.3.4. The DPP-4 antibody

DPP-4 can be found in circulation and is expressed on the endothelial lining of blood vessels. DPP-4 expression was primarily confirmed to the cell surface of islets with some cytoplasmic staining also (Figure 3.7).

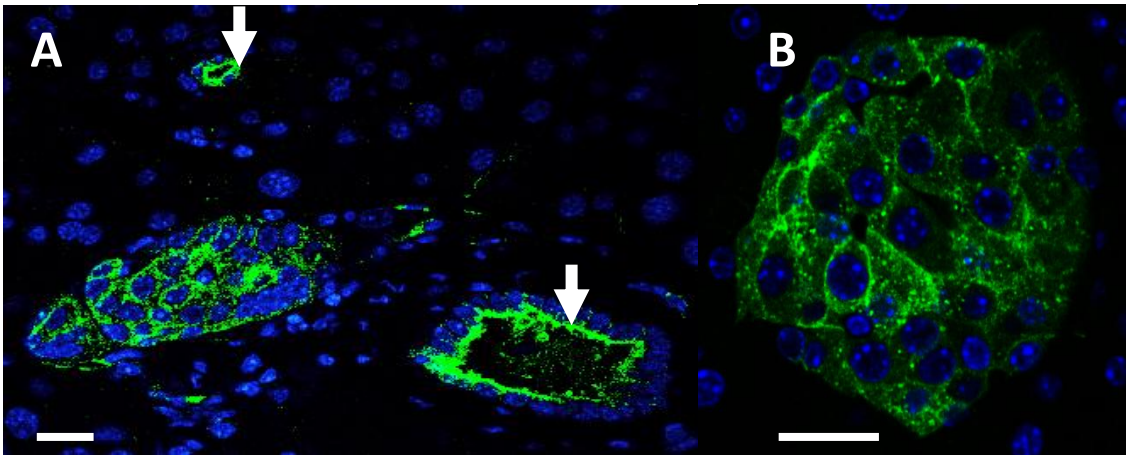

Figure 3.7: Validation of DPP-4 antibody in WT mice. Representative image showing immunostaining for (A) DPP-4 (green), blood vessels-immunoreactivity indicated by arrows (x 40). (B) Islet DPP-4 immunostaining in green at higher magnification (x 63). Nuclei are labelled with DAPI (blue). N = 8 mice per group, 6 sections per mouse. Reference line: 10 µm. *(For more detailed images, see supplementary data supplied; appendix II A1-A2).*

3.5.3.5. Assessing the distribution and localisation of PYY and DPP-4 within different islet cell subtypes in WT mouse pancreata.

3.5.3.5.1. PYY localisation in β-, α- and δ-cells.

To determine if PYY was localised to the β-cells, 5 µm pancreata sections from WT mice were immunostained for insulin in red and PYY in green. As expected, we found that PYY was not co-localised with insulin (Figure 3.8A-C). PYY was found to be present in glucagon positive cells (Figure 3.9A-D). However, PYY was found predominantly, but not exclusively co-localised with somatostatin positive cells, i.e. the δ-cells (Figure 3.9E-H).

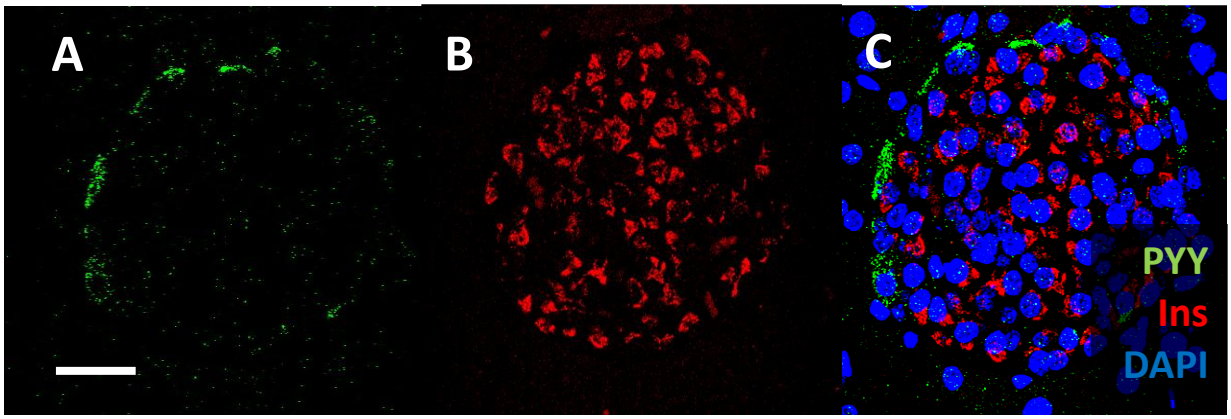

Figure 3.8: PYY is not localised in the β-cells. Representative image showing islet immunostaining in WT mice for (A) PYY (green) and (B) insulin (red). (C) Merging of the immunostaining. Nuclei are labelled with DAPI (blue). Magnification x 40. N = 8 mice per group, 6 sections per mouse. Reference line: 10 µm.

Figure 3.9: Islet PYY is present in the α- and δ-cells in WT mice. Islet immunostaining in WT mice for (A) glucagon α-cells (green), (B) PYY positive cells (red), (C-D) Merging of the immunostaining. (E) PYY cells (green) and (F) somatostatin δ-cells (red). (G-H) Merging of the immunostaining. Nuclei stained in DAPI (blue). Magnification x 40, and inset magnification x 63. N = 8 mice per group, 6 sections per mouse. Reference line: 10 µm.

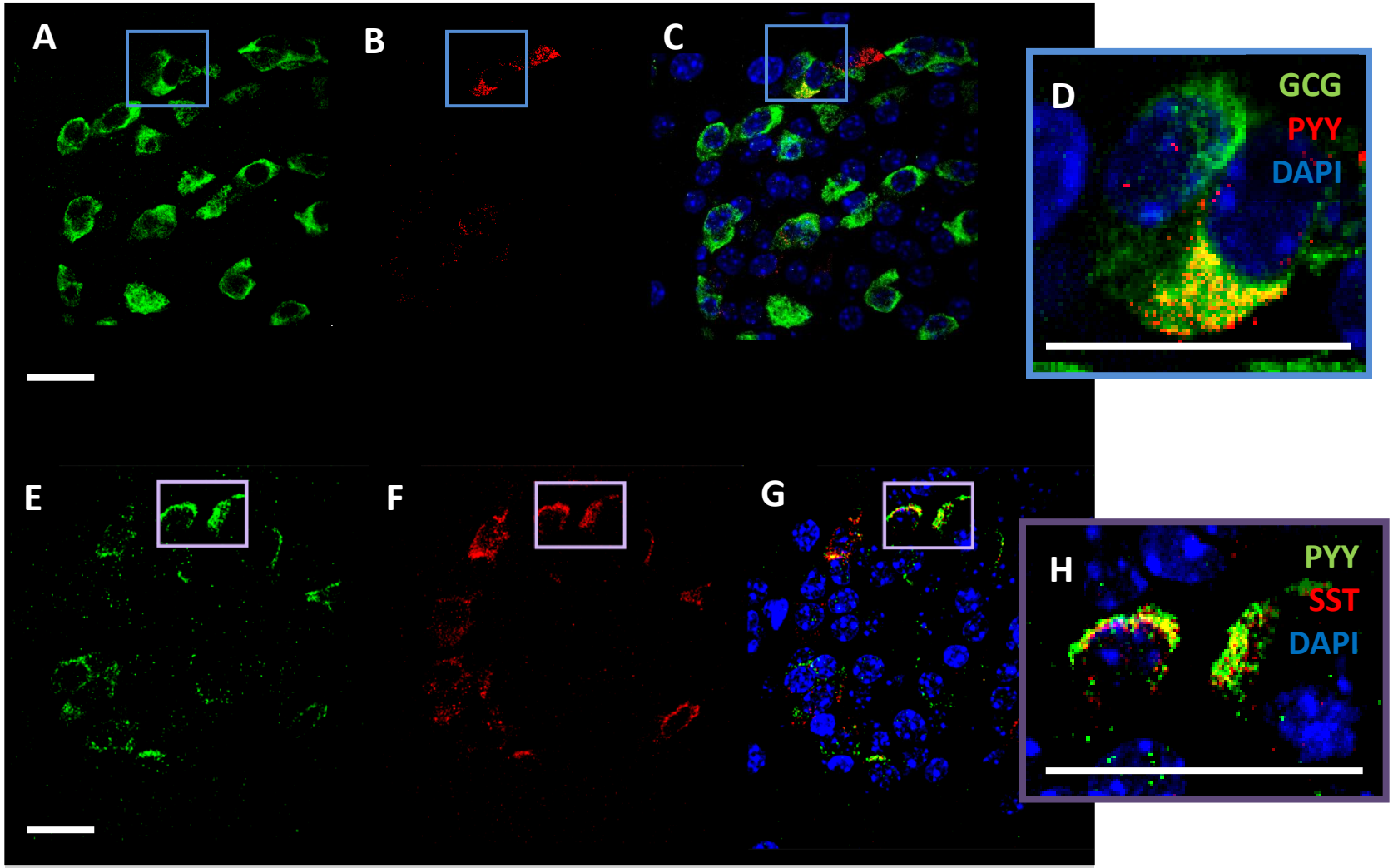

3.5.3.5.2. DPP-4 localisation in β-, α-, δ- and PYY positive cells

DPP-4 expression was localised to islet cell surfaces. DPP-4 appeared to be distributed on insulin positive β-cells (Figure 3.10A), and on a small population of glucagon positive cells (Figure 3.10B). However, the enzyme could not be found on somatostatin positive cells (Figure 3.10C). DPP-4 was also located on one population of PYY positive cells, but was absent on another PYY positive cell population in the WT mice (Figure 3.10D).

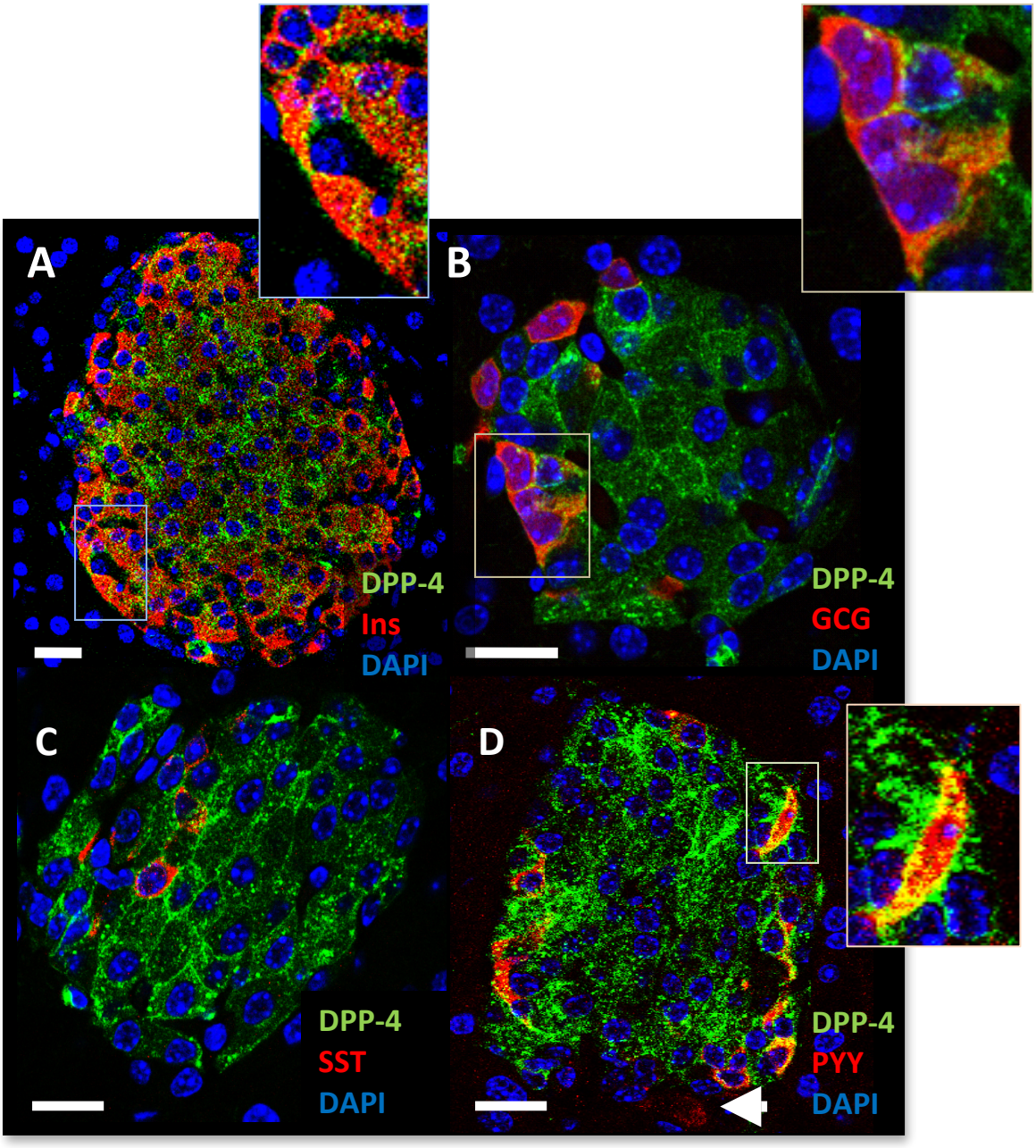

Figure 3.10: DPP-4 is localised on α-, β- and PYY positive cells but not with somatostatin in WT mice Islet immunostaining for DPP-4 (green) co-stained with (A) insulin (red), (B) glucagon (red), (C) somatostatin (red) and (D) PYY (red) in WT mice. Nuclei are labelled with DAPI (blue). Arrow indicates PYY positive cells absent of DPP-4 staining. Magnification x 20 and x 40. N = 8 mice per group, 6 sections per mouse. Reference line: 10 µm. *(For more detailed images, see supplementary data; appendix II A3-A8).*

3.5.3.6. Confirming the expression of the Y1R on β- and DPP-4 positive cells in WT mouse pancreata.

To determine if the Y1R was localised to the β-cells, 5 µm pancreata sections from WT mice were immunostained for insulin in red and Y1R in green. As expected, we found that Y1R was localised to the cell surface of insulin-positive β-cells (Figure 3.11A). In addition, Y1R was co-localised to DPP-4 positive cells (Figure 3.11B).

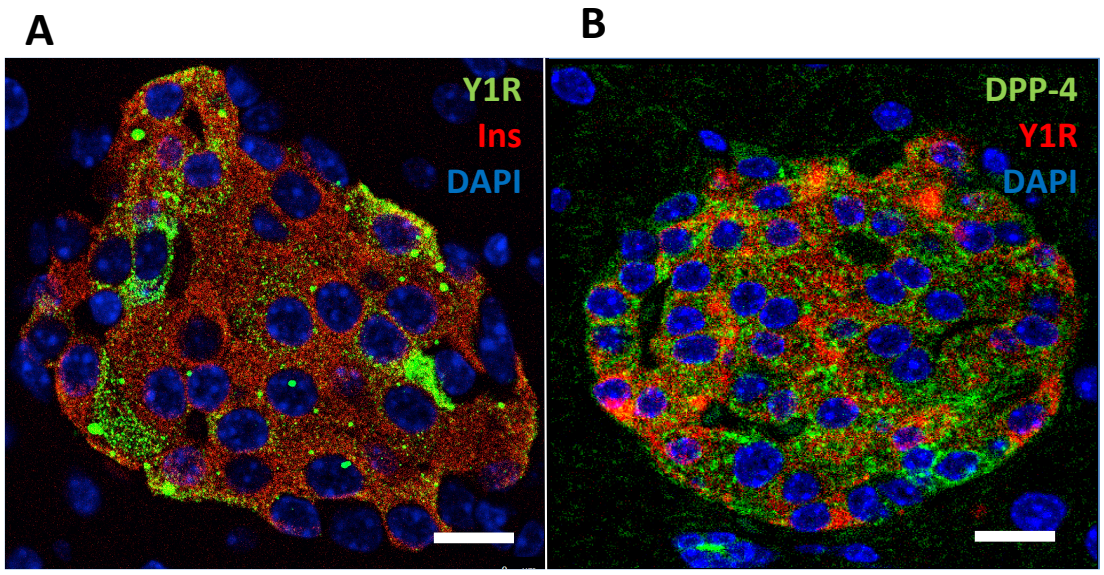

Figure 3.11: Y1R is localised on β-cells and DPP-4 positive cells in WT mice. Islet immunostaining in WT mice for (A) Y1R (green) co-stained with insulin (red) and (B) Y1R (green) co-stained with DPP-4 (green). Nuclei are labelled with DAPI (blue). Magnification x 40. N = 3 mice per group, 4 sections per mouse. Reference line: 10 µm. *(For more detailed images, see supplementary data; appendix II A9-A10).*

3.5.4. Evaluating the effect of pancreatic-specific & global *Pyy* deletion on islet morphology and expression

To assess changes in islet morphology of the pancreatic-specific and global *Pyy* KO mice, we stained pancreatic sections with the widely popular haematoxylin and eosin stain (H&E). H&E staining is routinely used to in pathological assessments for detection in changes of morphological tissue structure. The protocol involved applying an aluminium ion and haematoxylin complex, haemalum. This produced a blue nuclear staining. Eosin was then used to counterstain other cellular structures in various shades of red.

3.5.4.1. Morphological islet changes in the PdxPyy and Pyy mice

The *Pyy* KO and the *PdxPyy* KO mouse displayed an increased number of islet nuclei when compared to their respective controls (Figure 3.12).

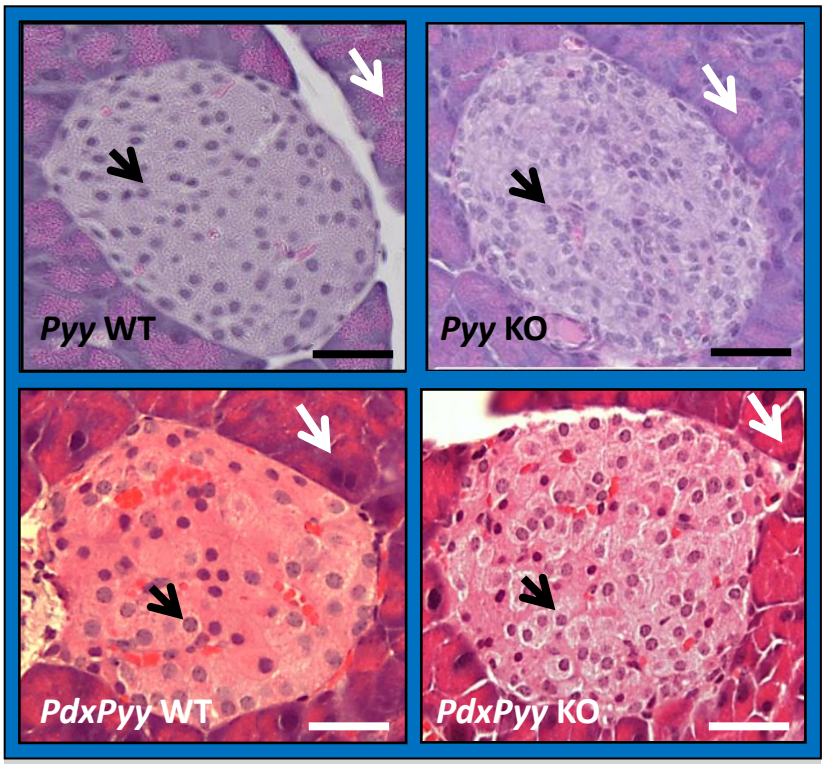

Figure 3.12: Changes in morphological structure the *Pyy* transgenic mice. Representative haematoxylin eosin (H&E) stained sections of islets in the *PdxPyy* KO and *Pyy* KO with their littermate control mice aged 12-14 weeks. Black arrows represent islet cell nuclear staining. White arrows represent acinar cells. Magnification x 20. N = 3-8 mice per group, 4 sections per mouse. Reference line: 25 µm.

3.5.4.2. Assessment to detect changes in pancreatic cell area expression of the Pyy KO mouse using IHC and qRTPCR

To determine the islet phenotype of the *Pyy* KO mice; we assessed the expression of islet genes and proteins in male 16-18 week old mice.

3.5.4.2.1. Pyy KO: Pancreatic insulin mRNA and β-cell area

No differences in pancreatic islet *Ins* expression (WT: 12.88 ± 0.34 vs. KO: 13.50 ± 0.36 AU) or β-cell area (WT: 0.0041 ± 0.00006 % vs. KO: 0.0041 ± 0.00004 % total area) was found between the *Pyy* WT and KO mouse (Figure 3.13).

3.5.4.2.2. Pyy KO: Pancreatic glucagon mRNA and α-cell area

There were no differences in pancreatic islet *Gcg* expression in the *Pyy* mice (WT: 12.89 ± 0.65 vs. KO: 11.67 ± 0.71 AU). However, there was a reduction in α-cell area of *Pyy* KO mice (WT: 0.0013 ± 0.00002 % vs. KO: 0.0012 ± 0.00001 % total area*)* (Figure 3.14).

3.5.4.2.3. Pyy KO: Pancreatic somatostatin mRNA and δ-cell area

When evaluating the *Sst* gene expression there was no change between the groups (WT: 17.94 ± 0.59 vs. KO: 18.05 ± 0.38 AU). Whereas, there was a difference in δ-cell area of the *Pyy* mice (WT: 0.00014 ± 0.000005 % vs. KO: 0.00030 ± 0.00006 % total area) (Figure 3.15).

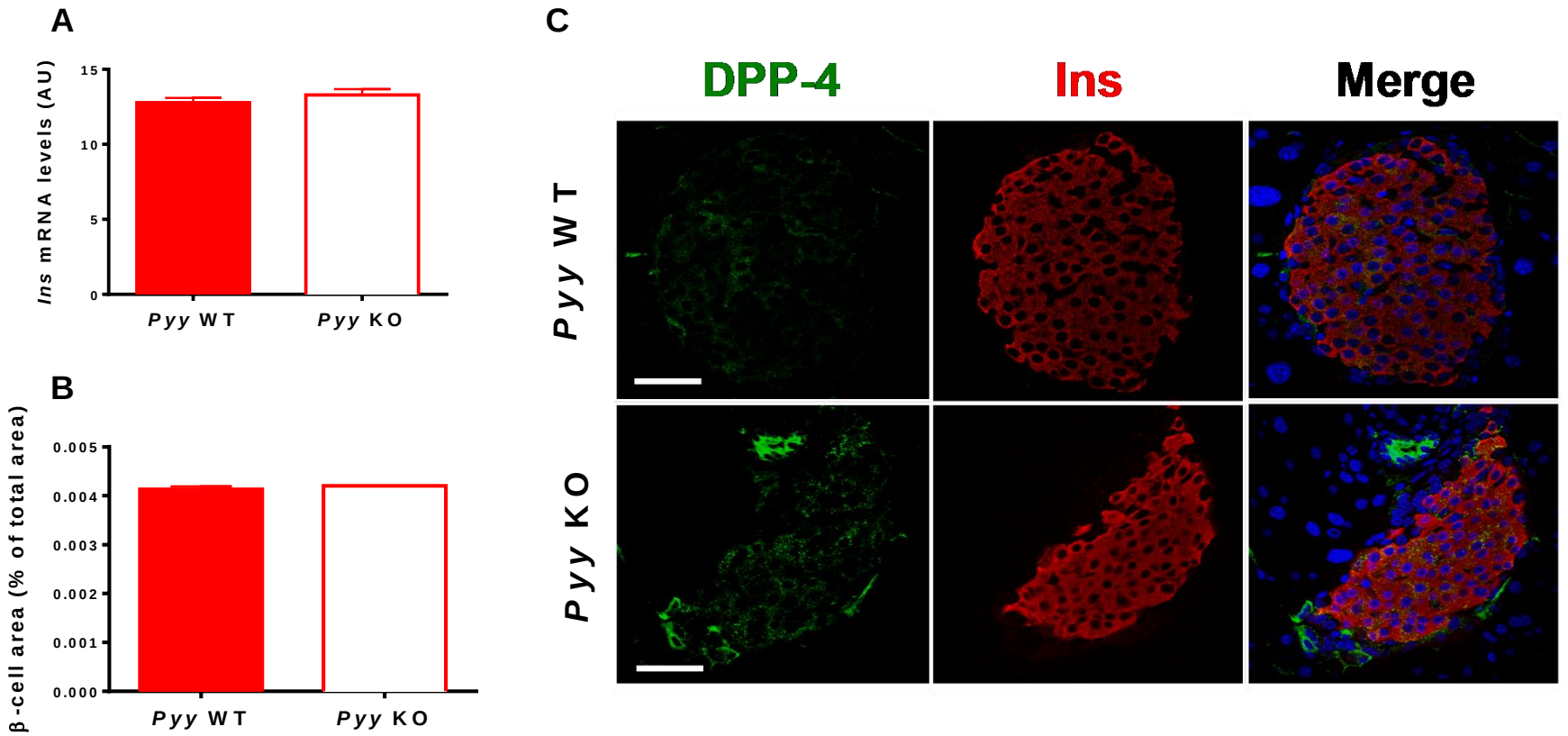

Figure 3.13: Global *Pyy* deletion has no effect on *Ins* gene expression or β-cell area. (A) Expression of *Ins* mRNA in whole pancreatic tissue samples of the *Pyy* WT and KO mice. B) Pancreatic β-cell area expression in the *Pyy* mice. C) Representative immunostained images of pancreatic islets of the *Pyy* WT and KO mice (DPP-4 green, insulin: red & nucleus: DAPI blue). Magnification x 40. Reference line: 20 µm. Gene expression: data shown as mean of duplicates + SEM, n= 9-11 mice per group. Pancreatic islet cell area: data shown as mean + SEM, n = 2 mice per group, 2 sections per mouse.

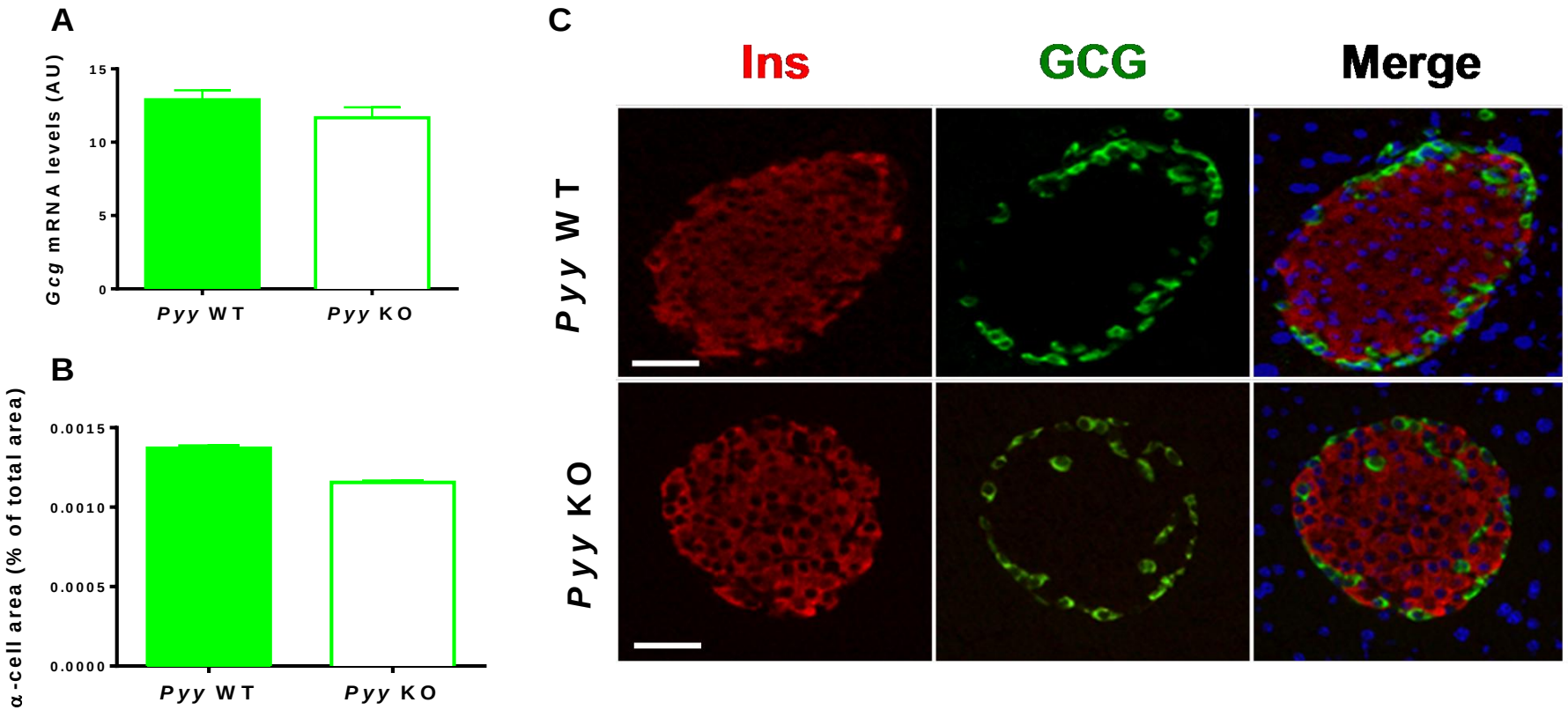

Figure 3.14: Global *Pyy* deletion leads to a reduction in α-cell area. (A) Expression of *Gcg* mRNA in whole pancreatic tissue samples of the *Pyy* WT and KO mice. B) Pancreatic α-cell area expression in the *Pyy* mice. C) Representative immunostained images of pancreatic islets of the *Pyy* WT and KO mice (GCG green, insulin: red & nucleus: DAPI blue). Magnification x 40. Reference line: 20 µm. Gene expression: data shown as mean of duplicates + SEM, n= 9-11 mice per group. Pancreatic islet cell area: data shown as mean + SEM, n = 2 mice per group, 2 sections per mouse.

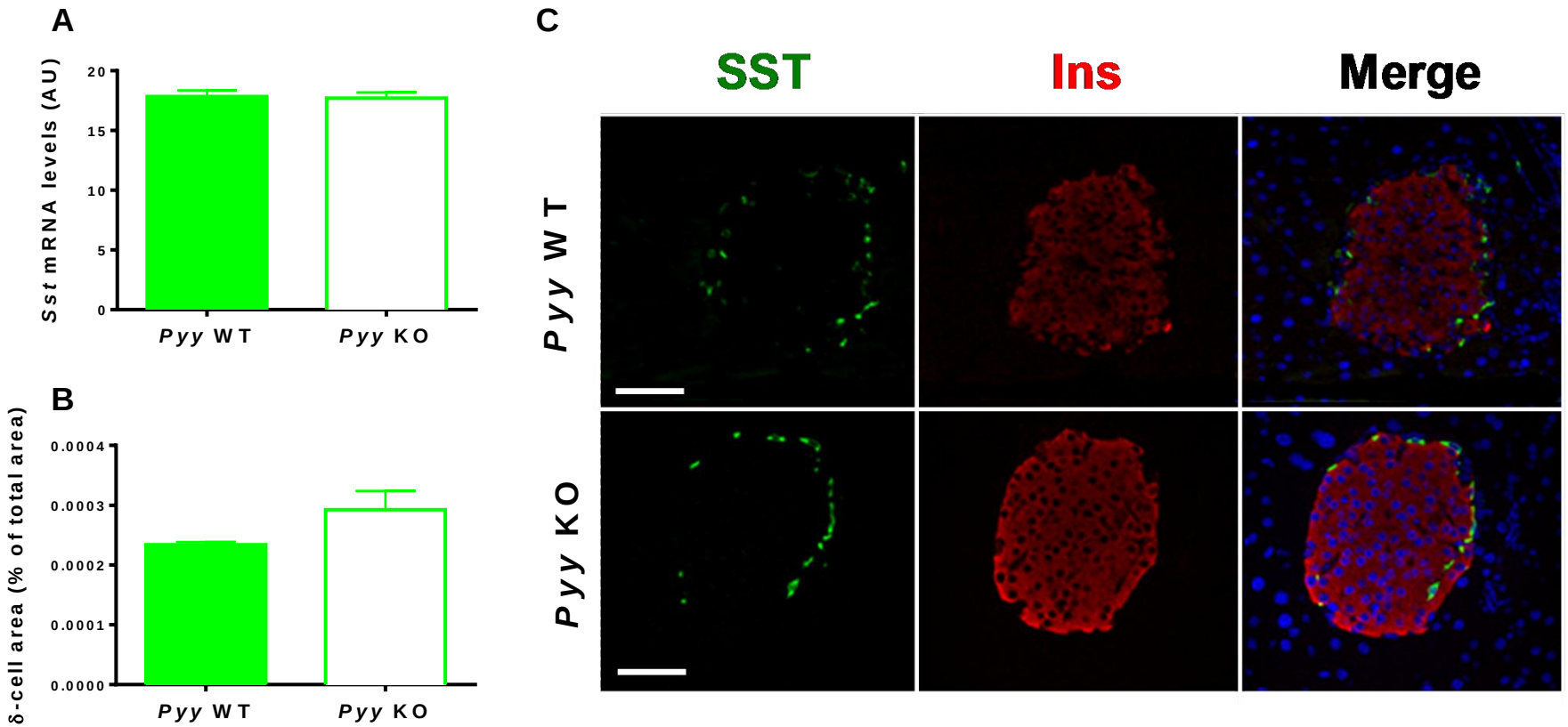

Figure 3.15: Global *Pyy* deletion leads to an increase in δ-cell area. (A) Expression of *Sst* mRNA in whole pancreatic tissue samples of the *Pyy* WT and KO mice. B) Pancreatic δ-cell area expression in the *Pyy* mice. C) Representative immunostained images of pancreatic islets of the *Pyy* WT and KO mice (SST green, insulin: red & nucleus: DAPI blue). Magnification x 40. Reference line: 20 µm. Gene expression: data shown as mean of duplicates + SEM, n= 9-11 mice per group. Pancreatic islet cell area: data shown as mean + SEM, n = 2 mice per group, 2 sections per mouse.

3.5.4.3. Morphometric assessment of islet-cell area in the PdxPyy KO mouse using IHC

To determine and compare the islet phenotype of the *PdxPyy* KO mouse to the *PdxPyy* WT mice, we assessed the islet cell morphometry, since no differences in islet gene expression was found amongst the *Pyy* mice. *PdxPyy* male mice aged 12-16 weeks were investigated.

3.5.4.3.1. PdxPyy KO: Changes in pancreatic β-cell area

No differences in pancreatic islet β-cell area were found between the *PdxPyy* WT and KO mice (WT: 0.0067 ± 0.00009 vs. KO: 0.0065 ± 0.00001 % total area) (Figure 3.16).

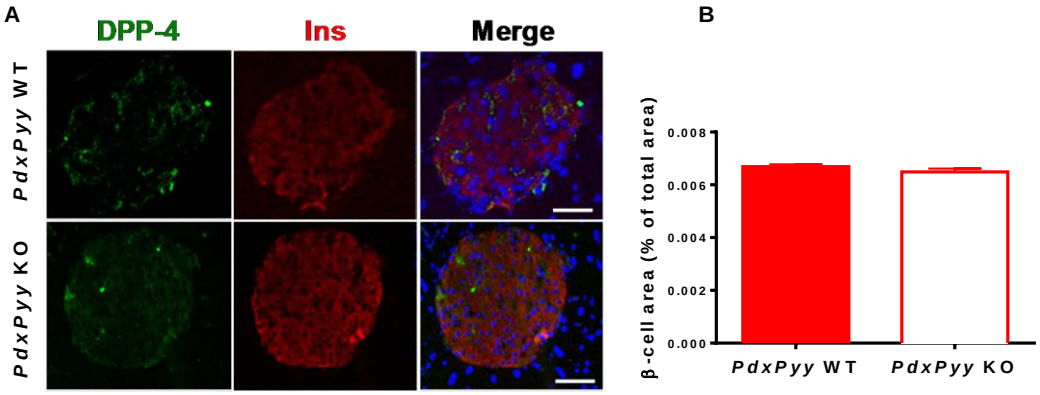

Figure 3.16: *PdxPyy* deletion has no effect on β-cell area. (A) Representative immunostained images of pancreatic islets of the *PdxPyy* WT and KO mice (DPP-4 green, insulin: red & nucleus: DAPI blue). Magnification x 40. Reference line: 20 µm. B) Pancreatic β-cell area expression in the *PdxPyy* WT and KO mice. Data shown as mean + SEM, n = 2 mice per group, 2 sections per mouse.

3.5.4.3.2. PdxPyy KO: Changes in pancreatic α-cell area

Like the *Pyy* KO mice, the *PdxPyy* null mice also showed a reduction in α-cell area when compared to the control mice (WT: 0.0016 ± 0.00007 vs. KO: 0.0014 ± 0.00006 % total area) (Figure 3.17).

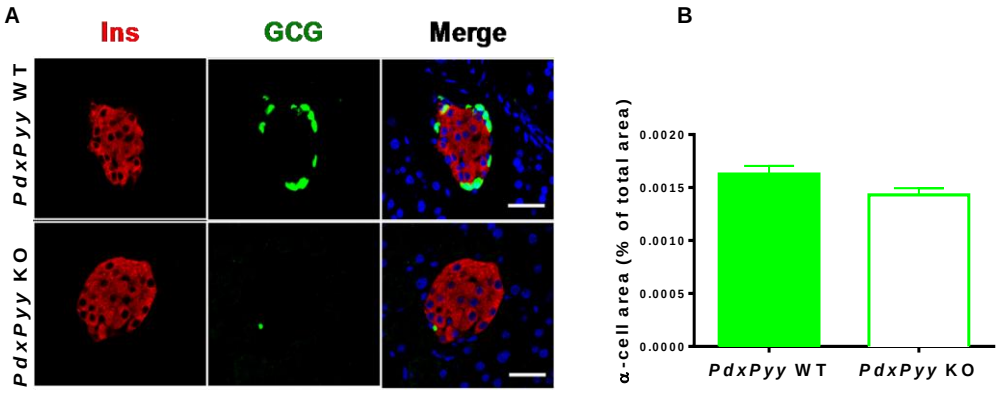

Figure 3.17: *PdxPyy* deletion results in a reduction in α-cell area. (A) Representative immunostained images of pancreatic islets of the *PdxPyy* WT and KO mice (GCG green, insulin: red & nucleus: DAPI blue). Magnification x 40. Reference line: 20 µm. B) Pancreatic α-cell area expression in the *PdxPyy* mice. Data shown as mean + SEM, n = 2 mice per group, 2 sections per mouse.

3.5.4.3.3. PdxPyy KO: Changes in pancreatic δ-cell area

Surprisingly, we found an increase in δ-cell area of the *PdxPyy* KO mice compared to the WT controls (WT: 0.00019 ± 0.000002 vs. KO: 0.00022 ± 0.000001 % total area) (Figure 3.18).

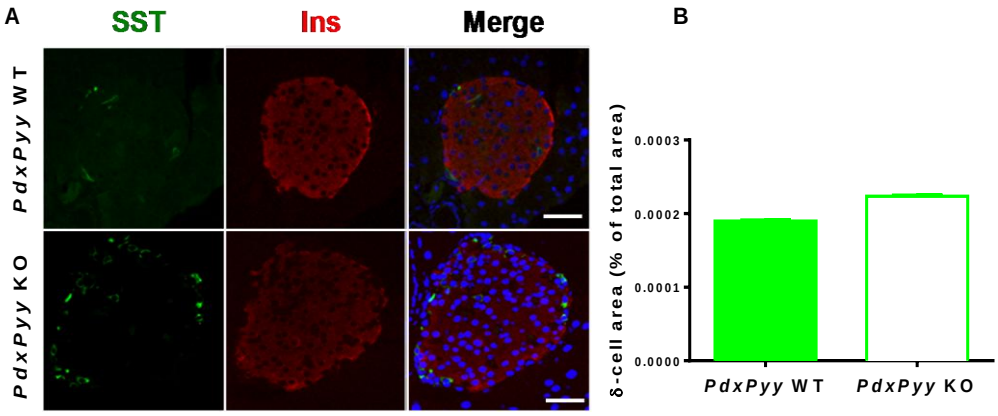

Figure 3.18: *PdxPyy* deletion results in an increase in δ-cell area. (A) Representative immunostained images of pancreatic islets of the *PdxPyy* WT and KO mice (SST green, insulin: red & nucleus: DAPI blue). Magnification x 40. Reference line: 20 µm. B) Pancreatic δ-cell area expression in the *PdxPyy* WT and KO mice. Data shown as mean + SEM, n = 2 mice per group, 2 sections per mouse.

3.6. Summary

Previous research and literature has highlighted a role for intra-islet PYY in glucose homeostasis, *in vivo* and *in vitro*. However, to date no studies have researched the intra-islet PYY system in-depth. Therefore, we pursued to characterise islet PYY and demonstrate the importance it has in mediating insulin control.

3.6.1. Islet isolation for gene expression analysis

Beginning with the optimisation of a murine islet isolation protocol, we subsequently evaluated the expression of islet *Yr*s. *Y2r* and *Y5r* were unexpressed in the pancreas. *Y1r* and *Y4r* were identified as the only two PYY receptors present in the pancreas, with *Y4r* expression almost six-fold higher than *Y1r* expression. RNA extracted from isolated islets was then checked for *Y1*- and *Y4r* expression. Islets only expressed *Y1r* mRNA in all 8 tissues samples (Ct <36).

3.6.2. Pancreatic localisation of PYY, DPP-4 and Y1R in the WT mouse

Confirmation of PYY protein expression was verified in the pancreatic islets using the *YfpPyy* reporter mouse. Antibodies were sourced from literature searches and corroborated to the correct immunostaining patterns of the islets. Using *Pyy* KO mice, we confirmed the specific staining of the PYY antibody. Next we assessed the distribution of PYY to specific cell-subtypes in the WT mouse. The δ-cell predominantly expressed PYY. The next most abundant PYY positive cells co-localised with DPP-4. The α-cells stained the least for PYY. Unlike PYY, DPP-4 mainly co-localised with the β-cells. Some DPP-4 expression was localised to the α-cells but immunostaining for the enzyme was completely absent from the δ-cells.

To understand whether PYY mediated its effects on insulin directly, we assessed the localisation of Y1R on β-cells or with DPP-4 positive cells. We found that Y1R was localised with both these proteins. However, since the Y1R antibody was inefficiently

weak during immunostaining, we were unable to assess if it co-localised with the other antibodies.

3.6.3. Determining changes in pancreatic expression in the *Pyy* transgenic mouse lines

Using H&E staining, we were able to detect islet morphological differences in both the *Pyy* transgenic mouse lines. Both *Pyy* KO and *PdxPyy* KO mice showed an increase in islet cell nuclei when compared to their respective controls. Moreover, changes in pancreatic *Ins, Gcg and Sst* gene expression as well as β-, α- and δ-cell area were measured in the both groups of the *Pyy* transgenic mice. Global *Pyy* KO mice showed no difference in pancreatic islet hormone mRNA levels compared to the *Pyy* WT mice. Additionally, β-cell area also remained unchanged by the deletion of *Pyy* in the *Pyy* mice. However, *Pyy* deletion caused a decrease in α-cell and increase in δ-cell area. Subsequently, morphometric analysis of the *PdxPyy* mice was evaluated. Like the *Pyy* KO mice, the *PdxPyy* KO mice also showed no difference in β-cell area, as well as reduced α-cell area and an increase in δ-cell area.

3.6.4. Conclusion

In conclusion, the data presented in this chapter is consistent with the intra-islet PYY mediating an inhibitory effect on insulin via the Y1R, and DPP-4 appears to regulate this action by converting it into an inactive form in the islets (PYY 3-36). Deletion of islet PYY appears to contribute to fall in α-cell area with an increase in δ-cell area in both the *Pyy* transgenic mouse models, suggesting a role for PYY in the development of at least α- and δ-cells. Collectively, these findings highlight the importance of PYY in islet development and function, and concurs with previous published data (Boey et al., 2006a, Batterham et al., 2006, Chandarana, 2009, Chandarana et al., 2013). However, more pharmacological and genetics studies are needed to understand this further.

Chapter 4

Investigating the *in vivo* role of intra-islet PYY in energy and glucose homeostasis

4. Investigating the *in vivo* role of intra-islet PYY in energy and glucose homeostasis

4.1. Introduction

PYY has been the focus of research in the past decade for its role in body weight regulation. Post-prandially, gut PYY reduces appetite by activating the anorectic hypothalamic homeostatic neurons and inhibiting the feeding-stimulating sites. However, prior to these findings, studies demonstrated the presence of PYY in islets and a role for PYY in regulating insulin secretion (Bottcher et al., 1989, Bottcher et al., 1993, Upchurch et al., 1994, Myrsén-Axcrona et al., 1997, Nieuwenhuizen et al., 1994). Subsequently, many studies followed which all aimed at understanding the physiological role of pancreatic PYY.

The first of a series of studies aimed at unravelling an *in vivo* role for PYY in energy and glucose homeostasis constructed a transgenic *Pyy* null mouse (Boey et al., 2006b). This mouse was absent of the *Pyy* gene and thus, of either isoform of PYY. The reported KO mouse was obese, hyperphagic but surprisingly HI post- GTT. This was accompanied by another *Pyy* KO mouse which reported a similar findings (Batterham et al., 2006). The obese phenotype of this mouse was reversed by administration of exogenous PYY 3-36 (Batterham et al., 2006). The following year, Boey and colleagues generated an overexpressing PYY mutant mouse which appeared to be protected from DIO but the investigators failed to assess the glucose tolerance in these mice. Moreover, when the mice were crossed with leptin deficient *ob/ob* mice they appeared to have a significant reduction in body weight gain and adiposity but this did not ameliorate the obese phenotype (Boey et al., 2007). A few years later, a PYY transgenic model was developed that deleted PYY in the adult mouse. This mouse was created that allowed deletion of PYY cells by diphtheria toxin. The resultant adult PYY KO mouse presented with hyperglycaemia attributed to a loss of β-cells and a disruption in islet morphology. The disturbance in islet phenotype was reduced after a long-acting PYY 1-36 analogue was administered (Sam et al., 2012). However, the systemic diphtheria toxin

administration deletes PYY in the gut, brainstem and pancreas so this mouse does not give insights into the role of pancreatic PYY. In addition, this approach destroys the cells and thus hormones that are co-localised with PYY. Subsequently, another report using a similar technology as Sam et al.'s produced an adult-onset PYY overexpressing mouse using tamoxifen. These mice displayed a reduction in fasting-induced food intake, an increase in respiratory exchange ratio, an increase in lipogenic activity and a trend towards a reduction in OGSIS (Shi et al., 2012). Furthermore, *Pyy* null mice fail to exhibit the improvement in glucose tolerance, post-bariatric surgery as seen in the control mice (Chandarana et al., 2011).

Data from chapter 3 coupled with previously published findings clearly suggest that PYY has a vital role in energy and glucose homeostasis, which is mediated by an alteration in insulin release. In particular, the global *Pyy* KO mouse, which despite having an obese phenotype shows a potentiation of GSIS (Batterham et al., 2006, Boey et al., 2006b). However, all these studies fail to determine the physiological role of intra-islet PYY independently of gut PYY action and the significance of this cell population still remains unclear.

Several reports have suggested a role of PYY in body weight and glucose balance (Boey et al., 2006b, Batterham et al., 2006, Batterham et al., 2002). The *Pyy* KO mice to date have exhibited global deletion and thus *Pyy* deletion throughout the GI tract, pancreas and brain. However, it is not known how much of a role intra-islet PYY may play in mediating these effects. To investigate the *in vivo* role of intra-islet PYY we generated a transgenic mouse with a pancreatic- specific promoter driven excision of the *Pyy* gene in the islets (*PdxPyy* KO). Thus, this mouse will enable us to potentially distinguish the role of the endocrine pancreas from GI and brain PYY and clarify the *in vivo* role of intra-islet PYY in energy and glucose balance.

4.2. Hypothesis

'Intra-islet PYY deletion mediates an improvement in glucose tolerance caused by hyperinsulinaemia'

4.3. Aims:

- To investigate the effects of pancreatic-specific *Pyy* deletion (*PdxPyy* KO) on food intake, body weight and adiposity, *in vivo.*
- To undertake a detailed *in vivo* glucose phenotyping of the *PdxPyy* KO mice and their wild-type littermate control mice.
- To assess the effects of *Pdx*-mediated *Pyy* deletion on neuro- and enteroendocrine mRNA levels that may contribute to the observed phenotypes.

4.4. Study Design:

PdxCre mice were crossed with *Pyy floxed*$^{+/-}$ to produce the *PdxPyy* KO mice (Gannon et al., 2000, Herrera, 2000). Since *Cre* recombinase alone has been shown to alter glucose tolerance we used *PdxCre+ Pyy* WT (*PdxPyy* WT) mice as controls (Fex et al., 2007). Using genotyping PCR, the targeted *Pdx*-mediated *Pyy* gene deletion was confirmed. Confirmation of islet PYY protein deletion was carried out by IHC. A detailed *in vivo* phenotype of these mice was investigated in both sexes. Changes in acute and chronic feeding and body weight of the *PdxPyy* mice were assessed from weaning. Additionally, an IPGTT, OGTT in both sexes, and OGSIS were carried out on 16-18 week old *PdxPyy* male mice. Body length and gonadal fat mass were determined. Furthermore, brainstem, ileal and colonic expression of *Pyy* were measured. Finally, duodenal *Cck* & *Pyy*, stomach g*hrelin,* ileal and colonic *proglucagon* mRNA expression was quantified by qRTPCR.

4.5. Results

4.5.1. Constructing the *Pdx*-specific *Pyy* null mouse

4.5.1.1. Confirmation of Pdx-specific Pyy gene deletion in the PdxPyy KO mouse using genotyping PCR.

The *Pdx-1* promoter is highly expressed during pancreatic, stomach antrum and duodenal murine ontogeny. Mouse *PdxPyy* WT and KO were produced by the *Cre/loxP* system (Gannon et al., 2000, Herrera, 2000) (Figure 4.1). Central and peripheral tissues were taken from *PdxPyy* KO mice and their littermate controls to assess genotype (Figure 4.2). As described previously, DNA was extracted from the sample and deletion was confirmed to the pancreas and duodenum only. The interleukin-2 (*IL2)* gene was used an internal control for the confirmation of DNA extraction.

Figure 4.1: *PdxPyy* mouse targeting strategy. Construction of the *PdxPyy* mice after recombination and deletion of the flanked *LoxP Pyy* gene. *Cre*-mediated deletion of the *Pyy*-coding region was confirmed using primers D1 and D2. The 326 bp product represents the presence of the *WT* allele, with the 350 bp demonstrating the floxed *Pyy* gene both obtained using the D1 and D2 primers. The 750 bp product indicates the *Pdx cre* gene with the presence of the *IL2* allele (324 bp) acting as an internal positive control for the presence of genomic DNA. Representative genotyping of *LoxP* and *PdxCre* PCR used to detect alleles of interest. N = 5 mice per group. *Heterozygote (Het), homozygous (Homo), wild type (WT), flanked LoxP sites (flox).*

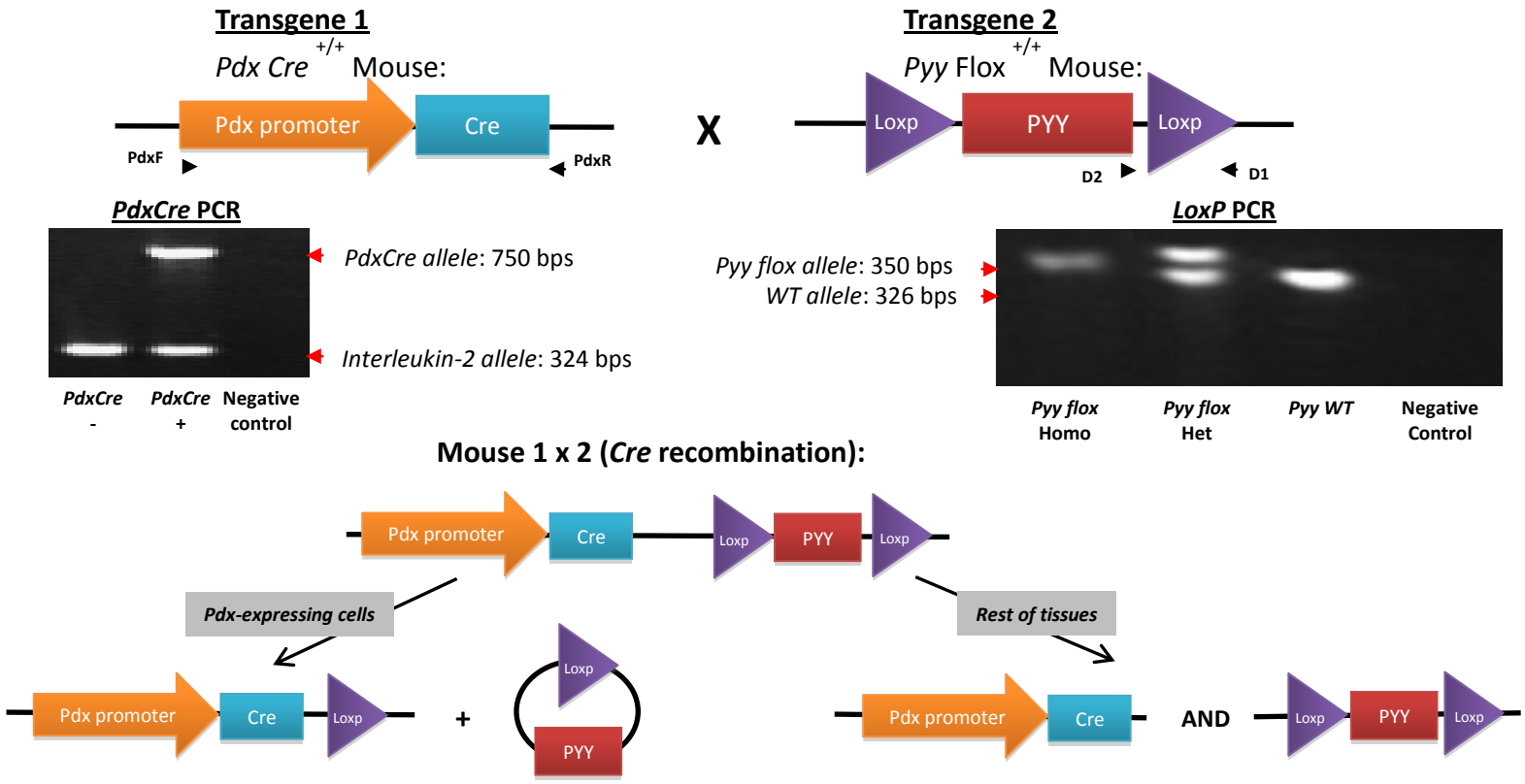

Figure 4.2: Evidence for the deletion of *Pyy* in the *PdxPyy* KO mouse. Representative genotyping PCR indicating the deletion of the *Pyy* gene in the duodenum and pancreas of the *PdxPyy* KO versus *PdxPyy* WT mice. C = cortex, Hy = Hypothalamus, BS = Brainstem, H = Heart, Lu = Lungs, L = Liver, K = Kidneys, M = Skeletal Muscle, F = Gonadal fat, Sp = Spleen, P = Pancreas, S = Stomach, D = Duodenum, J = Jejenum, I = Ileum, Co = Colon, + and - = controls. N = 10 mice per group.

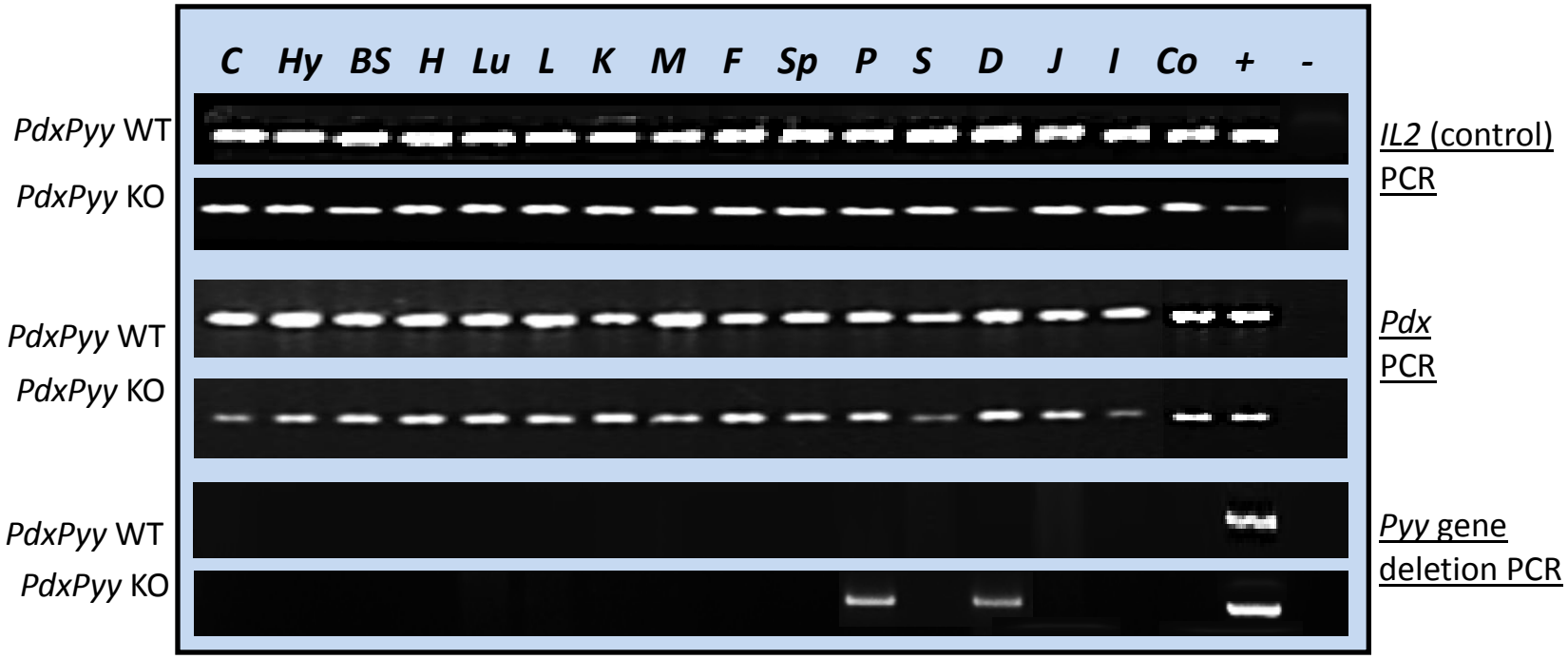

4.5.1.2. Evaluating the protein expression of PYY in pancreatic islets of the PdxPyy mice.

We evaluated whether we could detect PYY protein in the *PdxPyy* mice. Using insulin as a marker for islet localisation, we found PYY immunopositive cells in the *PdxPyy* WT mouse and confirmed PYY protein deletion in the *PdxPyy* KO mouse (Figures 4.3A-B).

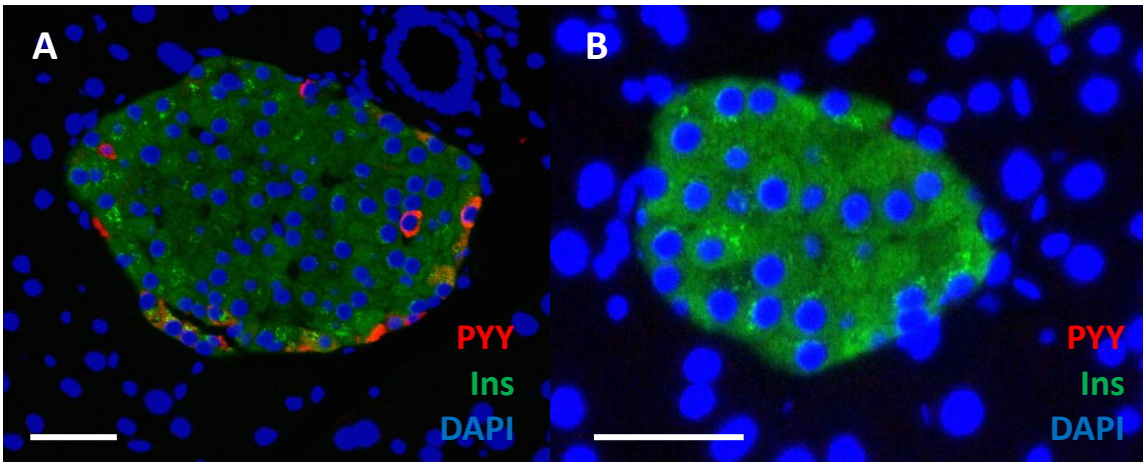

Figure 4.3: Assessment of *Pdx*-regulated PYY protein expression in the pancreas of the *PdxPyy* mice. Islet immunostaining for PYY (red), insulin (green) and nuclear staining in DAPI (blue) in A) *PdxPyy* WT and B) *PdxPyy* KO mice. N = 2 mice per group, 2 sections per pancreas, x 20 magnification, line represents: 20 µm.

4.5.2. *In vivo* evaluation of the physiological characteristics of intra-islet *Pyy* deletion on energy and glucose homeostasis

To assess the physiological role of islet PYY action in the appropriate regulation of appetite and body weight, we analysed cumulative food intake and weight gain in both male and female *PdxPyy* KO mice and their littermate controls.

4.5.2.1. Evaluating the effects of Pdx-mediated deletion of Pyy on food intake

Singly-housed mice were fed *ad libitum* chow and food weight per cage was recorded weekly and thus, food intake was calculated per week. Cumulative weekly food intake from weaning until the end of the study remained unchanged in both male and females (Figures 4.4A & C). However, when the *PdxPyy* KO mice were fasted for 16 hours and refed *ad libitum*, the male *PdxPyy* KO mice showed a significant decrease in cumulative acute food intake at 2h (1.0 ± 0.1 g, p= 0.02), 4h (1.2 ± 0.1 g, p= 0.01), 6h (1.6 ± 0.1 g, p= 0.02), and 8h hours (2.0 ± 0.2 g, p= 0.05) post-refeed when compared to WT controls (2h= 1.4 ± 0.1 g, 4h= 1.7 ± 0.1 g, 6h= 2.2 ± 0.1 g & 8h= 2.5 ± 0.2 g). However, eventually both groups were eating the same amount of food by 24 hours (WT= 5.8 ± 0.3 g & KO= 5.4 ± 0.4 g) (Figure 4.4B). The female mice showed no difference in acute feeding behaviour (Figure 4.4D).

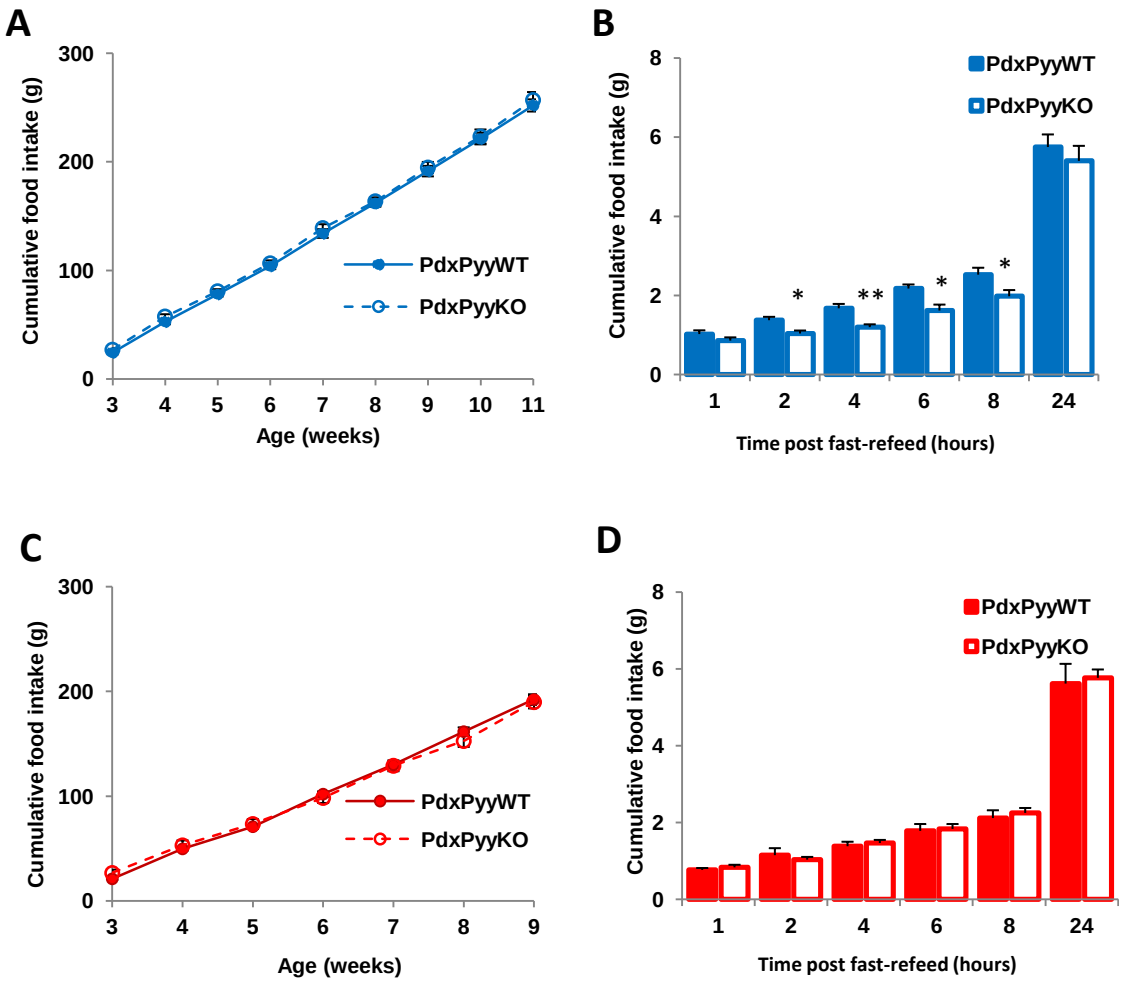

Figure 4.4: Assessment of food intake in the *PdxPyy* mice. Cumulative food intake in the: A) Male *PdxPyy* mice: blue. B) Female *PdxPyy* mice: red. N = 10 mice per group. Data represented as mean ± SEM. * $p < 0.05$, ** $p < 0.01$.

4.5.2.2. Evaluating the effects of Pdx-mediated deletion of Pyy on body weight

Deletion of *Pyy* in the *PdxPyy* mice of both sexes resulted in a significant reduction in weight gain during the study period when compared to the *PdxPyy* WT controls in both male and female mice. Male *PdxPyy* KO mice were significantly lighter from 8 weeks of age (p <0.05: Figure 4.5A), whereas, female *PdxPyy* KO mice were lighter from weaning (p <0.01: Figure 4.5C). This difference at weaning implies that pancreatic *Pyy* deletion affects growth, this will assessed further in section 4.5.2.3.

After a 16-hour fast, male *PdxPyy* WT mice weighed significantly less when fasted than when fed *ad libitum* (p <0.001), as did the *PdxPyy* KO mice (p <0.01). The male fasted or fed WT mice weighed more than the null mice (p <0.0.5: Figure 4.5B). On the other hand, female *PdxPyy* KO mice only significantly weighed more fed than fasted (p <0.05: Figure 4.5D).

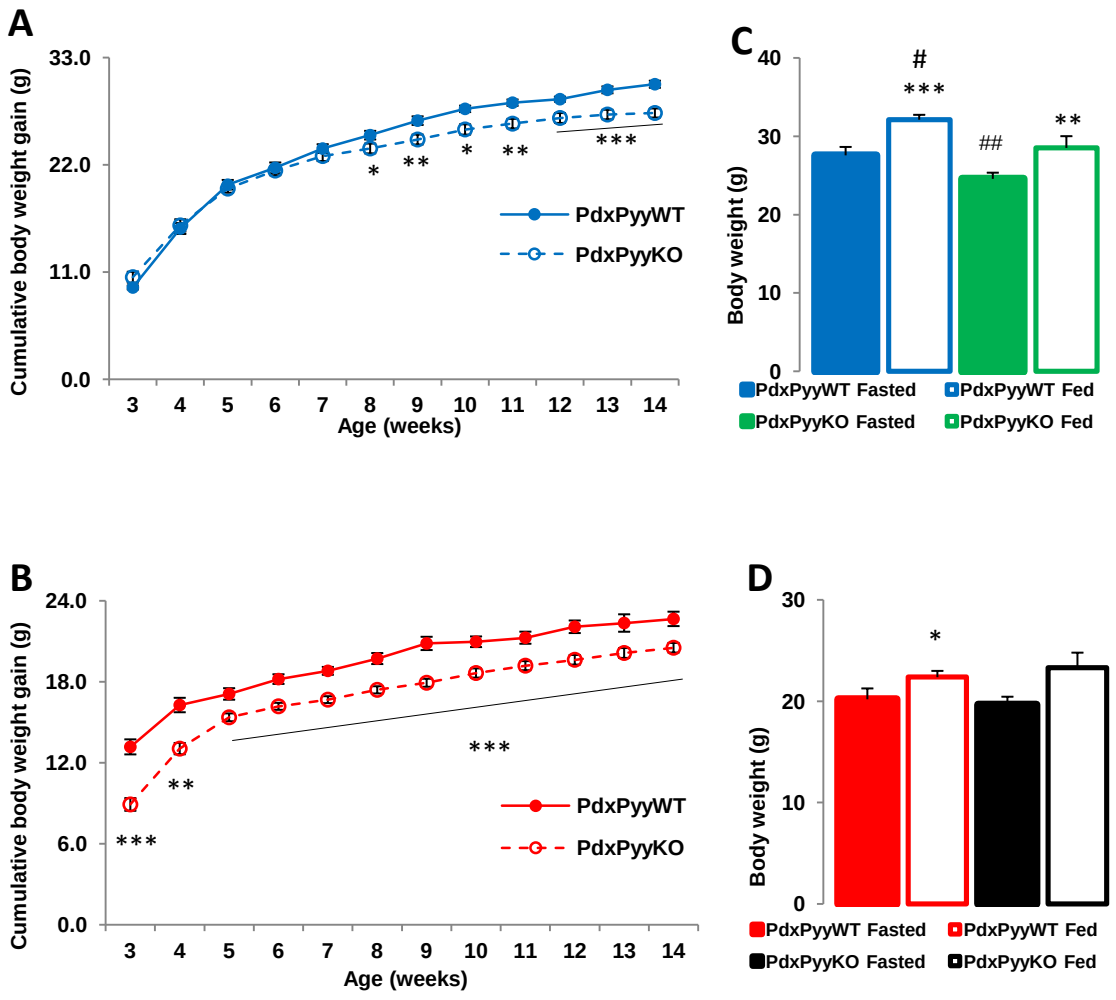

Figure 4.5: Body weight phenotype of the *PdxPyy* mice. Cumulative body weight gain in the: A) Male *PdxPyy* mice: blue. B) Female *PdxPyy* mice: red. Fasted or fed body weight in: C) Male *PdxPyy* mice: blue/green. D) Female *PdxPyy* mice: red/black. N = 15-25 mice per group. Data represented as mean ± SEM. **p<0.05*, ***p<0.01*, ****p <0.001* between genotypes. *#p < 0.05*, *##p < 0.01*, between the fasted or fed groups.

4.5.2.3. Evaluating the effects of Pdx-mediated deletion of Pyy on factors that may contribute to the observed body weight phenotype.

To ensure that the body weight difference was not due to somatic growth, in mice aged 16-18 weeks, we measured the length of the mouse (from nose to anus). The WT mice body lengths were not significantly different from the KO mice of both sexes (Male WT= 10.74 ± 0.08 cms *versus* KO= 10.48 ± 0.13 cms and female WT= 10.08 ± 0.17 cms *versus* KO= 9.9 ± 0.09 cms) (Figures 4.6A & B). Fat mass from the gonads was removed and weighed in 16-18 week old mice. Male *PdxPyy* WT mice fat mass was 0.48 ± 0.03 g and the null mice showed a reduction in gonadal fat (0.36 ± 0.04 g, p <0.001: Figure 4.6C-D). In female mice this difference was not apparent (Figure 4.6E).

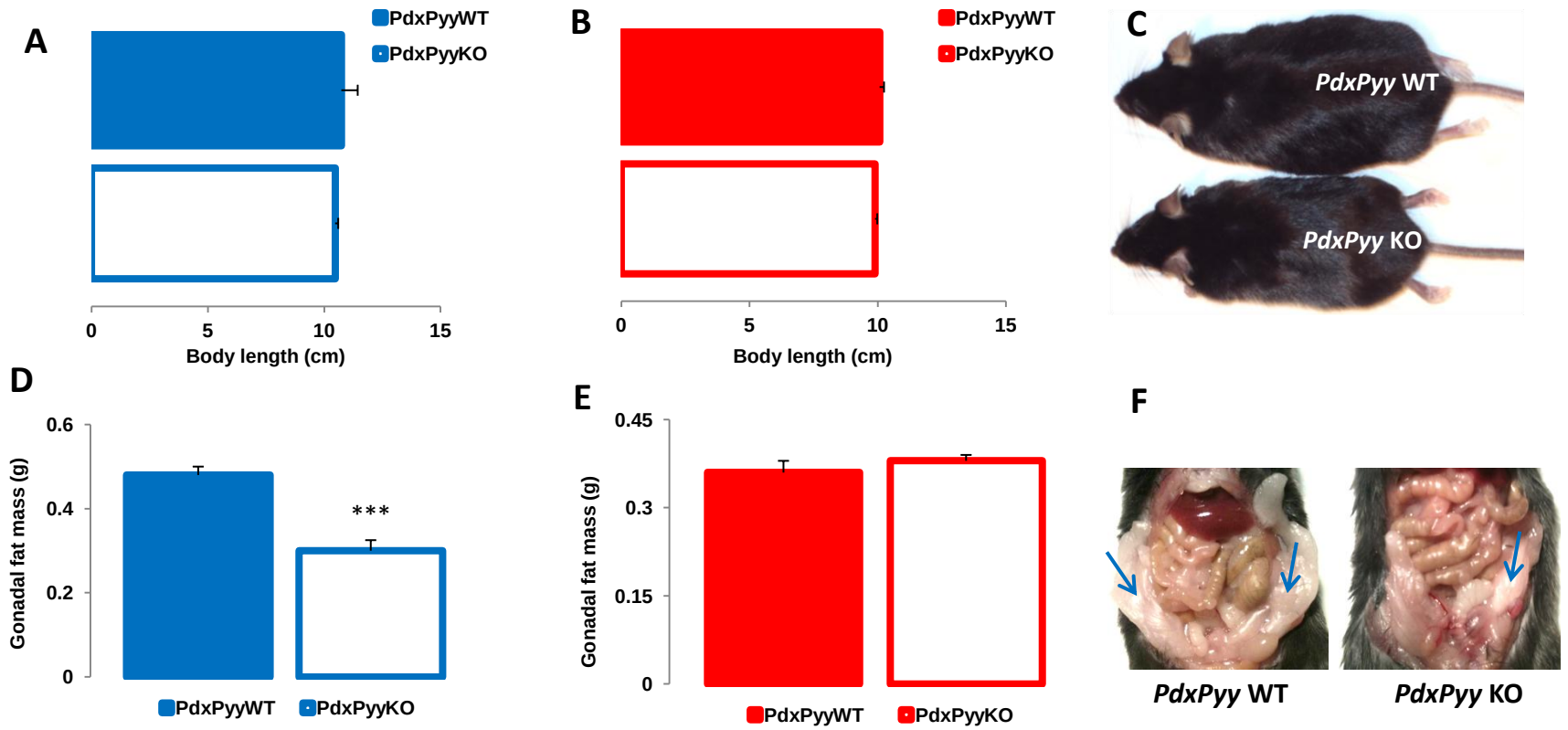

Figure 4.6: *PdxPyy* KO mice show decreased adiposity. A&B) Body length in the male (blue) and female (red) *PdxPyy* mice. C) Representative image of the *PdxPyy* mouse body size. D-E) Gonadal fat mass in the male (blue) and female (red) *PdxPyy* mice. F) Ventral representative image of fat pads of the *PdxPyy* mice. N = 8-10 mice per group aged 16-18 weeks. Data represented as mean + SEM. ****p < 0.001*.

4.5.2.4. Evaluating the effects of Pdx-mediated deletion of Pyy on glucose homeostasis.

Glucose homeostasis was assessed in 18-20 week old *PdxPyy* mice (body weights: males: WT: 28.4 ± 0.7 g, KO: 25.1 ± 0.9 g, p <0.01. Females: WT: 18.5 ± 0.5 g, KO: 20.4 ± 1.3 g). The glucose tolerance in these mice was done by performing an IPGTT, OGTT and an OGSIS. For the GTTs, a bolus i.p. injection or oral gavage with glucose (1g/kg body weight) was administered in age- and sex-matched *PdxPyy* KO mice and their controls. Blood was taken to measure glucose levels from the tail vein before and after the injection. For the GSIS, additional blood was taken for measurement of circulating insulin levels.

Fasted blood glucose of the *PdxPyy* WT mice was not significantly different from the KO mice in both male (WT: 3.0 ± 0.2 mM vs. KO: 3.0 ± 0.3 mM: Figure 4.7A) and female mice (WT: 3.5 ± 0.4 mM vs KO: 2.9 ± 0.2 mM: Figure 4.7B).

I. <u>IPGTT</u>

From the IPGTT, the P*dxPyy* KO mice showed a significant reduction in blood glucose levels at t90 and t120 post-injection in the males and t120 in females (Male t90: WT: 16.7 ± 2.1 mM, KO: 8.6 ± 1.5 mM, p =0.009, male t120: WT: 12.7 ± 2.0 mM, KO: 5.2 ± 0.5 mM p <0.005: Figure 4.7C, female t90: WT: 5.0 ± 0.3 mM, KO: 3.1 ± 0.3 mM p <0.002: Figure 4.7D). In addition, the $AUC_{60\text{-}120}$ IPGTT was significantly lower in the male *PdxPyy* KO mice (551.6 ± 87.4 mM/min) compared to the controls (968.8 ± 119.5 mM/min p <0.05) (Figure 4.7E). The female *PdxPyy* KO mice showed insignificantly reduced $AUC_{90\text{-}120}$ IPGTT (119.1 ± 11.6 mM/min) compared to the controls (162.4 ± 17.2 mM/min, p =0.059) (Figure 4.7F).

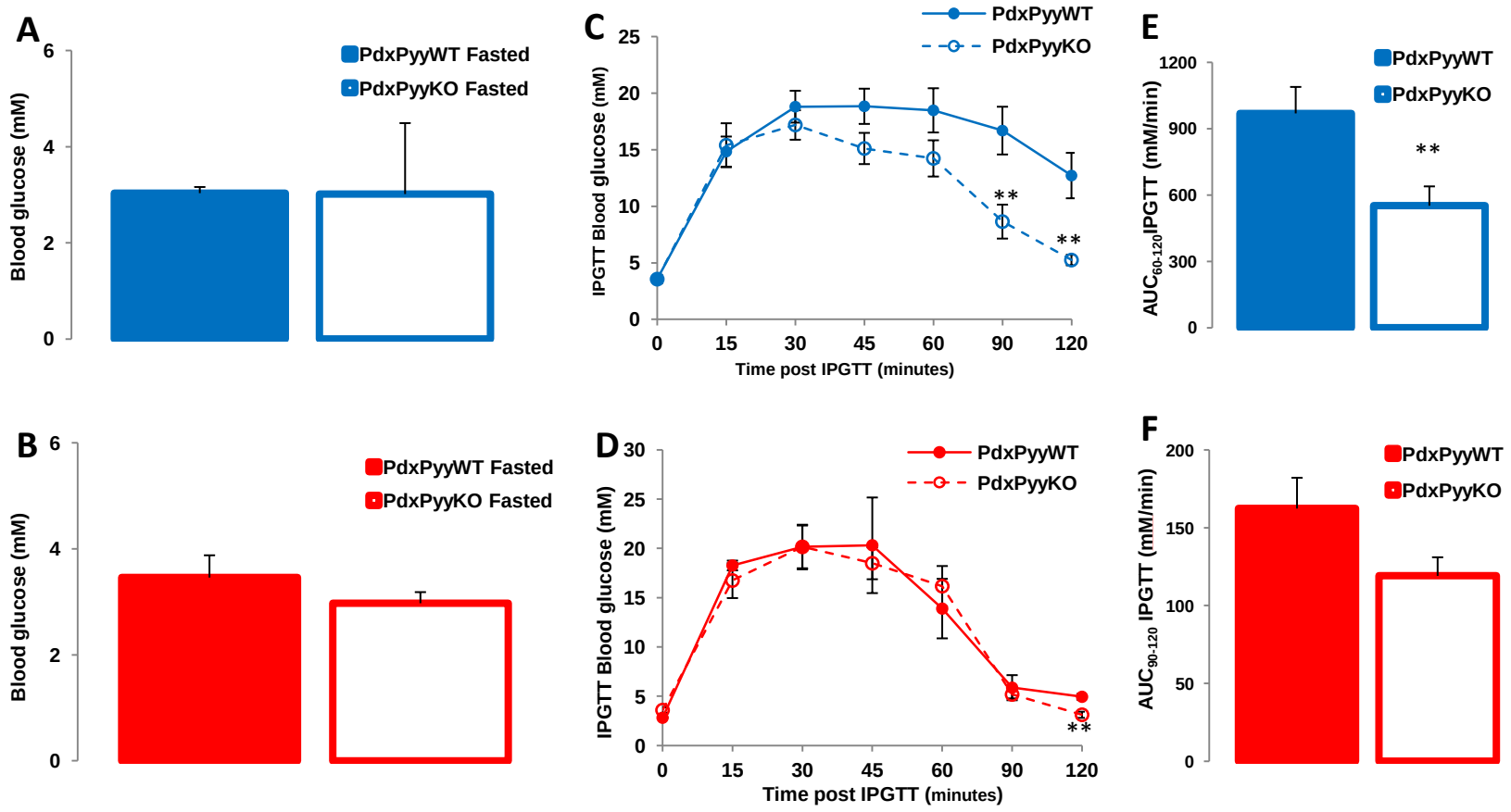

Figure 4.7: Assessment of IPGTT in the *PdxPyy* mice. Glucose homeostasis was assessed in age- and sex-matched *PdxPyy* mice. Glucose (1g/kg body weight) was injected i.p. and blood samples collected for measurement of blood glucose at time points indicated. Fasted blood glucose in A) males and B) females. Time course of IPGTT in C) males and D) females. AUC IPGTT in E) males and F) females. Data is shown as mean ± SEM of duplicates. N = 6-12 per group, * $p < 0.05$, ** $p < 0.01$.

II. OGTT and OGSIS

From the OGTT, the *PdxPyy* KO mice showed a significant reduction in blood glucose levels at t30 in male mice (15.8 ± 1.5 mM vs. WT: 20.9 ± 1.8 mM, p =0.04: Figure 4.8A). In female mice however, there was no difference in the OGTT response between the groups (Figure 4.8B). In addition, the $AUC_{30\text{-}120}$ OGTT was significantly lower in the male *PdxPyy* KO mice compared to the controls (WT: 1487.2 ± 159.9 mM/min vs. KO: 972.2 ± 83.3 mM/min: Figure 4.8C). Again, there was no difference in the AUC OGTT of the female different *PdxPyy* mouse groups (Figure 4.8D). Blood was also taken at the times indicated in the OGSIS for assessment of insulin release and measured by ELISA. At t15, *PdxPyy* KO mice significantly secreted more insulin (WT: 0.20 ± 0.04 ng/ml vs. KO: 0.31 ± 0.02 ng/ml, p =0.04), with the $AUC_{0\text{-}30}$ OGSIS showing a significant increase in the *PdxPyy* KO mouse (p =0.027) (Figures 4.8E-F).

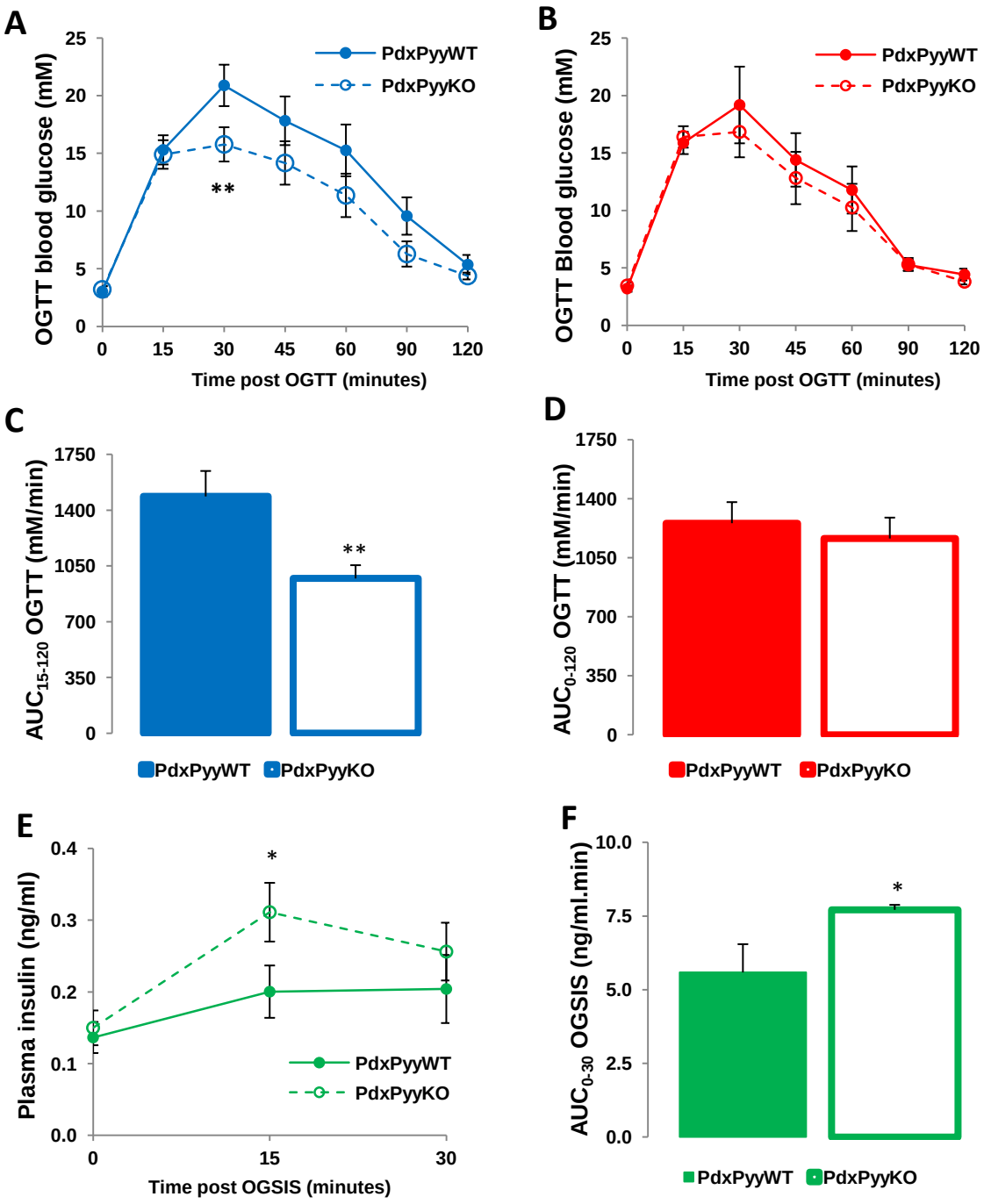

Figure 4.8: Assessment of OGTT and OGSIS in the *PdxPyy* mice. Glucose homeostasis administered orally and blood samples collected for measurement of blood glucose and GSIS at time points indicated. Time course of OGTT in A) males and B) females. AUC OGTT in C) males and D) females. E) Time course of OGSIS in males. F) $AUC_{0\text{-}30}$ OGSIS. Data is shown as mean ± SEM of duplicates. N = 5-9 per group, * $p < 0.05$, ** $p < 0.01$.

4.5.3. Investigating the possible compensatory factors that may contribute to the observed energy and glucose homeostatic phenotypes of the *PdxPyy* KO mouse

4.5.3.1. Assessing the hormonal changes that may contribute to the PdxPyy KO phenotype: PYY expressing sites.

Apart from the pancreas, PYY is found expressed in the gut which has known post-prandial anorectic action (Batterham et al., 2002, Batterham and Bloom, 2003, Batterham et al., 2003). However, PYY is also located in the brainstem but the physiological role of this set of cells remains unknown (Glavas et al., 2008, Gelegen et al., 2012). To determine if changes in gut and brainstem *Pyy* may be involved in the observed phenotypes, we measured *Pyy* gene expression from these tissues of the *PdxPyy* mice. Whole tissue qRTPCR were performed on the brainstem, ileum, and colon. Brainstem, ileal and colonic *Pyy* expression was not different between the groups (Figure 4.9).

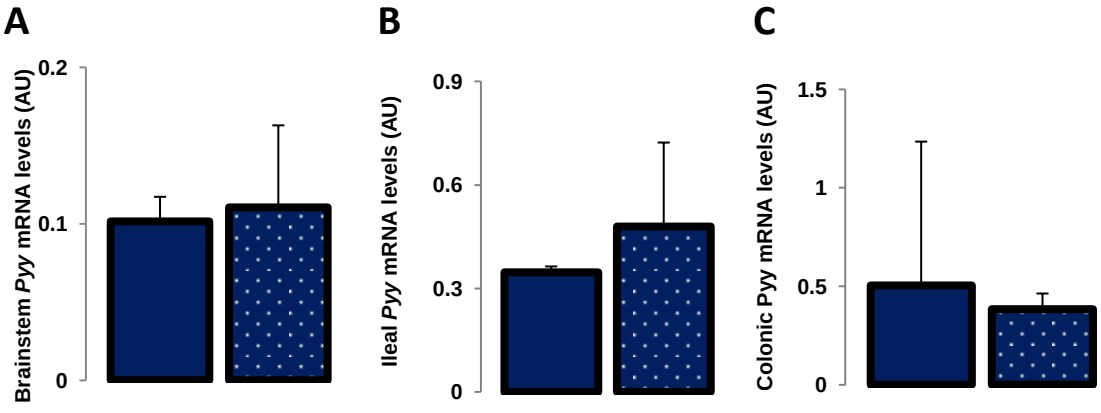

Figure 4.9: Assessment of *Pyy* mRNA in the *PdxPyy* mice. Whole tissue *Pyy* expression was measured by qRTPCR in A) Brainstem, B) Ileum and C) Colonic tissue. Results were normalized to *Ubc*. Filled bars: *PdxPyy* WT and patterned bars: *PdxPyy* KO. Data is shown as mean + SEM of duplicates. N= 4-7 per group.

4.5.3.2. Assessing the duodenal hormonal changes that may contribute to the PdxPyy KO phenotype.

To assess if the *Pdx*-directed deletion of *Pyy* affected duodenal expression of *Pyy*, we measured for changes in mRNA levels. There was no significant difference in duodenal *Pyy* expression between the *PdxPyy* WT (0.071 ± 0.005 AU) and *PdxPyy* KO mice (0.074 ± 0.02 AU) (Figure 4.10A). Cholesystokinin (CCK), a duodenal anorectic peptide was also assessed to determine whether the *Pdx*-targeting strategy was possibly causing compensation for the loss of the *Pyy* gene. *Cck* mRNA was measured by real-time qRTPCR and remained unchanged between 16-18 week old *ad libitum* fed *PdxPyy* KO mice and their control littermates (Figure 4.10B).

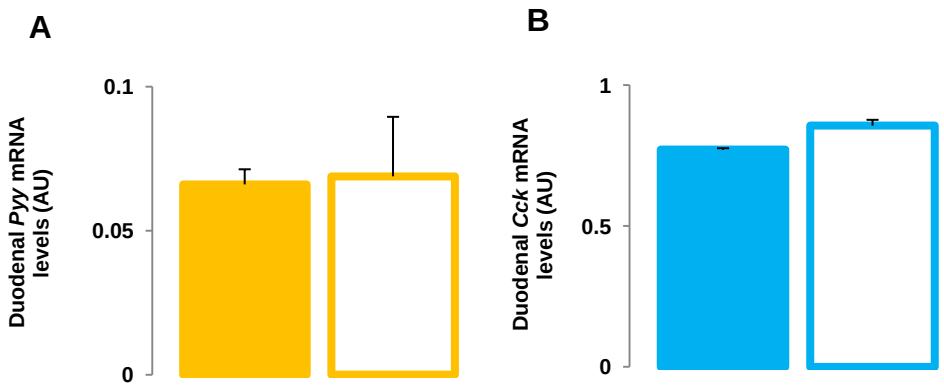

Figure 4.10: Assessment of duodenal gut hormone gene expression. Whole tissue gene expression was measured from the duodenum for A) *Pyy* expression and B) *Cck* in the *PdxPyy* mice. Results were normalized to *Ubc*. Filled bars: *PdxPyy* WT and patterned bars: *PdxPyy* KO. Data is shown as mean + SEM of duplicates. N=4-7 per group.

4.5.3.3. Assessing the gut hormone changes that may contribute to the PdxPyy KO phenotype.

In addition to the duodenum, other gut hormones were assessed; stomach *ghrelin*, ileal and colonic *proglucagon* gene expression were measured. There was no difference between the 16-18 week old *ad libitum* fed *PdxPyy* KO and the control mice (Figure 4.11).

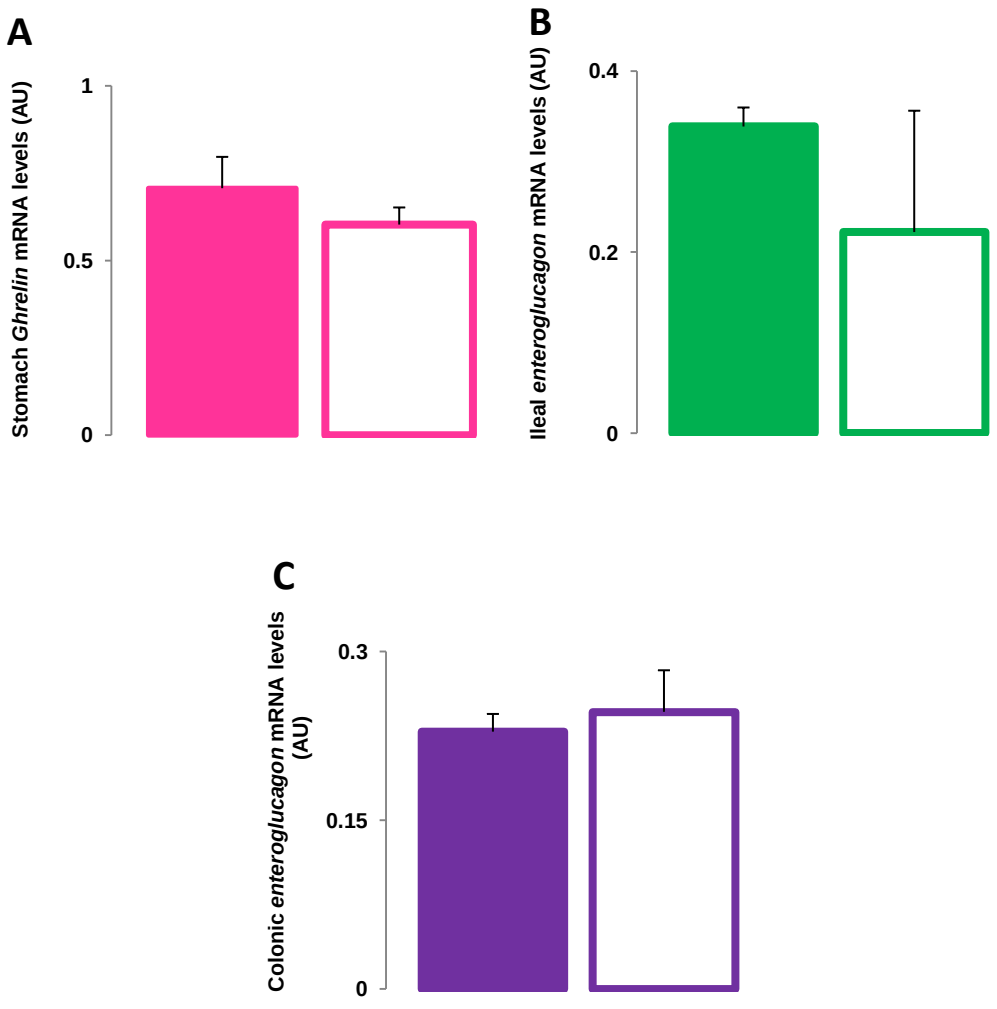

Figure 4.11: Assessment of gut hormone gene expression in the male *PdxPyy* mice. Whole tissue gut hormone expression was measured by qRTPCR: A) Stomach *ghrelin*, B) Ileum and C) Colonic *proglucagon* mRNA in the *PdxPyy* mice. Results were normalized to *Ubc*. Filled bars: *PdxPyy* WT and open bars: *PdxPyy* KO. Data is shown as mean + SEM of duplicates. N= 4-7 per group.

4.6. Summary

4.6.1. Analysis of *Pdx*-specific deletion of *Pyy*

To understand the specific *in vivo* role of islet PYY, a transgenic mouse was created; *PdxPyy* KO. *PdxCre* meditated recombination of the floxed *Pyy* gene was successful causing the deletion of the gene and protein. Duodenal *Pyy* mRNA levels remain unchanged in the *PdxPyy* KO mice in comparison to the control *ad libitum* fed mice. This work suggests a role for pancreatic PYY in the regulation of body weight and glucose metabolism.

4.6.2. *PdxPyy* deletion effects on body weight and appetite regulation

Deletion of pancreatic PYY resulted in no change to weekly cumulative food intake, but a significant reduction in food intake at a few time points post a fast-re-feed challenge in male mice. Additionally, there was also a reduction in cumulative body weight gain in both male and female *PdxPyy* KO mice compared to the *PdxPyy* WT from weaning to the end of the study.

To ensure the body weight phenotype was not a result of a difference in somatic growth, as was seen in the global $Pyy^{-/-}$ mouse (Boey et al., 2006b), we measured the length of the mice and found that *PdxPyy* KO and WT mice were of a similar body length in both male and females. Gonadal fat mass was also measured to see if this was contributing to the observed phenotype. Only male *PdxPyy* KO mice showed significantly less fat than the WT mice, this phenotype was not apparent in the female groups.

4.6.3. *PdxPyy* deletion and glucose homeostasis

The oral GTT challenge resulted in HI and a reduction in blood glucose in the *PdxPyy* null mouse. We also carried out an IPGTT to see whether the response was lost in absence of enteral stimulation and found a significant reduction in blood glucose levels but this was observed at a later time. Moreover, *in vivo* GSIS was markedly increased, with a reduction in blood glucose.

4.6.4. *PdxPyy* deletion and the gut

To assess whether there are compensatory changes to gut hormones as a result of the *PdxPyy* deletion, we initially measured *Pyy* mRNA in the brainstem (Glavas et al., 2008, Gelegen et al., 2012) and lower gut (Batterham et al., 2002, Batterham and Bloom, 2003). Subsequently, using qRTPCR *Pyy* expression from peripheral and central sites was quantified. This was followed by gut *ghrelin*, *Cck* and *enteroglucagon* measurements. This was undertaken to assess whether other gut hormones were contributing to the *in vivo* effects observed in these mice. However, no changes were observed in the gut hormone gene expression of the *PdxPyy* KO mice.

4.6.5. Conclusion

In summary, this chapter demonstrates that PYY-mediated systems are important for the regulation of body weight and glucose homeostasis. In particular, *Pdx*-specific deletion of *Pyy* led to the successful deletion of islet PYY protein and results in an exaggerated GSIS causally linked to a lean phenotype and decreases in adiposity.

Chapter 5

Characterising the role of gut hormones in hyperinsulinaemic hypoglycaemia

5. Characterising the role of gut hormones in hyperinsulinaemic hypoglycaemia

5.1. Introduction

Nesidioblastosis in adults or congenital forms of HH is characterised by persistent hypoglycaemia due to unregulated secretion of insulin from the pancreatic β-cells. Historically adult-onset nesidioblastosis has been rare and was mainly found due to the occurrence of non-insulinoma pancreatogenous hypoglycaemia syndrome (NIPHS) (Jabri and Bayard, 2004). Though the cause appears to be unknown, as of late there appears to be a surge in the frequency of cases. Increasing evidence has suggested this to be a result of the GBP weight-loss surgery (Service et al., 2005). At present, two theories exist for the reasoning behind nesidioblastoma formation as a complication of GBP surgery. The first suggests that obesity induces HI and islet hyperfunction. The second hypothesis is that HI is a consequence of GBP (Service et al., 2005, Cummings, 2005). However, support against the first hypothesis is that individuals with insulinomas are not morbidly obese and obese persons have normal islet cell morphology (Service et al., 2005). Due to such theories, a deeper understanding for the functional mechanisms purporting that bariatric surgery causes nesidioblastosis is becoming of great interest to diabetes research.

Many individuals who have undergone GBP have presented with the dumping syndrome. Reports have proposed this to be because of an increase in peripheral GLP-1 due to the rapid transit of nutrients to the distal gut (Miholic et al., 1991). GLP-1 is known to promote β-cell proliferation, neogenesis and inhibit apoptosis. Furthermore, a case study highlighted the persistence of post-prandial HH episodes in a person who previously had undergone a GBP. The individual required a subtotal pancreatectomy. However, 6 months post-surgery and apparent remission, HH returned and the person was managed on drugs (Qintar et al., 2012). Hence this case supports the theory that GBP has possibly either bypassed the proximal gut hormone(s) (such as GIP: foregut theory) and/or overstimulated the distal GI peptide(s) (such as GLP-1 and PYY: hindgut

theory) to induce exaggerated HI. This in turn would potentially mediate hypoglycaemia and nesidioblastosis. Moreover, DPP-4 regulates these gut hormones and thus, GBP may also be altering the biological activity of DPP-4 on these substrates. Furthermore DPP-4 inhibition is currently employed to promote the incretin effect in T2DM. Ultimately, if GLP-1 and other DPP-4 gut hormone substrates are factors involved in this condition, then it brings into question (1) the current practice of GBP as well as (2) the use of GLP-1R agonists and DPP-4 inhibitors as therapeutic treatments of obesity and T2DM.

Nesidioblastosis has also been reported in neonates (Rahier et al., 2000). It is more commonly referred to and accepted as CHI. CHI incidence is around 1 in 50,000 births of the general population and can be transient or persistent. In most cases, defects in the K_{ATP} channels (channelopathies) cause the congenital form of HH; K_{ATP}HI (Senniappan et al., 2013). Treatments of such cases usually require constant feeding and pharmacotherapy. In medically-unresponsive HH situations, surgical removal of the pancreas is required. The overall effect is to reduce insulin secretion and function as well as prevent brain damage that occurs as a result of recurring hypoglycaemia. However, the surgery has complications and often leads to pancreatic exocrine insufficiency and DM (Arya et al., 2013).

Gene deletion of *Sur-1* results in fasted hypoglycaemia and is similar to the human K_{ATP}HI condition (De Leon et al., 2008). WT mice treated with the GLP-1R antagonist exendin (9-39) have shown an increase in fasting blood glucose (De León et al., 2003). Therefore *Sur-1* null animals were treated with the exendin (9-39) or vehicle and blood glucose measured. The KO mice treated with exendin (9-39) had an increase in fasting blood glucose when compared to vehicle-treated KO mice. These changes were in the absence of body weight, glucose tolerance and insulin sensitivity adjustments (De Leon et al., 2008). This was followed by a pilot clinical study by the group. They infused the GLP-1R antagonist in patients with K_{ATP}HI and aimed to reduce HH (Calabria et al., 2012). They found a glucose increasing effect and insulin decreased without altering circulating glucagon or GLP-1 levels. Overall these studies implicate and support the

hypothesis that GLP-1 activity plays an important role in HH and thus, may have the potential as a therapeutic target for the treatment of this disease. However, these studies have also failed to assess if other gut hormone are involved in the pathophysiology of HH.

Collectively the data supports the theories that gut hormone changes promote HH as a result of K_{ATP}HI or due to GBP-induced nesidioblastosis. However, the mechanism of this effect remains unknown. Taken together, the interaction between the incretins, PYY and DPP-4 needs to be examined more closely if (1) we are to gain full therapeutic benefit and (2) avoid possible adverse effects of current drug treatments for HH.

5.2. Hypothesis

'Hyperinsulinaemic hypoglycaemia promotes changes in DPP-4 and its gut hormone substrates'

5.3. Aims:

- To determine changes in expression of pancreatic genes involved in energy and glucose balance.
- To characterise the distribution and localisation of islet PYY and DPP-4 in healthy pancreatic samples.
- To determine the proliferating islet-cell subtypes in the K_{ATP}HI pancreas.
- To assess circulating gut hormone changes in patients with K_{ATP}HI at HH.
- To evaluate correlations between metabolites analysed in patient with K_{ATP}HI.

5.4. Study Design:

Using gene expression analysis, we determined changes in mRNA of pancreatic genes that may contribute to the K_{ATP}HI phenotype of six K_{ATP}HI patients against two non-K_{ATP}HI controls. The localisation of PYY and DPP-4 expression in different islet cell subtypes were evaluated in eight healthy pancreata using IHC. Thereafter, we aimed to identify the proliferating islet-cell subtype in three K_{ATP}HI pancreatic tissues. In addition, five K_{ATP}HI patients were recruited and studied consecutively. All patients underwent a controlled hypoglycaemia screen (reducing i.v. glucose with no feeds) and blood was collected at normoglycaemia and at hypoglycaemia. Plasma glucose was measured by YSI and plasma insulin using RIAs. Active GLP-1 and total GIP were measured using ELISAs and active PYY was measured by RIAs. Finally correlation analysis was carried out in five K_{ATP}HI patients.

5.5. Results

5.5.1. Assessing the changes in expression of pancreatic genes involved in energy and glucose balance.

To begin we wanted to find possible gene contributors to the HH seen in K_{ATP}HI. Hence, we analysed the pancreatic gene expression of six K_{ATP}HI patients and compared them with two non- K_{ATP}HI controls. mRNA analysis of K_{ATP}HI patients showed an increase in *DPP-4* expression (control: 5.04 ± 0.39 AU versus K_{ATP}HI: 6.13 ± 0.11 AU) and a trend towards a down-regulation of *PYY* expression (control: 5.32 ± 0.01 AU versus K_{ATP}HI: 4.85 ± 0.08 AU, p = 0.09) when compared to control tissue. *Y1R* gene expression was also down-regulated but this was insignificant (control: 5.69 ± 0.35 AU versus K_{ATP}HI: 4.80 ± 0.34 AU, p = 0.31). Additionally, *SST* expression appeared to be significantly upregulated in K_{ATP}HI (control: 9.18 ± 0.94 AU versus K_{ATP}HI: 10.13 ± 0.04 AU). No changes were observed in the *GLP-1R*, *GIP*, *GCG* and in any pancreatic *PYY YR* subtypes (p >0.05) (Figure 5.1).

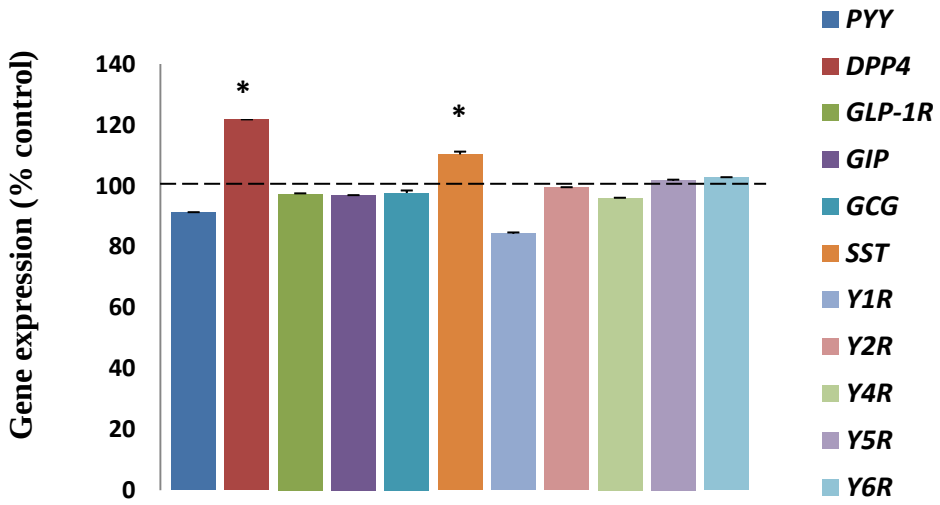

Figure 5.1: Gene expression results from pancreatic tissue samples of control and K_{ATP}HI patients. Gene expression of RNA isolated from K_{ATP}HI pancreata and control donors. N = 6 K_{ATP}HI and 2 control. Data shown as + SEM as % of control gene expression *p <0.05. Data reproduced from work carried out by Dr S. Senniappan, with permission.

5.5.2. Characterising the distribution and localisation of islet PYY and DPP-4 in normal healthy pancreas from children.

Primary and secondary antibodies (Chapter 2: Table 2.3) were used as previously described. Eight pancreata samples were obtained from healthy normal pancreatic tissue. This was following analysis and confirmation by the Histopathology Team at GOSH. Using immunofluorescent IHC, protein localisation of PYY and DPP-4 was determined.

5.5.2.1. PYY localisation in α-, β-, and δ-cells.

To determine if PYY was localised and was similar anatomically to the murine model; 5 µm pancreata sections from normal healthy and K_{ATP}HI patients were immunostained for individual cell-markers and PYY. As expected, we found that PYY was not co-localised with insulin (Figure 5.2A). PYY was found to be co-localised with glucagon in α-cells (Figure 5.2B). However, PYY was also absent from somatostatin δ-cells (Figure 5.2C).

5.5.2.2. DPP-4 localisation in α-, β-, and δ-cells.

DPP-4 expression appeared to be distributed in and on insulin positive β-cells (Figure 5.3), as well as with glucagon in α-cells (Figure 5.4). A small population of δ-cells were also positive for the expression of DPP-4 (Figure 5.5). However, DPP-4 was absent from PYY positive cell populations in normal healthy pancreatic islets (Figure 5.6).

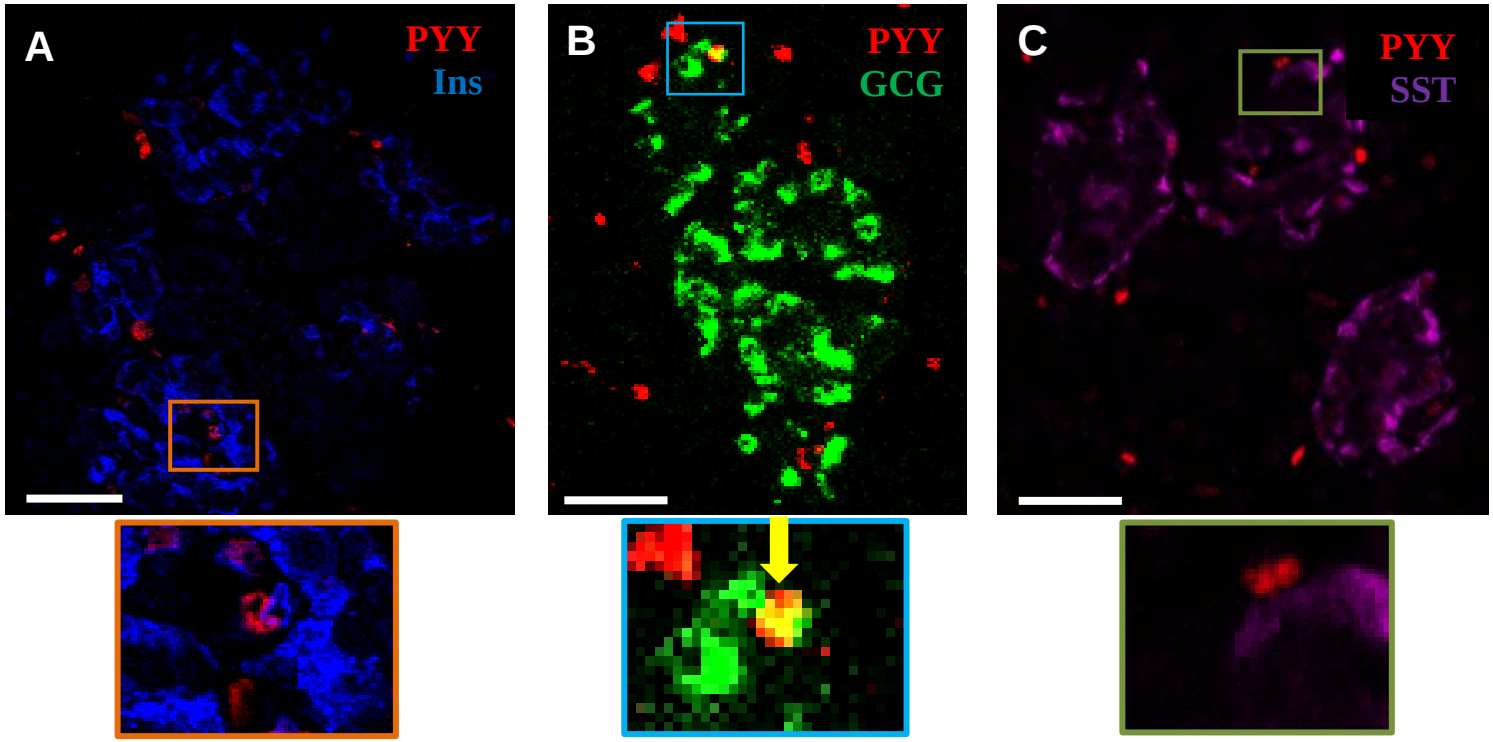

Figure 5.2: PYY is only localised to the human α-cells. Representative islet immunostaining in healthy children: (A) PYY (red) and insulin (blue) (B) Glucagon (green) and PYY (red). (C) Somatostatin (purple) and PYY (red). Yellow arrow indicates co-localisation of proteins. N = 8 with 2 sections per subject. Magnification x 20. Reference line: 50 µm.

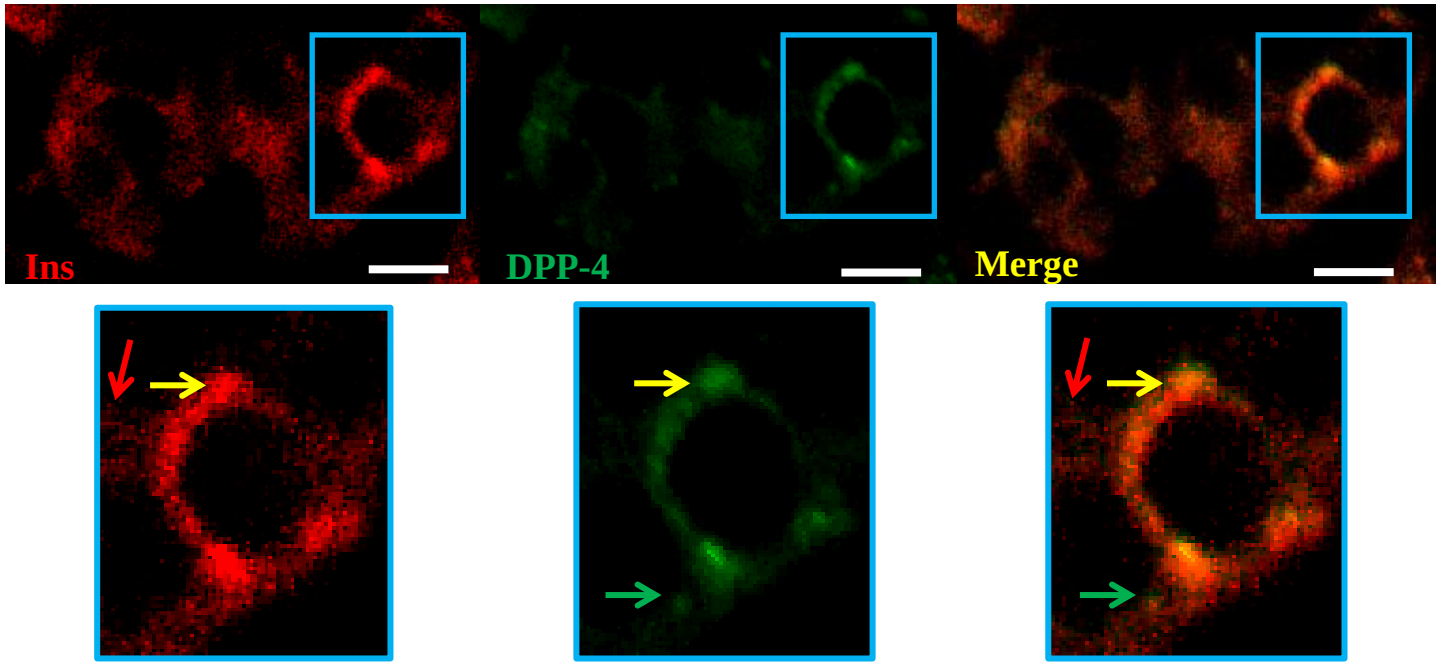

Figure 5.3: DPP-4 is localised in and on β-cells with insulin in healthy children pancreatic tissue. Representative islet immunostaining in healthy children: for insulin (red), DPP-4 (green) Red arrow indicates insulin only positive staining; green arrow indicates DPP-4 only positive staining with yellow arrow indicating co-localisation of the two proteins. N = 8 subjects, 2 sections per subject. Magnification x 63. Reference line: 10 µm.

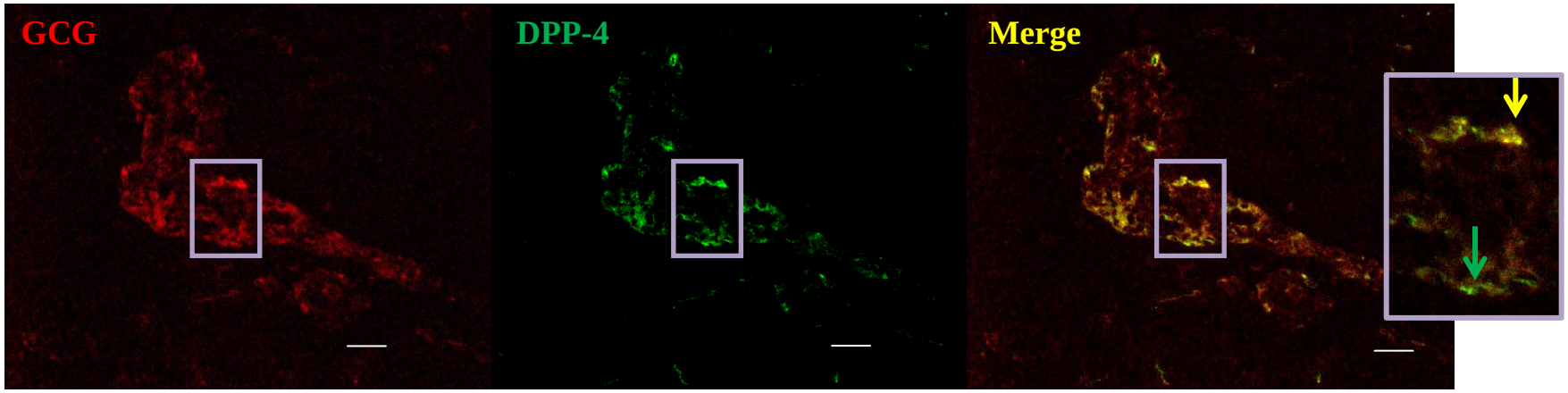

Figure 5.4: DPP-4 is localised in and on α-cells with glucagon in healthy children pancreatic tissue. Representative islet immunostaining in healthy children: for glucagon (red), DPP-4 (green). Green arrow indicates DPP-4 only positive staining with yellow arrow indicating co-localisation of the two proteins. N = 8 subjects, 2 sections per subject. Magnification x 20. Reference line: 20 µm.

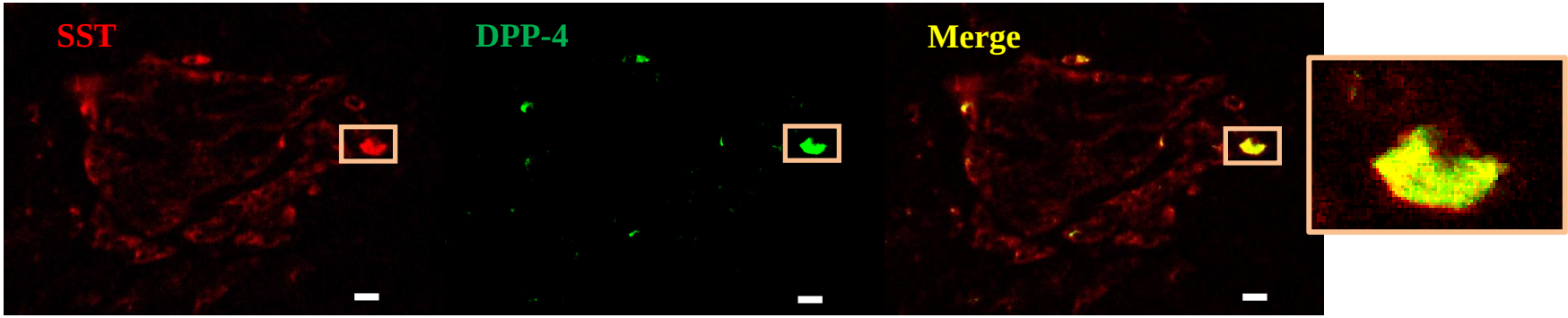

Figure 5.5: DPP-4 is localised in and on a few δ-cells with somatostatin in healthy children pancreatic tissue. Representative islet immunostaining in healthy children: for somatostatin (red), DPP-4 (green). Image inset indicating co-localisation of the two proteins. N = 8 subjects, 2 sections per subject. Magnification x 20. Reference line: 20 µm.

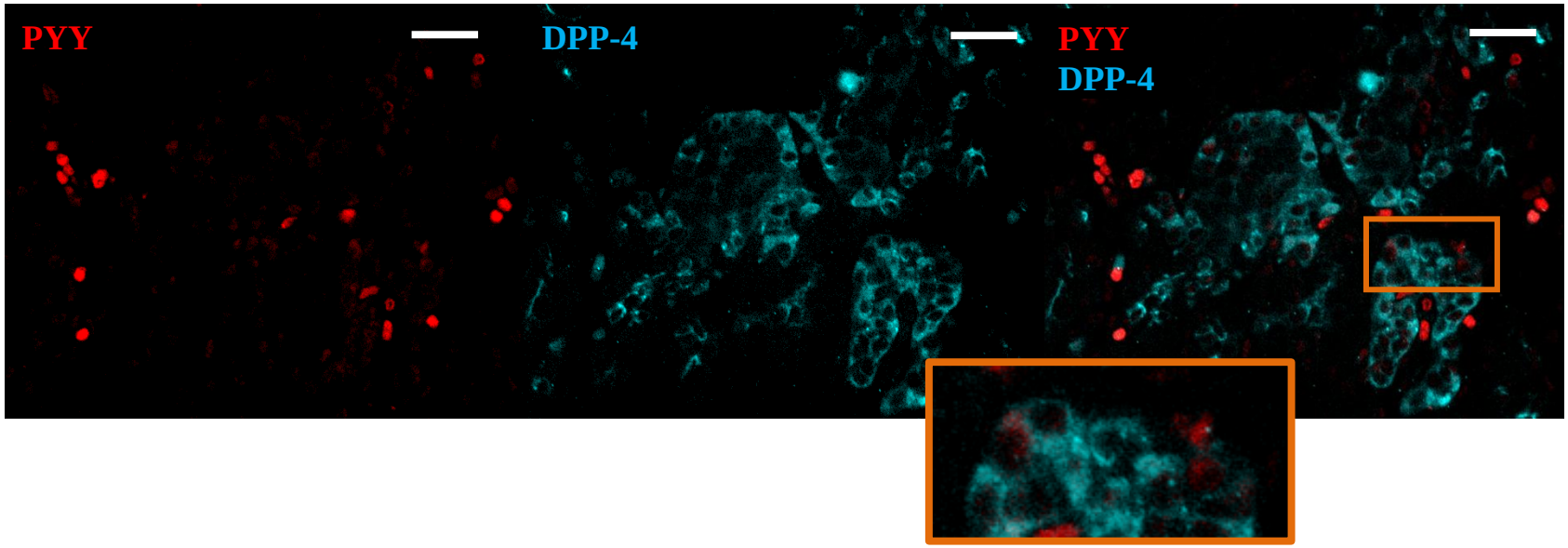

Figure 5.6: DPP-4 is not co-localised with PYY cells in healthy children pancreatic tissue. Representative islet immunostaining in healthy children: for PYY (red), DPP-4 (blue). N = 8 subjects, 2 sections per subject. Magnification x 20. Reference line: 25 µm.

5.5.3. Evaluating pancreatic changes in patients with K_{ATP}HI.

5.5.3.1. Morphological changes in patients with K_{ATP}HI.

Normal healthy pancreas was used as control and compared to K_{ATP}HI pancreas, which were obtained with consent from patients who have a near total pancreatectomy. Sections were cut and mounted on superfrost slides and H&E stained for visualisation of pancreata architecture. K_{ATP}HI pancreas generally had normal morphology and distribution of exocrine and endocrine cells however; they appeared to show characteristically large islet nuclei when compared to healthy pancreatic tissue (Figure 5.7).

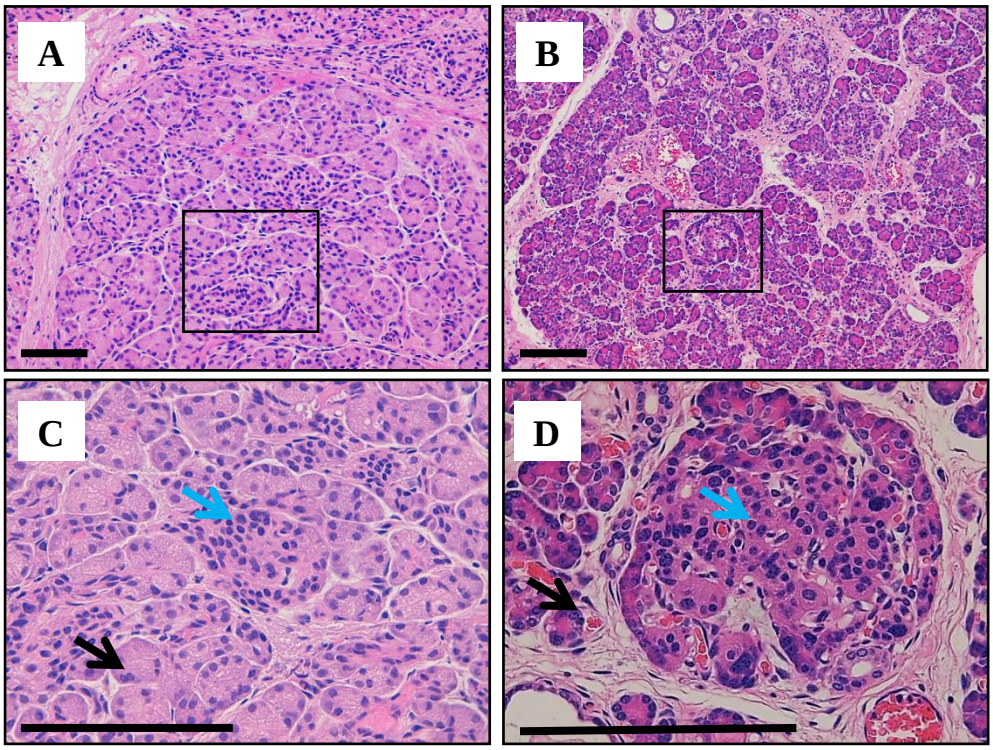

Figure 5.7: Normal and K_{ATP}HI pancreatic architecture. Representative images of haematoxylin & eosin (H&E) stained sections of pancreas in (A & C) normal and (B & D) K_{ATP}HI. Blue arrows indicate islet cell nuclear staining and black arrows indicate acinar cells (exocrine). (A & B) Magnification x 20, (C & D) magnification x 40. N = 8 subjects per group, 6 sections per patient. Reference line: 100 µm.

5.5.3.2. Proliferative changes in patients with K_{ATP}HI.

K_{ATP}HI and control pancreata were sectioned at 5 µm depth and stained for Ki67; a marker used to show proliferation. K_{ATP}HI pancreas showed an increased number of Ki67 nuclear immunostaining when compared to healthy pancreatic tissue (Figure 5.8). Performed with the assistance of GOSH histopathology lab.

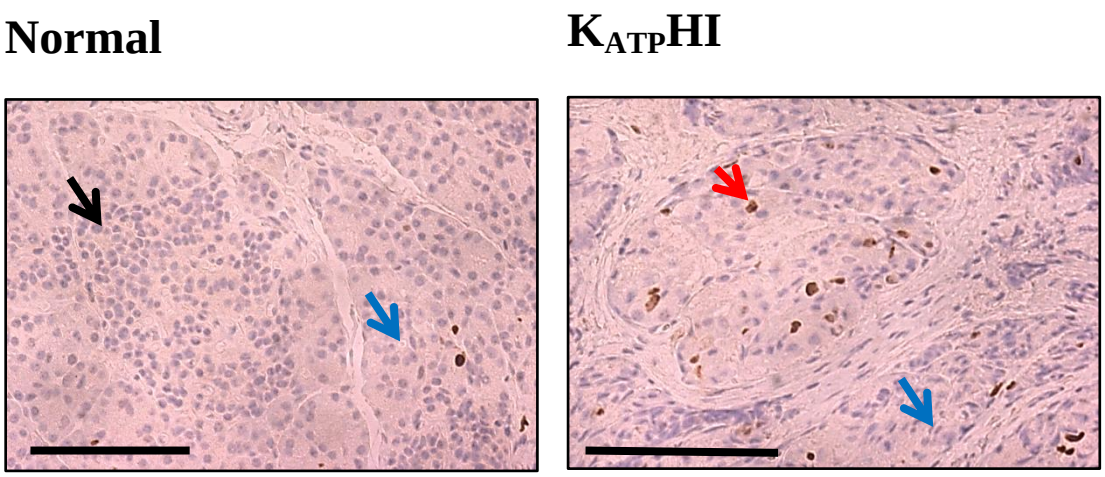

Figure 5.8: K_{ATP}HI promotes islet-cell proliferation. Representative immunostained sections of pancreas in normal and K_{ATP}HI using automated Leica stainer for Ki67 proliferation marker. Black arrow indicates the islet cell nuclear staining absent of Ki67 staining (brown). Blue arrows indicate Ki67+ acinar nuclear cell staining. Red arrow represents Ki67+ islet cell nuclear staining. Magnification x 40. N = 8 subjects per group, 2 sections per subject. Reference line: 50 µm.

5.5.3.3. Assessment to detect islet expression changes in patients with K_{ATP}HI.

Using IHC, we tried to determine the islet cell subtypes that may be proliferating and hence, contribute to the observed phenotype of these patients using Ki67 as a marker for proliferation.

K_{ATP}HI tissue appeared to show islet β-cell proliferation (Figure 5.9), which was absent for α-cells (Figure 5.10). Islet δ-cell showed positive immunostaining for the proliferative marker, Ki67 (Figure 5.11). In addition, PYY and DPP-4 expression were assessed against the proliferative marker. PYY positive cells showed no proliferation (Figure 5.12). Whereas, DPP-4 positive cells were clearly also expressing Ki67 (Figure 5.13).

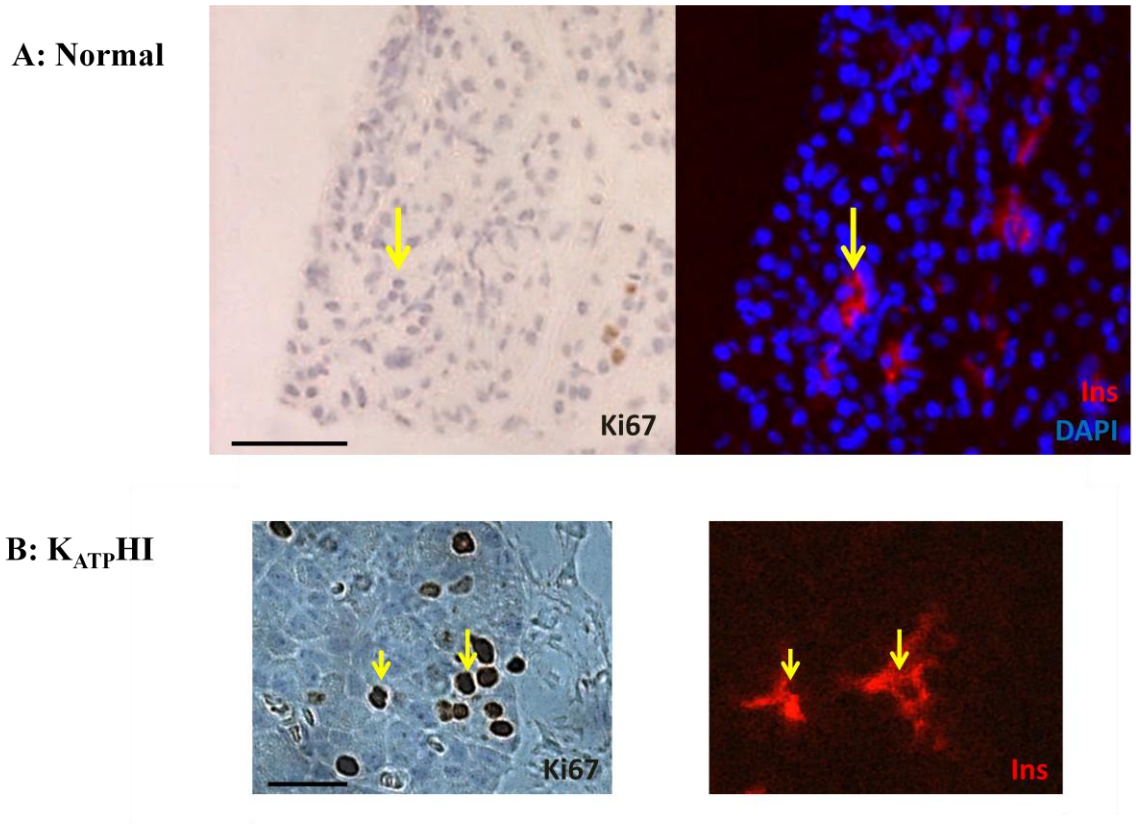

Figure 5.9: K_{ATP}HI promotes β-cell proliferation. Representative immunostained sections of pancreas in (A) normal and (B) K_{ATP}HI using automated Leica stainer for Ki67 proliferation marker. Immunofluorescent staining for insulin in red. Yellow arrows represent the islet cell nuclear staining positive for Ki67 staining (brown). DAPI stains nuclei blue. Magnification x 20 & x 40. N = 3 subjects per group, 2 sections per subject. Reference line: 50 µm.

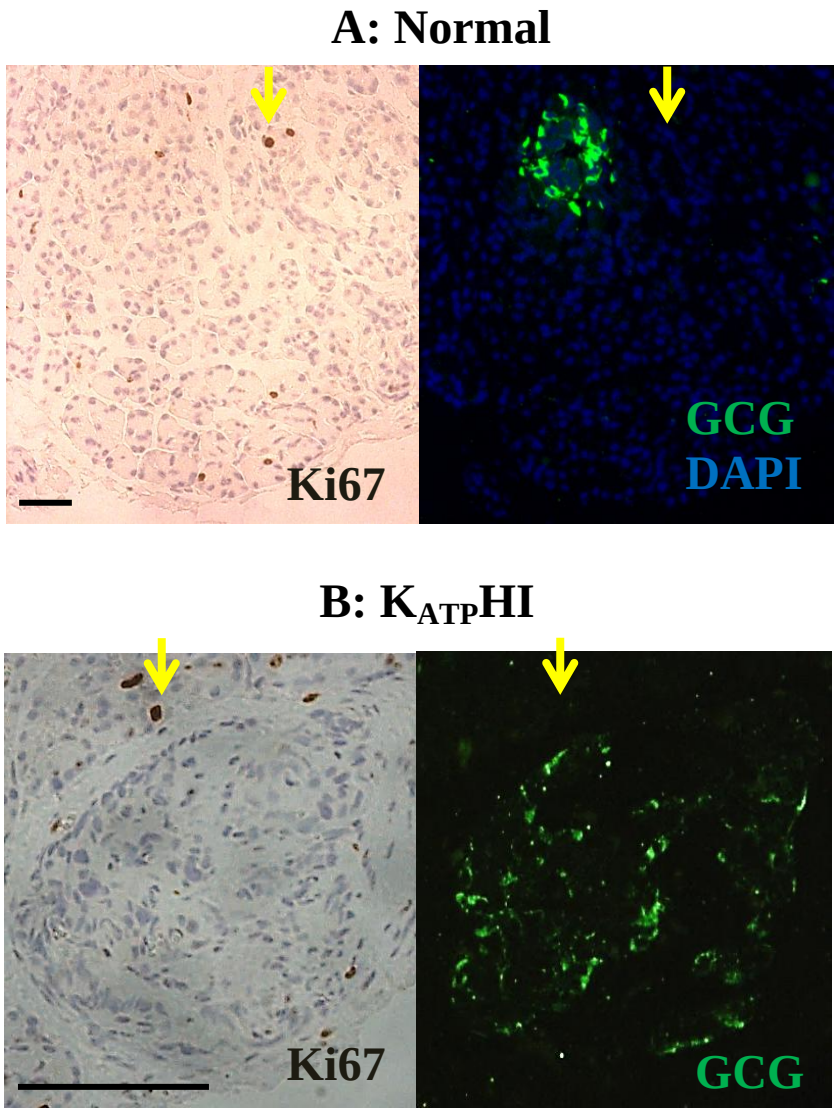

Figure 5.10: K_{ATP}HI is absent in α-cell proliferation. Representative immunostained sections of pancreas in (A) normal and (B) K_{ATP}HI using automated Leica stainer for Ki67 proliferation marker. Immunofluorescent staining for glucagon in green. Yellow arrows indicate the islet cell nuclear staining positive for Ki67 staining (brown). DAPI stains nuclei blue. Magnification x 20 & x 40. N = 3 subjects per group, 2 sections per subject. Reference line: 50 µm.

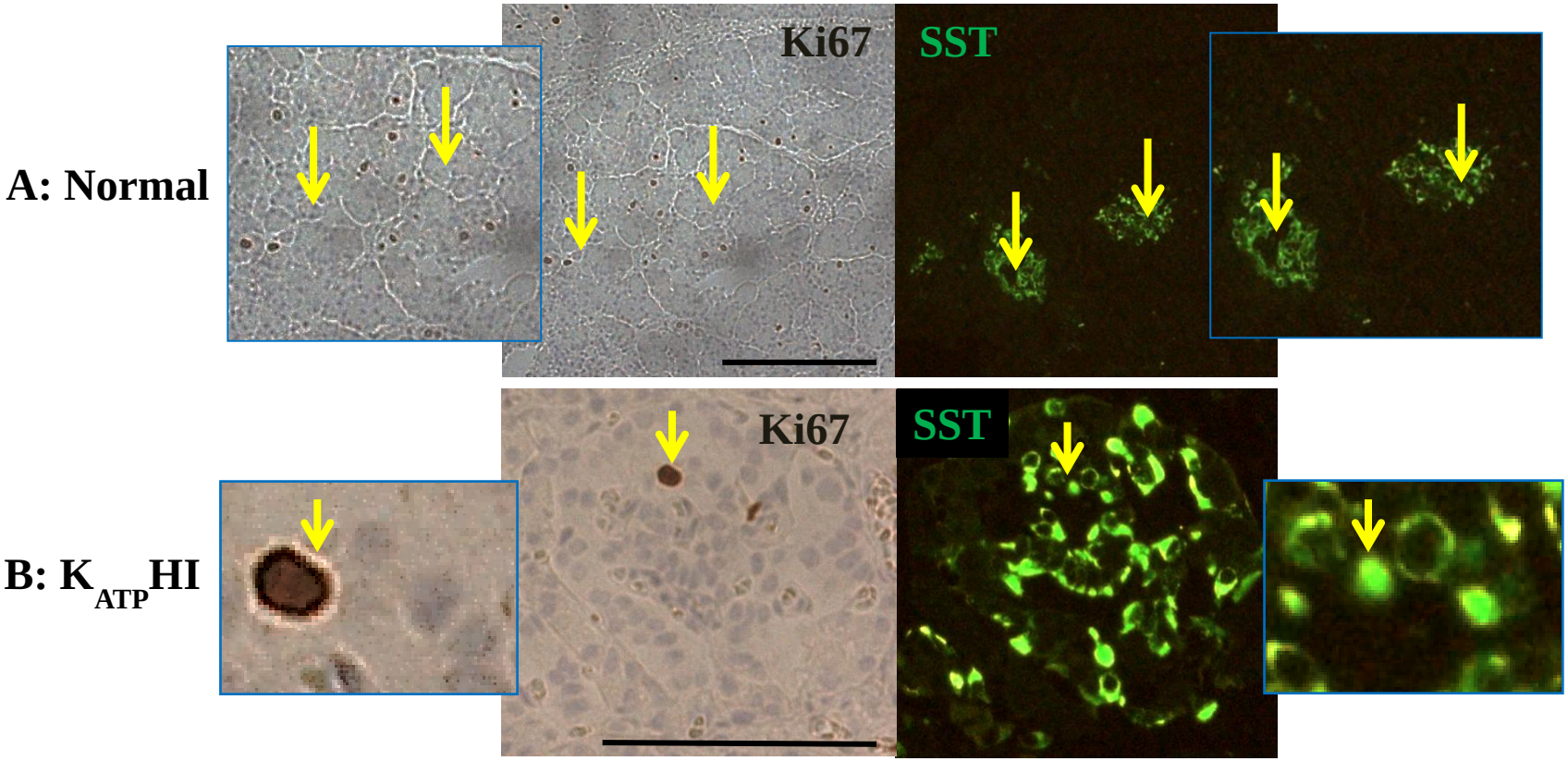

Figure 5.11: K_{ATP}HI promotes δ-cell proliferation. Representative immunostained sections of pancreas in (A) normal and (B) K_{ATP}HI using automated Leica stainer for Ki67 proliferation marker. Immunofluorescent staining for somatostatin in green. Yellow arrows indicate the islet cell nuclear staining positive for Ki67 staining (brown). Magnification x 20 and x 40. N = 3 subjects per group, 2 sections per subject. Reference line: 50 µm.

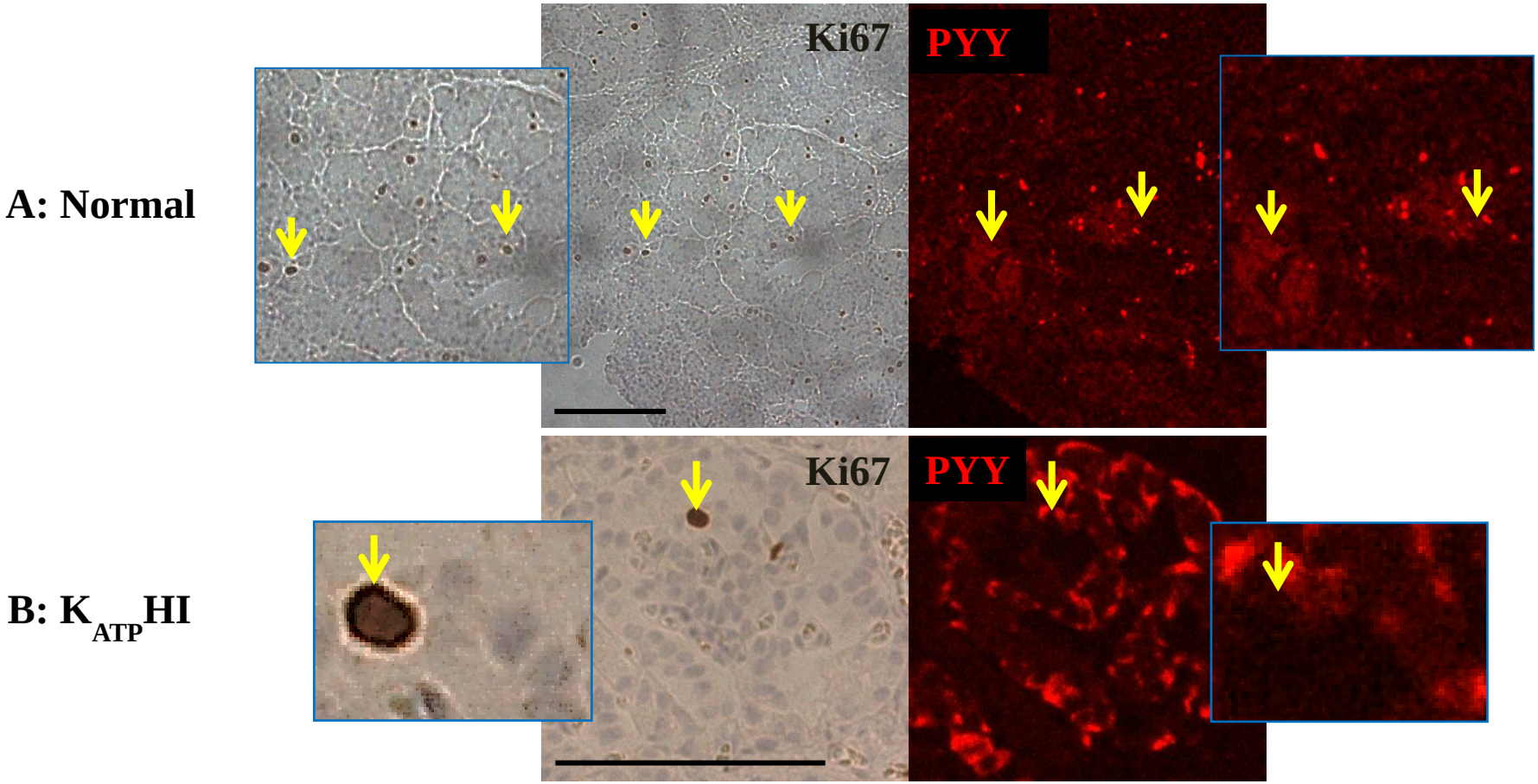

Figure 5.12: K_{ATP}HI does not promote PYY-positive cell proliferation. Representative immunostained sections of pancreas in (A) normal and (B) K_{ATP}HI using automated Leica stainer for Ki67 proliferation marker. Immunofluorescent staining for PYY in red. Yellow arrows represent the islet cell nuclear staining positive for Ki67 staining (brown). Red arrow represents Ki67+ islet cell nuclear staining. Magnification x 20 and x 40. N = 3 subjects per group, 2 sections per subject. Reference line: 50 µm.

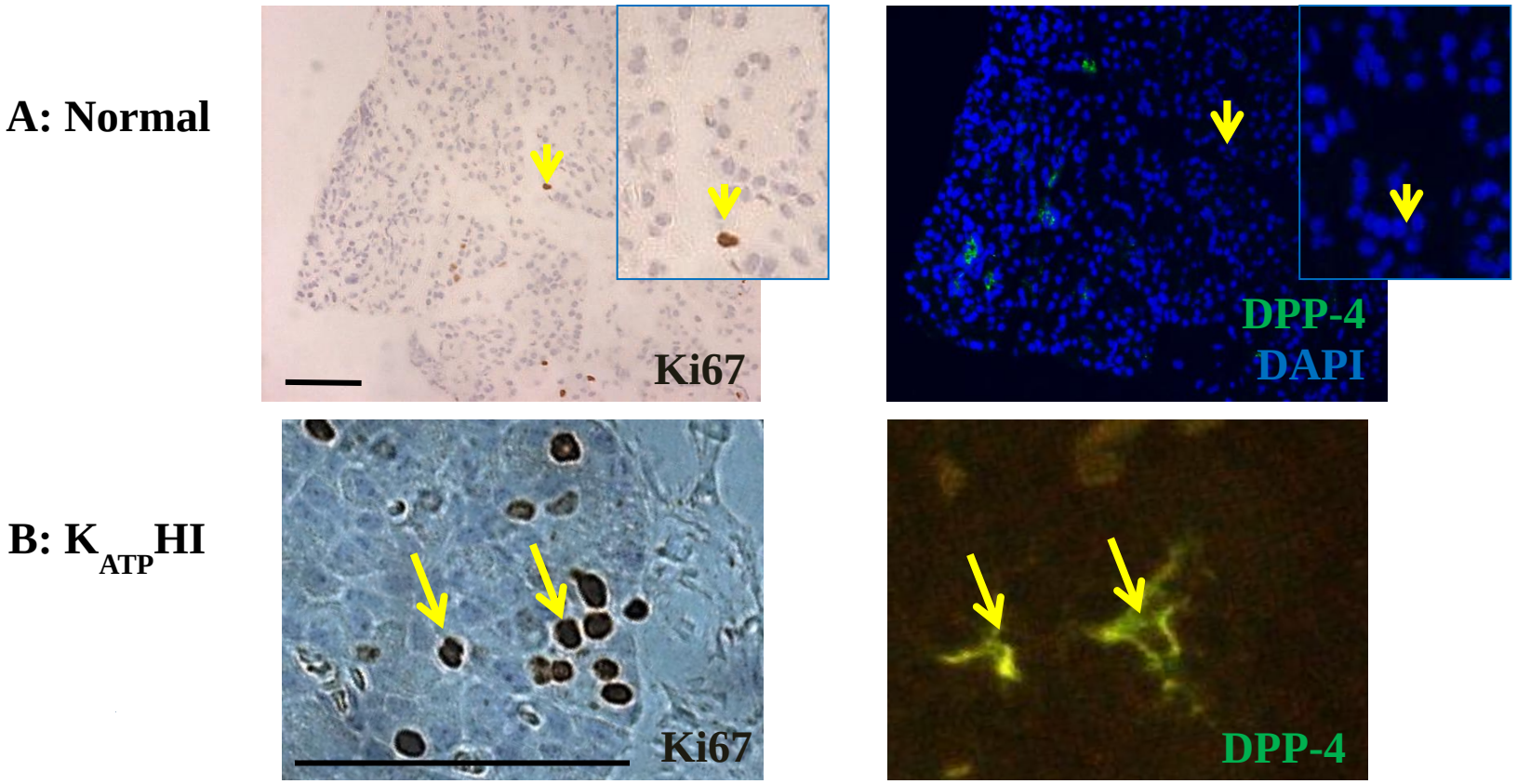

Figure 5.13: K_{ATP}HI causes DPP-4-cells to proliferate. Representative immunostained sections of pancreas in (A) normal and (B) K_{ATP}HI using automated Leica stainer for Ki67 proliferation marker. Immunofluorescent staining for DPP-4 in green. Yellow arrows represent the islet cell nuclear staining positive for Ki67 staining (brown). DAPI stains nuclei blue. Magnification x 20 & x 40. N = 3 subjects per group, 2 sections per subject. Reference line: 50 µm.

5.5.4. Changes in plasma gut hormone levels in patients with K_{ATP}HI.

Five patients were recruited for this study with consent obtained from parents/guardians. Since pancreatic *DPP-4* was significantly increased in K_{ATP}HI patients, we analysed the gut hormone substrates that may be affected.

5.5.4.1. Recruitment and biochemical characteristics of K_{ATP}HI patients

The age of the patients was 4.8 ± 1.6 weeks (mean ± SD) weeks and body weight 4.5 ± 0.6 kgs. The mean plasma insulin levels were 18.6 ± 8.6 mU/L at normoglycaemia and decreased to 10.9 ± 2.9 mU/L (p =0.289) at hypoglycaemia. Plasma glucose levels significantly decreased from 6.1 ± 1.0 to 2.4 ± 0.2 mmol/L (p =0.02) (Table 5.1).

5.5.4.2. Assessing circulating gut hormone levels in patients with K_{ATP}HI

Circulating gut hormone peptides were measured using commercially available assays and corrected for body weight. Circulating active PYY levels decreased from 223.7 ± 63.6 to 215.3 ± 52.1 pg/ml/kg (p =0.772) at hypoglycaemia from euglycaemia. Plasma levels of active GLP-1 insignificantly increased at hypoglycaemia (1.5 ± 0.5 to 0.8 ± 0.5 pM/kg (p =0.514). Total GIP levels fell from 28.1 ± 9.8 to 19.5 ± 7.4 pg/ml/kg (p =0.083) at hypoglycaemia (Figure 5.14).

5.5.4.3. Assessing correlations between circulating metabolites in patients with K_{ATP}HI at normoglycaemia and at hypoglycaemia

The difference between hypoglycaemia and baseline (normoglycaemia) were determined for each metabolite and then corrected for body weight. Correlation analysis was carried out using these values and relationship between plasma metabolites evaluated. No correlation existed amongst any of the metabolites except GLP-1 and PYY (Figure 5.15).

		Patient Information				
		AI	**DT**	**RD**	**JE**	**LA**
	Gestational weight at delivery	3.0kgs	4.5kgs	3.2kgs	4.3kgs	2.1kgs
	Age of presentation	Birth	Birth	Birth	Birth	Birth
	Current age (weeks)	2	2	2	8	5
	Histology	Diffuse	Diffuse	Transient HI	Diffuse	Unknown
	Genetics	Homozygous ABCC8 mutation	Maternal heterozygous ABCC8 mutation	ABCC8/KCJN11 mutation negative	Unknown-Awaiting results	ABCC8/KCJN11 mutation negative
	Sex	Male	Male	Male	Female	Female
	Weight	3.1kgs	4.5kgs	3.18kgs	5.6kgs	2.86kgs
	Treatment	Sirolimus, Octreotide Omeprazole, Domperidone Rantidine	Diazoxide Chlorothiazide 120ml/kg/day 25% dextrose	Continue to monitor annually	16mls/hr 40% dextrose	10ml/hr 30% dextrose
	Pre-screen preparation	Fasted 4 hours	Fasted 6 hours	Fasted 5.5hrs	Fasted 4 hours	Fasted 3.5 hours
Normal	**BM (mM)**	7.5	4.9	4.7	9.7	3.8
	Glucose (mM)	6.7	6.7	4.2	9.2	3.9
	Insulin (mU/L)	7.9	7.9	10.7	52.7	14
Hypo	**BM (mM)**	3.1	2.6	2.7	2.4	2.7
	Glucose (mM)	2.0	2.0	2.8	2.8	2.5
	Insulin (mU/L)	9.3	9.3	2.7	20.4	12.6
	NOTES	• Consanguineous parents • Diazoxide-unresponsive • Gastro-oesophageal reflux • Right Hydrocele	• Shoulder dystocia • Lethargic at birth • IV dextrose given at birth • Cardiac murmur: further investigation proved negative	• Polycythaemia at birth • Eventually diagnosed as transient HI	• Diazoxide-unresponsive	• Diazoxide-unresponsive • Gastro-oesophageal reflux: resolved • Cardiac murmur

Table 5.1: K_{ATP}HI patient details. Five patients presenting with K_{ATP}HI were recruited to the study and underwent a hypoglycaemia screen. Data presented from patient notes. *Hypo- hypoglycaemia.*

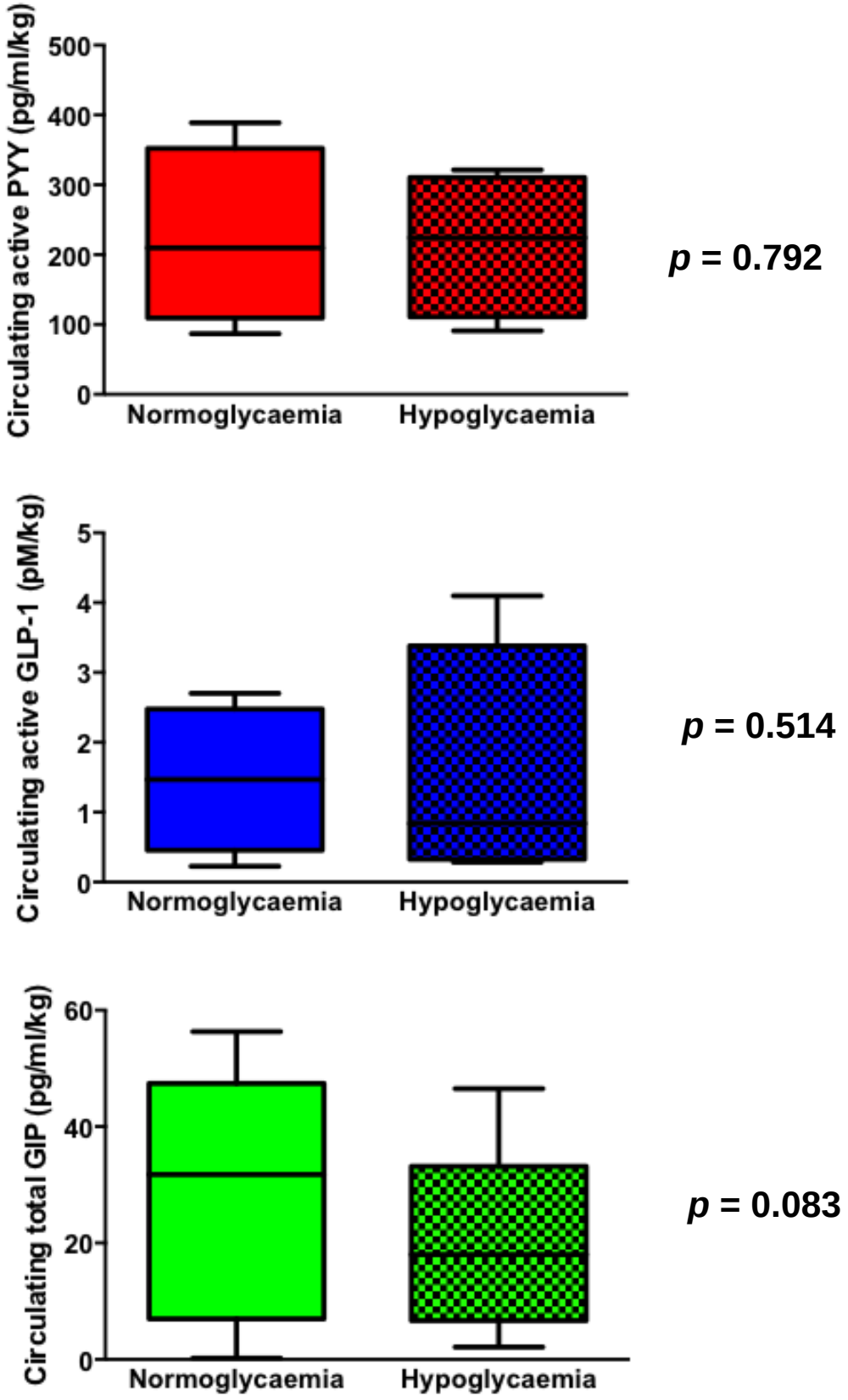

Figure 5.14: Assessment of circulating DPP-4-regulated gut hormones in patients with K_{ATP}HI. Box represents the interquartile range. Horizontal lines within boxes represent medians. Whiskers extend the range of gut hormone values and shown as ± SEM. N= 4-5 paired values.

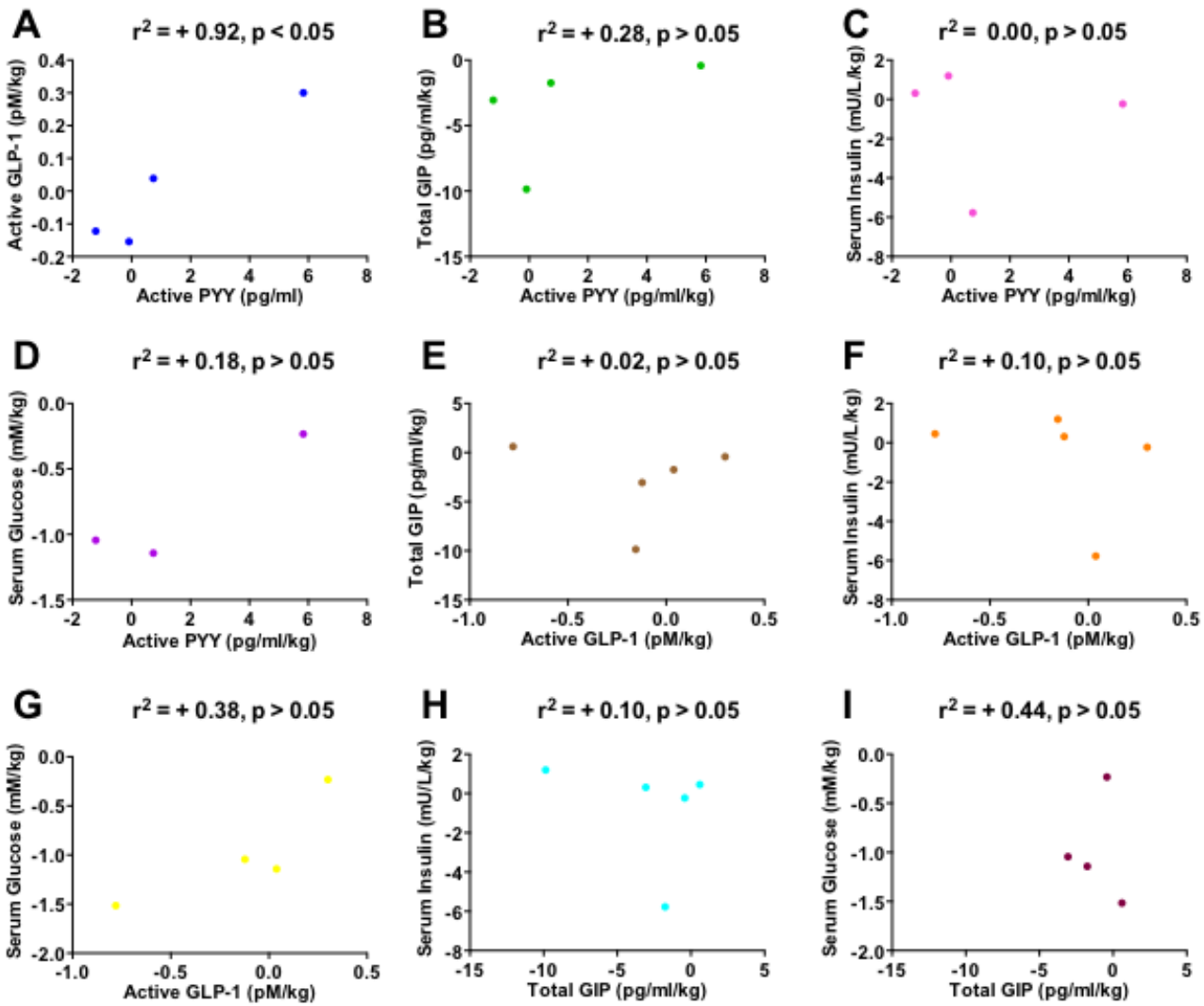

Figure 5.15: Correlation analysis between circulating metabolite levels in patients with K_{ATP}HI. Values taken from the difference between normoglycaemia and hypoglycaemic state. Correlating relationship between: PYY and (A) GLP-1 or (B) GIP or (C) insulin or (D) serum glucose. Correlating relationship between: GLP-1 and (E) GIP or (F) insulin or (G) serum glucose. Correlating relationship between: GIP and (H) insulin or (I) serum glucose. N= 3-5 paired values. R^2 = +1 represents positive correlation, r^2 = 0 represents no correlation, r^2 = -1 represents negative correlation. *P < 0.05* is deemed significant.

5.6. Summary

Chapter 5 reveals the significance of DPP-4 in mediating gut peptides in HH and potentially highlights an undervalued regulator of HI. Understanding the role of DPP-4 and its gut hormone substrate may aid in manipulating regulatory pathways in nesidioblastosis-induced HH. Overall, this data provides a mechanistic understanding of current drug treatments and the potential of therapeutic strategies in combating metabolic disorders.

5.6.1. mRNA analysis of pancreatic genes involved in energy and glucose homeostasis

Genes involved in appetite and glucose metabolism were analysed in pancreatic tissue of K_{ATP}HI and control subjects. Pancreatic *DPP-4* and *SST* gene expression were significantly up-regulated in K_{ATP}HI tissue with a trend for a reduction in *PYY* mRNA levels. These findings provide evidence of candidate genes involved in the pathology of K_{ATP}HI, which have not previously been shown.

5.6.2. PYY and DPP-4 localisation and expression in the healthy pancreas

Using IHC, PYY localisation was determined. Unlike the mouse, the healthy human pancreas largely expressed PYY to an unknown islet cell, with small amounts being expressed with glucagon in α-cells. PYY was absent from both β- and δ-cells as well as DPP-4 positive cells. On the other hand, in all tissue samples assessed, DPP-4 was expressed in the three islet cell-subtypes: α-, β- and δ-cells.

5.6.3. Changes in islet hormone expression of K_{ATP}HI patients

Islets from K_{ATP}HI tissue were assessed for morphological changes that may contribute to the islet phenotype. K_{ATP}HI resulted in more proliferative cellular nuclei of both endocrine and exocrine portions of the pancreas. Since Ki67 was markedly increased in K_{ATP}HI pancreatic tissue, we attempted to determine the identification of the islet-cell subtype that appeared to be proliferating in the endocrine areas. In K_{ATP}HI samples, β-, δ- and DPP-4 positive cells all

immunostained for Ki67. In contrast, α- and PYY positive cells were absent for the proliferating marker.

5.6.4. Role of gut hormones in K_{ATP}HI

Since DPP-4 mediates gut hormone action and the gene expression suggested the *DPP-4* is up-regulated, we assumed there was a possibility that circulating gut hormones may have changed as a result. Plasma PYY and GLP-1 both remained unchanged at hypoglycaemia, however, there was trend for a reduction in GIP levels. Correlation analysis unsurprisingly revealed a positive relationship between PYY and GLP-1. No other correlations existed between circulating metabolites analysed except between the co-localised active GLP-1 and active PYY.

5.6.5. Conclusion

Pancreatic *DPP-4, SST* and *PYY* genes as well as plasma GIP all appear to play a potential role in K_{ATP}HI. Moreover, DPP-4 regulates a number of gut hormones; PYY, GLP-1 and GIP and all of these hormones have been implicated to have role in glucose homeostasis, but limited data is available to suggest a role in K_{ATP}HI. The IHC reveals that DPP-4 positive cells are proliferating; hence all findings imply a role of DPP-4 activity in HH pathogenesis. This chapter provides the basis for further investigations into assessing the role of gut hormones in HH.

Chapter 6

Discussion and conclusions

6. Discussion

6.1. Chapter 3: Characterisation of the intra-islet PYY system

The hormones released from the enteroinsular axis play a key role in appetite control, glucose regulation and interact to regulate homeostasis of food intake and energy expenditure. These effects are known to be mediated through the action of gut hormones (Murphy and Bloom, 2006). One such gut hormone is PYY. PYY is secreted post-prandially from L-cells in the distal GI tract (Ballantyne, 2006). Enzymatic activity by DPP-4 changes the isoform from the full length protein; PYY 1-36 to PYY 3-36, and this truncated isoform has well known and established anorectic effects acting on the Y2R (Batterham et al., 2002, Batterham and Bloom, 2003, Batterham et al., 2006). However, PYY is also found to be expressed in the pancreatic islets of Langerhans with evidence suggesting a role of islet PYY in glucose homeostasis (Boey et al., 2006b, Boey et al., 2007, Sam et al., 2012, Shi et al., 2012, Zhang et al., 2012). But the physiological role and regulation of this population of islet PYY cells still remain largely unknown.

PYY exerts its action via the YRs; a group of GPCRs. PYY has been previously shown to inhibit insulin secretion *in vitro* (Bertrand et al., 1992). However, it is not known which receptor mediates this process. Hence, a murine islet isolation protocol was established (Liao, 2012). After the islet isolation protocol was optimized, *Yr* expression was confirmed by qRTPCR analysis. On investigation *Y4r* was confined to the exocrine pancreas since the expression of the receptor was present abundantly in pancreatic tissue but absent from islet RNA. The ratio of *Y4r*:*Y1r* expression was high in the whole pancreas possibly, due to the fact that endocrine islets account for only 1-2% of total pancreatic volume. The PP-preferential Y4R is known to have a role in exocrine secretion (Park et al., 1993), so it comes as no surprise that this receptor subtype is located in the pancreatic exocrine portion. However, currently no commercially available Y4R compounds exist so little is known of this receptor.

Unlike Chandarana et al., who found both *Y1r* and *Y4r* mRNA in the pancreatic endocrine tissues, we found *Y1r* as the only PYY receptor-subtype expressed in islets

in our studies (Chandarana et al., 2013). There is a possible difference in methods used. Whilst handpicking islets and dissociation of isolated islets from the exocrine tissue is difficult, we ensured we handpicked the islets three times, each time placing these into new dishes and washing to remove any unwanted exocrine debris that we found can pass through the cell strainers. This enabled us to pick islets clear of unwanted tissue. This could explain the difference between the two findings. Therefore it is possible that exocrine tissue attached to the islets was amplified and hence, the detections of the *Y4r* transcript by Chandarana and co-workers.

PYY 1-36-mediated reduction in insulin release is assumed to have been via the Y1R insolated murine islets, but this has not been confirmed to date (Sam et al., 2012, Chandarana et al., 2013). These findings are supported by the *in vivo* phenotype of the global *Y1r* KO mouse which displays a potentiation of GSIS with post-prandial HI (Burcelin et al., 2001). Similarly, NPY, an endogenous Y1R ligand has also been shown to inhibit GSIS, *in vitro*. *In vivo, Npy*$^{-/-}$ mice display enhanced nutrient-stimulated HI (Imai et al., 2007). Moreover, Morgan et al. reportedly removed NPY's GSIS inhibition by co-incubation with a Y1R antagonist, *in vitro* (Morgan et al., 1998). On the other hand, the PYY 3-36 isoform does not appear to produce a change to insulin secretion, *in vitro* or ß-cell content *in vivo* (Chandarana, 2009, Sam et al., 2012, Chandarana et al., 2013). This is further supported by the absence of *Y2r* gene expression (Chandarana et al., 2009, Chandarana et al., 2013) and suggests that islet PYY 1-36, Y1R and DPP-4 are important physiological regulators of glucose homeostasis. However, further work is required to establish if the deletion of islet *Pyy* will alter the expression of islet *Y1r* and *Dpp-4* mRNA. In addition, investigations into the use of Y1R compounds on insulin and other islet hormones, such as glucagon and somatostatin release need further exploration to understand if this effect is mediated directly or on a secondary basis.

To physiologically understand the islet PYY system, it was important to assess the anatomical distribution of PYY expressing cells within islets. Using IHC, we confirmed the absence of PYY from β-cells and found co-expression of PYY within a small population of glucagon in α-cells in WT mice (Upchurch et al., 1994, Myrsén-Axcrona et al., 1997). α- and β-cells both expressed DPP-4 on their cell-

surfaces this has previously not be shown (Poulsen et al., 1993, Grondin et al., 1999). Understandably, the enzyme that regulates PYYs activity on β-cells secretion will be located on PYY responsive cells. So far we have reported some novel observations; PYY was predominantly expressed with somatostatin in δ-cells. This cell population also appeared to be absent of DPP-4 expression. A second cell population stained abundantly for PYY and expresses DPP-4 in and on the cell-surface. However, the identification of this cell subtype requires further analysis. Perhaps the two PYY cell populations, i.e. the δ-cell PYY and the unidentified PYY positive cell which shows co-expression of DPP-4, suggests PYY may be an intracellular signalling molecule or that PYY may be regulated differently in the two islet-cells and potentially have different roles within the islet system.

PYY exerts its insulinotropic effects through its YRs and as previously demonstrated *Y1r* was the only receptor to be expressed in the isolated islets. If the effect of PYY on insulin secretion is direct than we would expect Y1R to be present on responsive cells. Consequently, we used IHC to localise Y1R expression on β-cells. The Y1R was expressed on insulin positive cells, however, due to antibody inefficiency, we were unable to assess if Y1R was expressed on any other islet-cell subtype. However, we were able to assess and find DPP-4 co-expression with Y1R. Physiologically, prolonging PYYs action on the β-cell via Y1R could be seen as detrimental; hence it is understandable that DPP-4 would ensure a rapid removal of PYY 1-36 effects on inhibiting insulin secretion. Y1R-immunostaining has been found on PYY-positive cells (Jackerott et al., 1996). Hence, it is possible that PYY is an autocrine regulator via the Y1R and thus, would explain the close proximity of DPP-4 to remove this effect.

The islet phenotype of the PYY transgenic mouse models; global *Pyy* KO and the *PdxPyy* null mouse were evaluated to shed light on the published *in vivo* and *in vitro* glucose phenotypes (Boey et al., 2006b, Chandarana, 2009). Initially, histological examination on both the transgenic mouse groups revealed hyperplasia in the islets of the *Pyy*- and *PdxPyy* null mice with respect to their controls. However, further work with the use of proliferating markers such as bromodeoxyuridine (BrdU) or Ki67 could confirm this and further characterise this phenotype.

Evaluation of the gene expression in the global *Pyy* mice was performed to shed light on the *in vivo* glucose phenotype reported (Boey et al., 2006b). No changes in pancreatic *Ins, Gcg* or *Sst* were found in the *Pyy* null mice in comparison to their littermate controls. Subsequently work analysing the pancreatic morphometry was carried out in both the *Pyy* and *PdxPyy* mice. Global and pancreatic-specific *Pyy* deletion led to a significant reduction in pancreatic α-cell area, an increase in δ-cell volume. However no changes were found in β-cell area in the pancreas of the KO mice of both groups compared to their respective controls. Work previously carried out by Upchurch and co-workers suggested a role for PYY in development and differentiation of specialised colonic enteroendocrine cells (Upchurch et. al, 1996). PYY has been identified as one of the earliest peptides to be detected during development. Additionally, they showed PYY co-expression in all the colonic cells prior to differentiation. Common precursor cells of the lower intestine were confirmed to all arise from a PYY-producing endocrine progenitor. However, once these cells differentiate they were rarely expressing PYY or dividing (Jackerott et al., 1996).

This PYY lineage relationship was also explored in the pancreatic endocrine cells (Upchurch et al., 1994, Myrsén-Axcrona et al., 1997, Liu et al., 2006). Here they examined the co-expression of PYY with different islet cell subtypes. It was revealed that embryonically, PYY co-expresses with all islet hormones including insulin as cell clusters. Eventually, the insulin positive cells differentiate from the PYY cells and remained like this post-natally and through adulthood. Both these findings led to the theory that PYY is a possible developmental differentiation endocrine regulator and are made up of one lineage branch. On the contrary, a study ablating *Pyy* found normal development of endocrine cells, yet this mouse model appeared to have also deleted the closely located *Pp* gene (Schonhoff et al., 2005). Sam et al. also deleted PYY cells in the adult mouse and this resulted in β-cell loss (Sam et al., 2012). This phenotype is rescued by a PYY1-36 analogue. Hence, it is suggests Y1R activation causes anti-apoptotic effects in ß-cells, which could be compensated for by islet NPY (Y1R ligand) in our mice. In addition, itt remains to be seen whether the targeting strategy used in Sam et al.'s mice may have destroyed gap junctions, which are known to be important in islet cell-cell communication (Rocheleau et al., 2006).

Additionally, both these reports fail to assess the impact of *Pyy* deletion on other islet hormones.

Limited data exist regarding the role of PYY on glucagon and somatostatin secretion. Bertrand et al. have produced data in which they showed no effect of PYY on glucagon secretion, *in vitro* (Bertrand et al., 1992). Though the data from this thesis could not confirm or disprove this, we did find PYY to regulate the α- and δ-cells, *ex vivo*. One possible explanation is that over time the islet isolation protocol has evolved and been manipulated to provide better islet yields and quality as shown in this chapter (Li et al., 2009, Liao, 2012). However it is essential to get high-quality islets and ensure reproducibility of isolation from mice. During evaluation of the islet isolation protocol, quality and yield of islets were found to be impacted by various conditions including the method of collagenase administration, the concentration of collagenase used, the temperature and the duration of digestion. Since both islet-cell subtypes are located on the mantle of the islet complexes it is possible that damage due to digestion by Bertrand and co-workers have led to the absence of the glucagon effect. Additionally, it is also plausible that PYY's effect in our mice is due to PYY's role in the development of other islet hormones as previously explained.

Since both *Pyy*- and *PdxPyy* KO mice have shown enhanced GSIS *in vivo*, it comes as a surprise that pancreatic *Ins* and β-cell area remain unaltered with respect to control mice. Moreover, the loss of α-cell mass in both *Pyy* transgenic KO mice may be the possible explanantion to the exaggerated GSIS phenotype, *in vivo*. In the glucose intolerant- HI state GLP-1R activity is retained but GIPR action is lost which jointly leads to a reduction in glucagon levels (Nauck et al., 1993). Conversely, T1DM; where the β-cells are destroyed by autoimmunity, lose their capability to synthesize endogenous insulin are also known to have post-prandial hyperglucagonaemia (Brown et al., 2008). These studies highlight a clear link between the deregulation of glucagon function and insulin signaling. Furthermore the increase in δ-cell area of both the *Pyy* and *PdxPyy* null mice implies that this could also be a reason for the difference in pancreatic glucagon expression. In support of this finding is the phenotype of the *Sst* KO mice which lose their glucose-

dependent suppression of glucagon release (Hauge-Evans et al., 2009). Hence, there is a possibility of an augmented somatostatin inhibition on glucagon seen in the global- and *Pdx- Pyy* KO mice and thus promotes a reduction in glucagon cell content. However, as yet, no studies have undertaken investigations into assessing the effects of various conditions on the secretion of islet PYY. Therefore, a novel PYY detection system requires setting up and optimisation to see whether PYY release could be measured, *in vitro*. In doing so, a study to understand and provide an insight into the intra-islet PYY system regulation can be devised and can eventually identify a novel pathway(s) that islet PYY regulates in a functional approach and to complement the data we have produced.

In light of all this evidence, it is possible that loss of PYY, and thus, its loss of function in developmental regulation may result in the changes of some insulinotropic inhibitory hormones (such as glucagon and somatostatin that it co-expresses with during postnatal differentiation). In addition, these hormones may contribute to the nutrient-stimulated HI, *in vivo* seen in the global *Pyy* KO mouse and the *PdxPyy* KO mouse (Boey et al., 2006b, Chandarana, 2009). Investigations using isolated islets from *Pyy* KO mice incubated with exogenous PYY would contribute to confirm if PYY affects somatostatin and/or glucagon release or synthesis to be measured by static incubation studies and qRTPCR. In doing this, novel mechanisms could be uncovered in the regulation of the intra-islet PYY system.

In conclusion, chapter 3 has provided the basis on which the intra-islet PYY system can be investigated further for a role in islet function. Islet DPP-4 also appears to be a major regulator in this system, possibly initiating the removal of insulin inhibition produced by PYY 1-36s action and converting it to the islet inactive form; PYY 3-36. The GSIS inhibition appears to be mediated at the Y1R located directly on the β-cells with DPP-4. Moreover, the *in vivo* data has revealed that deletion of the *Pyy* gene in the islets leads to an augmented GSIS by an indirect change in the insulin-inhibitory hormones; glucagon and somatostatin. More functional work is needed to understand how intra-islet PYY regulates pancreatic endocrine function. Finally, this chapter evidently supports the historical data of a possibility of PYY in regulating

the development and differentiation of other specialised islet cells and their hormone gene expression.

6.2. Chapter 4: Investigating the *in vivo* role of the intra-islet PYY in energy and glucose homeostasis.

Literature to date and the data produced in chapter 3 together demonstrate that PYY may have a role in islet function and thus glucose and energy control. Many studies have used transgenic models to understand the *in vivo* role of pancreatic PYY. However, they have failed to differentiate between the effects of gut and pancreatic PYY. In this thesis we generated data from the first pancreatic-specific *Pyy* KO mouse. Using this mouse model we were able to physiologically understand the specific role of islet PYY, *in vivo.*

To begin, we evaluated the feeding phenotype of the *PdxPyy* mice and found no difference in weekly cumulative food intake between the groups. The potential reason for this could be that our study was underpowered as the effect may be far too small to determine by the means we used. It has been suggested that the use of more mice is necessary to accurately measure food intake (Speakman, 2010). Further work using weight-matched controls or pair-feeding could provide a better way to understand if pancreatic PYY mediates feeding behaviour. Since this was not possible, we continued to investigate if changes in acute feeding patterns were present. We identified that the *PdxPyy* KO mice were eating less at a number of time points. Furthermore, *PdxPyy*$^{-/-}$ animals weighed less than their littermate controls, *in vivo*, in both the male and female groups. As a result, we hypothesised that a post-prandial factor was acutely being released that inhibited an orexigenic factor and given that *Pdx* deletes in the antrum of the stomach this may have reduced ghrelin. However, as *ghrelin* levels remained unchanged in the *PdxPyy* null animals it appears not to be the case. On the other hand, the factor could have promoted more satiation in the *PdxPyy* null group. It was therefore postulated that the factor(s) may be a pancreatic endocrine influence on the nutrient-stimulated insulin release, since gut hormone mRNA levels were unchanged in the KO group.

Apart from hypoglycaemia, sympathetic and parasympathetic nervous stimulation activates the α-cell granules to be released (Ahren et al., 1999) but there are limitations to the understanding of factors that influence α-cell secretion. PYY has

been found to be co-stored with glucagon in α-cell granules (Bottcher et al., 1989). Thus far it has been thought that these two peptides' activity on β-cell is in a paracrine manner (Nieuwenhuizen et al., 1994). PYY is reported to do this through the secondary GPCR messenger: cAMP. Therefore, PYYs inhibitory effect is reliant on the inhibition of both the production and effect of cAMP, independent of cytosolic Ca^{2+} (Nieuwenhuizen et al., 1994). Surprisingly, glucagon acts on β-cell GCGRs to stimulate tonic insulin release (Ahren et al., 1999). This dual inhibitory and stimulatory action by the α-cells to regulate insulin function is yet to be determined. On the other hand, in parallel to β-cells, δ-cell somatostatin release is also activated by glucose and parasympathetic nerve activation. Conversely, sympathetic stimulation leads to inhibition of somatostatin secretion (Ahren et al., 1999). Whilst somatostatin is known to inhibit insulin, islet somatostatin has been shown to inhibit intra-islet glucagon secretion via SSTR2, independently of its effects on insulin (Cejvan et al., 2003). Overall, the intra-islet system appears to work in a local (paracrine) fashion.

Alternatively, other changes may also arise from the gut. To assess if the *PdxPyy* deletion resulted in compensatory changes of duodenal CCK, mRNA levels were measured. *Cck* gene expression was unaltered in the fed state of the mouse lacking the *PdxPyy* gene. However, the expression may need confirming in the fasted state to confirm no compensatory changes by the *Pdx*-targeted strategy. Additionally, *Pyy* expression in the brainstem and GI tract was assessed to ensure that other areas were not counterbalancing the effects of the transgenesis. These PYY synthesis sites showed no alteration in gene expression but this requires further clarification in the fasted state and different time points since gut hormones are dynamic depending on feeding status. Finally, mRNA levels of other gut hormones known to have an effect in energy and glucose metabolism are known were assessed. Gut *ghrelin* and *enteroglucagon* expression were unchanged in the KO mice. In light of all this data it appears that the effect of the intra-islet *Pyy* deletion did not affect peripheral sites of PYY. Hence the observed changes were possibly due to alterations in local islet function. More research into examining the effects of pancreatic *Pyy* deletion on other islet hormones expression and plasma concentrations (such as PP involved in body weight regulation and glucose metabolism) are required.

Overall, our *in vivo* investigations found male mice to have a more pronounced difference in their phenotypes which was mostly absent in the female animals. Our studies concur with Boey et al.'s findings that reported gender differences in their studies (Boey et al., 2006b). Their male *Pyy* KO mice also exhibited a more pronounced phenotype. They attributed this result to an increased level of circulating testosterone. Moreover, other researchers have also found gender differences in studies when assessing PYY (Kim et al., 2005, Jackson et al., 2010, Wong et al., 2012). In particular, oestrogen is hypothesised to blunt Y1R activation in studies assessing hindlimb blood flow (Jackson et al., 2010). Since we were unable to determine if this was the case in our mice, we are unable to comment on whether the phenotypic differences were due to sex hormone differences. Further analysis could aid in confirming the findings of these reports.

As previously discussed, the *PdxPyy* KO mice displayed an exaggerated HI response to nutrient-stimulation *in vivo* and *in vitro* (Chandarana, 2009). This is similar to the reported phenotype of the *Pyy* KO mouse (Boey et al., 2006b). However, the *PdxPyy*$^{-/-}$ mice also show an increase in glucose disposal. These findings could be attributed to the elevated post-prandial plasma insulin concentrations found in the *PdxPyy* null mice. Insulin is known to act as an anorectic hormone, travelling to the hypothalamus and stimulating the inhibitory feeding centres (Gerozissis, 2004). In addition, high circulating insulin levels have been suggested to contribute to the promotion of leptin secretion from the adipose tissue. This would result in a reduction in body weight and adiposity which is the phenotype we observed in our mice (Barr et al., 1997). However, we were unable to measure leptin levels in either the plasma or white adipose tissue (WAT). Assessment into leptin concentrations of the *PdxPyy* mice would require investigation to confirm if leptin is involved in the body weight difference of the *PdxPyy* animals. In addition, differences in body weight composition could be assessed by echoMRI analysis of the animals. This would allow the identification of lean to fat mass ratio and provide the factor that is contributing to the differences in body weight. PYY overexpressing transgenic animals have been reported to show changes in hypothalamo-pituitary-somatotrophin (HPS) hormones and accordingly a theory was proposed that PYY may play a role in somatic growth (Boey et al., 2008). We therefore crudely assessed if changes in

somatic growth were contributing to differences in body weight. However, no change was found between groups in both male and female animals. To gain a better understanding for the role of PYY in growth, further work looking into circulating levels of IGF could be assessed. Another hypothesis is that the obese phenotype of the *Pyy* KO mouse was due to the deletion of the circulating anorectic isoform of PYY (PYY 3-36) (Batterham et al., 2006). This isoform is also known to activate the improvement in glucose tolerance by Y2R in the hepatoportal system (Chandarana et al., 2013a). Consequently, the loss of this bioactive circulating isoform causes obesity and glucose intolerance which is observed in the *Pyy* KO mice (Boey et al., 2006b, Batterham et al., 2006). To investigate this hypothesis, further work is required to assess the concentrations of peripheral PYY in the *PdxPyy* mice in the hepatoportal system.

In conclusion of chapter 4, differences in body weight phenotypes of the *Pyy*- and *PdxPyy* KO mice indicate towards a differential role of intra-islet PYY and gut-derived PYY in energy and glucose homeostasis. It appears like enteroendocrine PYY; islet PYY may mediate body weight and appetite effects. PYY deletion consequently promotes exaggerated post-prandial insulin release by the regulation of other pancreatic hormones in a paracrine manner. In light of these findings, islet PYY may be a marker which may act as an important surrogate to assess an individual's susceptibility to HI (Figure 6.1).

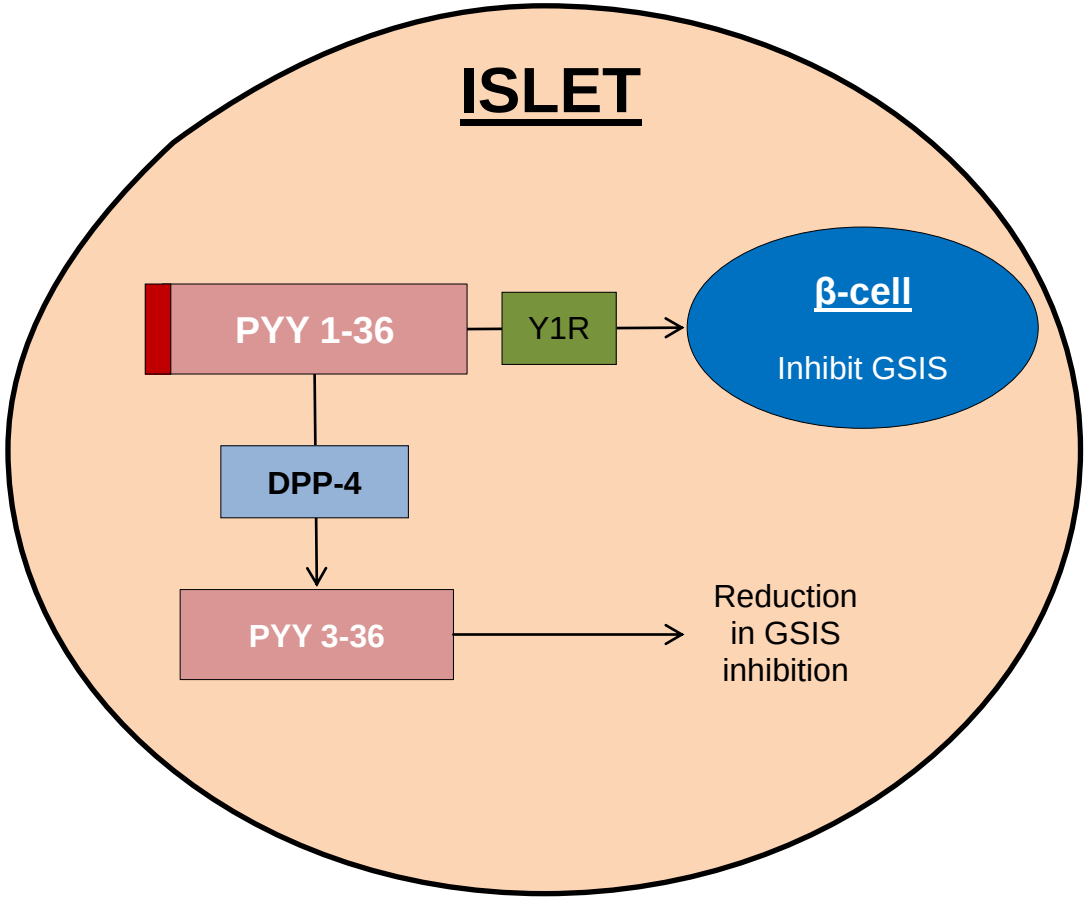

Figure 6.1: Potential regulatory pathways of the intra-islet PYY system. Intra-islet PYY 1-36 inhibits GSIS via the Y1R. DPP-4 changes the biological activity of PYY by converting it to an islet inactive isoform. Overall, this promotes a reduction in the inhibition of nutrient-stimulated insulin release.

6.3. Chapter 5: Characterising the role of gut hormones in hyperinsulinaemic hypoglycaemia

Whilst DPP-4 and its gut hormone substrates have been extensively researched in the past decade, the physiological roles of these regulators in glucose homeostatic processes are not fully understood. Traditionally it was viewed that congenital mutations in the genes that encoded for the K_{ATP} channel subunits caused most cases of HH. However, recently nesidioblastosis-induced HH has been reported in many cases as a complication of weight-loss GBP surgery. But it still remains elusive as to how the bypass procedure may cause physiological dysregulation of the pancreata and thus promotes hypoglycaemia (Service et al., 2005, Vella and Service, 2007, Singh and Vella, 2012). To our knowledge, apart from GLP-1s effects in HH, other DPP-4 gut hormones substrates have not yet been investigated or examined (De León et al., 2003, De Leon et al., 2008, Calabria et al., 2012). Hence studies in this thesis aimed to characterise a role for DPP-4 and its gut hormone substrates in HH to elucidate a role for these regulators in this condition.

The gene expression data from chapter 5 has shown there to be a potential role for pancreatic PYY in HI, since there was the trend for a reduction in pancreatic *PYY* from K_{ATP}HI tissue. Low levels of serum PYY have been previously found to be indicative of the predisposition to insulin resistance in first-degree relatives of T2DM persons (Boey et al., 2006a). However, this action appears to be mediated by gut PYY and not pancreatic PYY (Chandarana et al., 2013a). Hence, we measured plasma PYY levels to see if changes could be observed at hypoglycaemia, but no difference was found. This suggests two things; (1) pancreatic PYY has a role in HI independently of enteroendocrine PYY and (2) the reducing trend of pancreatic *PYY* mRNA seen in HH persons could be due to the increase in pancreatic *DPP-4* gene expression. This would in turn lead to a reduction in islet *PYY* and thus cause an overall decrease in Y1R-activated inhibition on GSIS. The lack of significance in the expression data may be potentially due to the study lacking statistical power. Nonetheless crucial roles for pancreatic PYY and DPP-4 have been identified in HH. To date a lack of research in identifying the localisation of pancreatic PYY or its regulatory enzyme in the human pancreas limits what is known about their role in

glucose metabolism since most work carried out to date has been focussed on animal models (Upchurch et al., 1994, Myrsén-Axcrona et al., 1997, Hinke et al., 2000, Schonhoff et al., 2005). Therefore, the distribution of PYY and DPP-4 expression in the pancreatic endocrine system was assessed in humans. PYY was found localised to the α-cells only (Boey et al., 2007). This finding could in part explain why there was probably an absence of a correlation/association between PYY and the metabolites analysed. On the other hand, GLP-1 is co-expressed with PYY in ileal L-cells; and thus explains the significant positive correlation when analysed in the study.

Subsequently, DPP-4 expression was evaluated in the control human tissue. DPP-4 immunoreactivity has been previously localised to porcine α-cells granules but as yet no other species have been assessed (Poulsen et al., 1993, Grondin et al., 1999). We therefore investigated and confirmed DPP-4 expression to the α-, β- and δ-cells in normal human pancreatic samples. Thereafter islet phenotyping of K_{ATP}HI samples were evaluated for an insight into the histological characteristics of the disease. As already known, K_{ATP}HI tissue samples have more proliferating pancreatic cells than the control tissue (Alexandrescu et al., 2010). Therefore, we identified the proliferating pancreatic endocrine cells as β-, δ- and DPP-4 positive cells. Given this result, it comes as no surprise that *DPP-4* mRNA was significantly increased in K_{ATP}HI patients.

Moreover, *SST* gene expression was also significantly increased in K_{ATP}HI persons which complements the IHC data. Currently, no reports have clearly substantiated a role for somatostatin dysfunction in the pathogenesis of HH. Treatment for the HH condition include the use of somatostatin mimetics (Yorifuji et al., 2013). However, the mechanism of somatostatin analogue action for the success in suppressing HI remains unknown. Interestingly, this result is similar to the global and *Pdx- Pyy* KO mouse islet phenotype discussed earlier in the thesis. Hypothetically, there is a possible link between pancreatic PYY and somatostatin in promoting HI. The proliferating δ-cells are in-line with the mRNA data that implicates K_{ATP}HI to induce an up-regulation of the *SST* gene and also confirms it as a likely regulator of HH. Nonetheless more detailed studies of somatostatin physiology are needed to unravel

its function in glucose metabolism. Overall, it appears that pancreatic somatostatin, PYY and DPP-4 all have a role in HH. However, to gain a better understanding further work is required.

DPP-4 rapidly inactivates the incretin gut hormones and terminates their biological function. Post-prandially, the incretins stimulate GSIS and *PROINS* gene transcription via their respective receptors located on β-cells (Baggio et al., 2000) and promote a change in plasma glucagon levels (Drucker, 2002). Principally GIP acts to induce glucose-dependent insulin release post-meal (Drucker, 2007). To unravel a glucoregulatory function of the incretins, investigations into GLP-1/R and GIP/R signalling in WT and transgenic mice have been carried out (Baggio et al., 2000). *Gipr* KO mice exhibit defective glucose clearance despite having normal fasting blood glucose and tolerance in response to an IPGTT, *in vivo* (Miyawaki et al., 1999). Additionally, GIPR blockade by antisera promotes hyperglycaemia also in the presence of normal fasting glucose (Baggio et al., 2000). Together all this data supports GIPs role as a glucose-dependent, classical 'incretin', which requires enteral stimulation to promote its glucoregulatory effects (Irwin et al., 2010). While GIP has been well-studied in its effects in T2DM, there is no data on its role in HH. Hence, we aimed at determining if a link existed. At hypoglycaemia (reducing i.v. dextrose) K_{ATP}HI subjects showed a trend for a reduction in plasma GIP levels. A possible explanation for this finding could be a result of reducing plasma glucose in absence of enteral stimulation. These two main factors are required for GIPs incretin response. Another explanation is HI may be caused by a reduction in the levels of plasma GIP which is seen in persons who have undergone weight-loss surgery (Guidone et al., 2006).

Medically-unresponsive HH persons require a pancreatectomy to prevent recurrent hypoglycaemia. However, complications of such invasive treatment include; (1) insulin-dependence and (2) reoccurrence of HH as a result of re-routing GI tract by the GBP procedure. Currently, there is no literature except case reports assessing how the GBP promotes recurrent HH and nesidioblastosis even after pancreatectomy (Qintar et al., 2012). Hence an understanding in how gut hormones regulate this glucose dysfunction needs further evaluation. On the other hand, a mouse model

displaying the features in the pathophysiology of K_{ATP}HI was constructed in 1996 (Scrocchi et al., 1996). In this mouse, the gene that encodes for the K_{ATP} subunit *Sur-1* was deleted and this resulted in mild fasting HH and post-prandial hyperglycaemia. From the data in chapter 5, we found that the topography of the human pancreas is dissimilar to the mouse (chapter 3). Hence, it is possible the pancreatic anatomical variation is the explanation for the differences in the hypoglycaemia phenotype of the *Sur-1* KO mice versus those seen in K_{ATP}HI subjects. Despite these differences, it is widely accepted that this model allows the development of an understanding of K_{ATP}HI pathophysiology. Using acetylcholine and GLP-1, Doliba and co-workers restored glucose-sensing in *Sur-1* KO islets, *in vitro* (Doliba et al., 2004). GLP-1 action in the hepatoportal system causes an increase glucose clearance by peripheral tissue independently of insulin action. This function appeared to require GLP-1R activation which is lost in *Glp-1r* KO mice and on the administration of exendin (9-39) (Chandarana et al., 2013a). Thus, GLP-1R signalling may therefore have a role in HH (Service et al., 2005).

For many years, rodent models have been employed to evaluate the capability of pancreatic regeneration (Bonner-Weir, 2000). In particular the partial pancreatectomy model (Ppx) has shown at 8 weeks post-surgery there is an induction to restore both endocrine and exocrine portions (42% of β-cell volume and 27% of total weight of sham-control mice) (Brockenbrough et al., 1988, Bonner-Weir et al., 1983). GLP-1 is known for its role in islet β-cell neogenesis, and regeneration (Drucker, 2007). But due to its rapid inactivation by DPP-4, GLP-1R has limited capacity. Hence, exendin-4 (a DPP-4 resistant, long acting GLP-1R agonist) was was used. Administration of exendin-4 for 10 days post-operatively in the Ppx mice resulted in an attenuation of Ppx-induced hyperglycaemia and promoted β-cell neogenesis and proliferation (Bonner-Weir et al., 1983, Brockenbrough et al., 1988, Xu et al., 1999, Bonner-Weir, 2000). On the other hand DPP-4 inhibitors do not appear to be involved in islet cell neogenesis. This has been shown in STZ-induced DM rats treated with DPP-4 inhibitors appear to show no reversal or improvement in pancreatic morphology (Pospisilik et al., 2003). Additionally, *Exendin-4* overexpressing mice have normal glucose tolerance thought to be a result of the down-regulation of endogenous GLP-1R (Baggio et al., 2000). To test this

hypothesis, *Glp-1r* KO were given a Ppx and at 5 weeks post-pancreatectomy, WT mice recovered from the Ppx-induced changes in glucose excursions (De León et al., 2003). However, this effect was absent in the transgenic Ppx group. Clearly this data demonstrates that under GLP-1/R action, pancreatic endocrine cells have the capacity to redevelop. Conversely, a truncated form of exendin-4; exendin (9-39) is a potent GLP-1R antagonist. A single injection of exendin (9-39) given to mice promoted a reduction in plasma insulin and an increase in fasting glucose levels (Baggio et al., 2000). With chronic administration, the effect continued without altering pancreatic insulin expression levels. This was one of the first studies identifying a role for GLP-1/R antagonism in the inhibition of HH.

Individually, GLP-1R and GIPR antagonism induce hyperglycaemia and potently reduce GSIS in the +/+ mouse (Baggio et al., 2000). Subsequent research has shown that GLP-1R agonists such as exendin-4 have fewer incidences of hypoglycaemic events since the drug works in line with the incretin effect and is currently prescribed for T2DM. On the other hand, GLP-1R antagonism has shown promise to increase blood glucose and lower GSIS (Baggio et al., 2000, De Leon et al., 2008, Calabria et al., 2012). It is therefore being researched for its capabilities in improving the effects of HH seen in patients with K_{ATP}HI and potentially other conditions that induced HH such as nesidioblastosis. STZ-induced islet destruction has also shown an increase in both islet and circulating GLP-1 levels; hypothetically this is as a response to counteract the islet damage (Nie et al., 2000). Treatment in these rodents with GLP-1 analogues has been shown to improve islet architecture and function (Drucker and Nauck, 2006). However, all these studies have failed to assess whether GIP (another hormone involved in β-cell function) may be involved in the observed effects. During HI, the K_{ATP}HI subjects appeared to show no change to circulating GLP-1 levels which confirms previous reports (De León et al., 2003). It could be plausible that GLP-1 concentrations in K_{ATP}HI patients at hypoglycaemia or on treatment with GLP-1R antagonist were potentially missed since measurements were made from systemic blood. As it appears that the hepatoportal system may have been the site to take for accurate GLP-1 measurements (Chandarana et al., 2013a).

In conclusion of chapter 5, we found proliferation of β- and δ-cells as well as the co-localised DPP-4 protein in K_{ATP}HI pancreatic tissues. These subjects also have an increase in pancreatic *DPP-4* potentially promoting a reducing trend for pancreatic *PYY* gene expression. Pancreatic reduction in *PYY* appears to mediate an increase in pancreatic *SST* mRNA as seen in the *PdxPyy* KO mice. Furthermore, it appears that a reduction in plasma GIP concentration (possibly due to a lack of glucose-mediated enteral stimulation) causes or exaggerates hypoglycaemia in K_{ATP}HI individuals.

6.4. Overall conclusion

It appears that the impact of PYY in the pancreas has been under-recognised. The full contribution of intra-islet PYY to the problem of obesity and/or diabetes is unknown but it may be substantial. Thus it is important to study and establish a role of pancreatic PYY in energy and glucose balance, independently of gut or brain PYY effects.

Hence, we constructed a *Pdx*-specific *Pyy* null mouse and studied it against its littermate controls and the global *Pyy* KO mice. Pancreatic deletion of *Pyy* led to abnormal islet-cell development and thus caused an indirect dysregulation of post-prandial insulin secretion. The loss of pancreatic *Pyy* results in alterations in the expression of other pancreatic hormones analysed. Both the transgenic *Pyy* mouse models analysed have post-prandial HI potentially due to changes in other islet hormones. The difference in body weight phenotypes and glucose disposal suggest a role of gut PYY in mediating a difference in appetite and energy expenditure. It is well-established that circulating PYYs anorectic action and glycaemia control is produced by the activity of truncated PYY 3-36 (Batterham et al., 2002, Batterham and Bloom, 2003, Batterham et al., 2003, Chandarana et al., 2013a). Hence, it is thought that the enzyme DPP-4 has the potential of improving the satiety and glucose tolerance effects. However, DPP-4 also appears to be a major regulator in this system, possibly initiating the removal of insulin inhibition produced by islet PYY 1-36 action. In conclusion to chapters 3 and 4, more work is needed to understand if DPP-4 inhibitor use may limit pharmacological therapeutic effectiveness and/or produce undesired side effects which are indicated by the current findings.

In summary of chapters 3 & 4, intra-islet PYY 1-36 appears to activate Y1R and mediate the inhibition of insulin secretion. Additionally pancreatic PYY demonstrates a role in the development of α- and δ-cells which also has the potential to indirectly regulate insulin release. Thus, *Pdx*- expressing PYY inhibition may be a target for weight-loss and improved glycaemic control.

Overall, chapter 5 suggests that hypoglycaemia may potentially be a result of changes in pancreatic insulinotropic genes which includes *DPP-4*, *PYY* and *SST*. Plasma GIP concentrations are lower in these persons. Thus there may be potential for GIPR-based compounds to be developed for the therapy of conditions that have hypoglycaemia. But further research is needed to develop a deeper understanding.

Overall, data collated from this thesis concludes that gut hormones play an important role in energy and glucose homeostasis.

References

References

ACCILI, D., DRAGO, J., LEE, E. J., JOHNSON, M. D., COOL, M. H., SALVATORE, P., ASICO, L. D., JOSE, P. A., TAYLOR, S. I. & WESTPHAL, H. 1996. Early neonatal death in mice homozygous for a null allele of the insulin receptor gene. *Nat Genet,* 12**,** 106-9.

AHREN, B., HOWELL, S. L. & BITTAR, E. E. 1999. *Potentiators and Inhibitors of Insulin Secretion. The Biology of the Pancreatic B-Cell : Advances in Molecular & Cell Biology. ed. Stamford, CT: Jai Press.,* Stamford, CT, Jai Press.

ALEXANDRESCU, S., TATEVIAN, N., OLUTOYE, O. & BROWN, R. E. 2010. Persistent hyperinsulinemic hypoglycemia of infancy: constitutive activation of the mTOR pathway with associated exocrine-islet transdifferentiation and therapeutic implications. *Int J Clin Exp Pathol,* 3**,** 691-705.

ALI-RACHEDI, A., VARNDELL, I. M., GAPP, D. A., VAN NOORDEN, S., ADRIAN, T. E., BLOOM, S. R. & POLAK, J. M. 1983. Peptide tyrosine (PYY) is co-stored with glucagon-related immunoreactants in endocrine cells of the gut and pancreas. *Regulatory Peptides,* 7**,** 272.

ALI, S., LAMONT, B. J., CHARRON, M. J. & DRUCKER, D. J. 2011. Dual elimination of the glucagon and GLP-1 receptors in mice reveals plasticity in the incretin axis. *J Clin Invest,* 121**,** 1917-29.

ARNES, L., HILL, J. T., GROSS, S., MAGNUSON, M. A. & SUSSEL, L. 2012. Ghrelin Expression in the Mouse Pancreas Defines a Unique Multipotent Progenitor Population. *PLoS One,* 7**,** e52026.

ARYA, V., SENNIAPPAN, S., GUEMES, M. & HUSSAIN, K. 2013. Neonatal Hypoglycemia. *The Indian Journal of Pediatrics***,** 1-8.

ASTRUP, A. & FINER, N. 2000. Redefining Type 2 diabetes: 'Diabesity' or 'Obesity Dependent Diabetes Mellitus'? *Obesity Reviews,* 1**,** 57-59.

BAGGIO, L., KIEFFER, T. J. & DRUCKER, D. J. 2000. Glucagon-Like Peptide-1, But Not Glucose-Dependent Insulinotropic Peptide, Regulates Fasting Glycemia and Nonenteral Glucose Clearance in Mice. *Endocrinology,* 141**,** 3703-3709.

BAGGIO, L. L. & DRUCKER, D. J. 2007. Biology of Incretins: GLP-1 and GIP. *Gastroenterology,* 132**,** 2131-2157.

BALLANTYNE, G. 2006a. Peptide YY(1-36) and Peptide YY(3-36): Part I. Distribution, Release and Actions. *Obesity Surgery,* 16**,** 651-658.

BALLANTYNE, G. H. 2006b. Peptide YY(1-36) and peptide YY(3-36): Part II. Changes after gastrointestinal surgery and bariatric surgery. *Obes Surg,* 16**,** 795-803.

BANKS, W. A., CLEVER, C. M. & FARRELL, C. L. 2000. Partial saturation and regional variation in the blood-to-brain transport of leptin in normal weight mice. *Am J Physiol Endocrinol Metab,* 278**,** E1158-65.

BARR, V. A., MALIDE, D., ZARNOWSKI, M. J., TAYLOR, S. I. & CUSHMAN, S. W. 1997. Insulin Stimulates Both Leptin Secretion and Production by Rat White Adipose Tissue. *Endocrinology,* 138**,** 4463-4472.

BATTERHAM, R. L. & BLOOM, S. R. 2003. The Gut Hormone Peptide YY Regulates Appetite. *Annals of the New York Academy of Sciences,* 994**,** 162-168.

BATTERHAM, R. L., COHEN, M. A., ELLIS, S. M., LE ROUX, C. W., WITHERS, D. J., FROST, G. S., GHATEI, M. A. & BLOOM, S. R. 2003. Inhibition of Food Intake in Obese Subjects by Peptide YY3–36. *New England Journal of Medicine,* 349**,** 941-948.

BATTERHAM, R. L., COWLEY, M. A., SMALL, C. J., HERZOG, H., COHEN, M. A., DAKIN, C. L., WREN, A. M., BRYNES, A. E., LOW, M. J., GHATEI, M. A., CONE, R. D. & BLOOM, S. R. 2002. Gut hormone PYY3-36 physiologically inhibits food intake. *Nature,* 418**,** 650-654.

BATTERHAM, R. L., FFYTCHE, D. H., ROSENTHAL, J. M., ZELAYA, F. O., BARKER, G. J., WITHERS, D. J. & WILLIAMS, S. C. R. 2007. PYY modulation of cortical and hypothalamic brain areas predicts feeding behaviour in humans. *Nature,* 450**,** 106-109.

BATTERHAM, R. L., HEFFRON, H., KAPOOR, S., CHIVERS, J. E., CHANDARANA, K., HERZOG, H., LE ROUX, C. W., THOMAS, E. L., BELL, J. D. & WITHERS, D. J. 2006. Critical role for peptide YY in protein-mediated satiation and body-weight regulation. *Cell Metabolism,* 4**,** 223-233.

Bayliss W, Starling EH (1902). "The mechanism of pancreatic secretion". *J. Physiol. (London)* 28: 325–353.

BELLINGER, L. L. & BERNARDIS, L. L. 2002. The dorsomedial hypothalamic nucleus and its role in ingestive behavior and body weight regulation: Lessons learned from lesioning studies. *Physiology & Behavior,* 76**,** 431-442.

BERTRAND, G., GROSS, R., ROYE, M., AHRKN, B. & RIBES, G. 1992. Evidence for a Direct Inhibitory Effect of PYY on Insulin Secretion in Rats. *Pancreas,* 7**,** 595-600.

BINGHAM, N. C., ANDERSON, K. K., REUTER, A. L., STALLINGS, N. R. & PARKER, K. L. 2008. Selective Loss of Leptin Receptors in the Ventromedial Hypothalamic Nucleus Results in Increased Adiposity and a Metabolic Syndrome. *Endocrinology,* 149**,** 2138-2148.

BOEY, D., HEILBRONN, L., SAINSBURY, A., LAYBUTT, R., KRIKETOS, A., HERZOG, H. & CAMPBELL, L. V. 2006a. Low serum PYY is linked to

insulin resistance in first-degree relatives of subjects with type 2 diabetes. *Neuropeptides,* 40**,** 317-324.

BOEY, D., LIN, S., ENRIQUEZ, R. F., LEE, N. J., SLACK, K., COUZENS, M., BALDOCK, P. A., HERZOG, H. & SAINSBURY, A. 2008. PYY transgenic mice are protected against diet-induced and genetic obesity. *Neuropeptides,* 42**,** 19-30.

BOEY, D., LIN, S., KARL, T., BALDOCK, P., LEE, N., ENRIQUEZ, R., COUZENS, M., SLACK, K., DALLMANN, R., SAINSBURY, A. & HERZOG, H. 2006b. Peptide YY ablation in mice leads to the development of hyperinsulinaemia and obesity. *Diabetologia,* 49**,** 1360-1370.

BOEY, D., SAINSBURY, A. & HERZOG, H. 2007. The role of peptide YY in regulating glucose homeostasis. *Peptides,* 28**,** 390-395.

BONNER-WEIR, S. 2000. Perspective: Postnatal pancreatic beta cell growth. *Endocrinology,* 141**,** 1926-9.

BONNER-WEIR, S., TRENT, D. F. & WEIR, G. C. 1983. Partial pancreatectomy in the rat and subsequent defect in glucose-induced insulin release. *The Journal of Clinical Investigation,* 71**,** 1544-1553.

BOTTCHER, G., AHREN, B., LUNDQUIST, I. & SUNDLER, F. 1989. Peptide YY: intrapancreatic localization and effects on insulin and glucagon secretion in the mouse. *Pancreas,* 4**,** 282-8.

BOTTCHER, G., SJOBERG, J., EKMAN, R., HAKANSON, R. & SUNDLER, F. 1993. Peptide YY in the mammalian pancreas: immunocytochemical localization and immunochemical characterization. *Regul Pept,* 43**,** 115-30.

BROCKENBROUGH, J. S., WEIR, G. C. & BONNER-WEIR, S. 1988. Discordance of Exocrine and Endocrine Growth After 90% Pancreatectomy in Rats. *Diabetes,* 37**,** 232-236.

BROWN, R. J., SINAII, N. & ROTHER, K. I. 2008. Too Much Glucagon, Too Little Insulin: Time course of pancreatic islet dysfunction in new-onset type 1 diabetes. *Diabetes Care,* 31**,** 1403-1404.

BRUNING, J. C., GAUTAM, D., BURKS, D. J., GILLETTE, J., SCHUBERT, M., ORBAN, P. C., KLEIN, R., KRONE, W., MULLER-WIELAND, D. & KAHN, C. R. 2000. Role of brain insulin receptor in control of body weight and reproduction. *Science,* 289**,** 2122-5.

BURCELIN, R., BRUNNER, H.-R., SEYDOUX, J., THORENSA, B. & PEDRAZZINI, T. 2001. Increased insulin concentrations and glucose storage in neuropeptide Y Y1 receptor-deficient mice. *Peptides,* 22**,** 421-427.

CALABRIA, A. C., LI, C., GALLAGHER, P. R., STANLEY, C. A. & DE LEÓN, D. D. 2012. GLP-1 Receptor Antagonist Exendin-(9-39) Elevates Fasting Blood Glucose Levels in Congenital Hyperinsulinism Owing to Inactivating Mutations in the ATP-Sensitive K+ Channel. *Diabetes,* 61**,** 2585-2591.

CALLE, E. E. & THUN, M. J. 2004. Obesity and cancer. *Oncogene,* 23**,** 6365-6378.

CEJVAN, K., COY, D. H. & EFENDIC, S. 2003. Intra-Islet Somatostatin Regulates Glucagon Release via Type 2 Somatostatin Receptors in Rats. *Diabetes,* 52**,** 1176-1181.

CHAMBERS, A. P., JESSEN, L., RYAN, K. K., SISLEY, S., WILSON-PEREZ, H. E., STEFATER, M. A., GAITONDE, S. G., SORRELL, J. E., TOURE, M., BERGER, J., D'ALESSIO, D. A., WOODS, S. C., SEELEY, R. J. & SANDOVAL, D. A. 2011. Weight-independent changes in blood glucose homeostasis after gastric bypass or vertical sleeve gastrectomy in rats. *Gastroenterology,* 141**,** 950-8.

CHANDARANA, K. & BATTERHAM, R. L. 2012. Shedding pounds after going under the knife : Metabolic insights from cutting the gut. *Nat Med,* 18**,** 668-669.

CHANDARANA, K., CANTLEY, J., HARROW, P.W., HERRERA, P.L., WITHERS D.J., AND BATTERHAM, R.L. 2009. Poster Discussion Sessions. *Journal of Diabetes,* 1**,** A33-A82.

CHANDARANA, K., GELEGEN, C., IRVINE, E. E., CHOUDHURY, A. I., AMOUYAL, C., ANDREELLI, F., WITHERS, D. J. & BATTERHAM, R. L. 2013. Peripheral activation of the Y2-receptor promotes secretion of GLP-1 and improves glucose tolerance. *Molecular Metabolism,* 2**,** 142-152.

CHANDARANA, K., GELEGEN, C., KARRA, E., CHOUDHURY, A. I., DREW, M. E., FAUVEAU, V., VIOLLET, B., ANDREELLI, F., WITHERS, D. J. & BATTERHAM, R. L. 2011. Diet and gastrointestinal bypass-induced weight loss: the roles of ghrelin and peptide YY. *Diabetes,* 60**,** 810-8.

CHEY, W. Y. & CHANG, T.-M. 2003. Secretin, 100 years later. *Journal of Gastroenterology,* 38**,** 1025-1035.

CHRISTESEN, H. B., TRIBBLE, N. D., MOLVEN, A., SIDDIQUI, J., SANDAL, T., BRUSGAARD, K., ELLARD, S., NJOLSTAD, P. R., ALM, J., BROCK JACOBSEN, B., HUSSAIN, K. & GLOYN, A. L. 2008. Activating glucokinase (GCK) mutations as a cause of medically responsive congenital hyperinsulinism: prevalence in children and characterisation of a novel GCK mutation. *Eur J Endocrinol,* 159**,** 27-34.

COLEMAN, D. L. 1978. Obese and diabetes: two mutant genes causing diabetes-obesity syndromes in mice. *Diabetologia,* 14**,** 141-8.

CORDOBA-CHACON, J., GAHETE, M. D., POZO-SALAS, A. I., CASTANO, J. P., KINEMAN, R. D. & LUQUE, R. M. 2013. Endogenous somatostatin is critical in regulating the acute effects of L-arginine on growth hormone and insulin release in mice. *Endocrinology,* 154**,** 2393-8.

CREUTZFELDT, W. 1979. The incretin concept today. *Diabetologia,* 16**,** 75-85.

CUMMINGS, D. E. 2005. Gastric Bypass and Nesidioblastosis — Too Much of a Good Thing for Islets? *New England Journal of Medicine,* 353**,** 300-302.

CUOMO, R., D'ALESSANDRO, A., ANDREOZZI, P., VOZ-ZELLA, L. & SARNELLI, G. 2011. Gastrointestinal regulation of food intake: do gut motility, enteric nerves and entero-hormones play together? *Minerva Endocrinol,* 36**,** 281-93.

DE LEÓN, D. D., DENG, S., MADANI, R., AHIMA, R. S., DRUCKER, D. J. & STOFFERS, D. A. 2003. Role of Endogenous Glucagon-Like Peptide-1 in Islet Regeneration After Partial Pancreatectomy. *Diabetes,* 52**,** 365-371.

DE LEON, D. D., LI, C., DELSON, M. I., MATSCHINSKY, F. M., STANLEY, C. A. & STOFFERS, D. A. 2008. Exendin-(9-39) corrects fasting hypoglycemia in SUR-1-/- mice by lowering cAMP in pancreatic beta-cells and inhibiting insulin secretion. *J Biol Chem,* 283**,** 25786-93.

DE LEON, D. D. & STANLEY, C. A. 2007. Mechanisms of Disease: advances in diagnosis and treatment of hyperinsulinism in neonates. *Nat Clin Pract End Met,* 3**,** 57-68.

DE SMET, B., DEPOORTERE, I., MOECHARS, D., SWENNEN, Q., MOREAUX, B., CRYNS, K., TACK, J., BUYSE, J., COULIE, B. & PEETERS, T. L. 2006. Energy homeostasis and gastric emptying in ghrelin knockout mice. *J Pharmacol Exp Ther,* 316**,** 431-9.

DEACON, C. F., NAUCK, M. A., MEIER, J., HUCKING, K. & HOLST, J. J. 2000. Degradation of endogenous and exogenous gastric inhibitory polypeptide in healthy and in type 2 diabetic subjects as revealed using a new assay for the intact peptide. *J Clin Endocrinol Metab,* 85**,** 3575-81.

DOLIBA, N. M., QIN, W., VATAMANIUK, M. Z., LI, C., ZELENT, D., NAJAFI, H., BUETTGER, C. W., COLLINS, H. W., CARR, R. D., MAGNUSON, M. A. & MATSCHINSKY, F. M. 2004. Restitution of defective glucose-stimulated insulin release of sulfonylurea type 1 receptor knockout mice by acetylcholine. *Am J Physiol Endocrinol Metab,* 286**,** E834-43.

DRUCKER, D. J. 2002. Gut adaptation and the glucagon-like peptides. *Gut,* 50**,** 428-435.

DRUCKER, D. J. 2007a. Dipeptidyl Peptidase-4 Inhibition and the Treatment of Type 2 Diabetes. *Diabetes Care,* 30**,** 1335-1343.

DRUCKER, D. J. 2007b. The role of gut hormones in glucose homeostasis. *J Clin Invest,* 117**,** 24-32.

DRUCKER, D. J. & NAUCK, M. A. 2006. The incretin system: glucagon-like peptide-1 receptor agonists and dipeptidyl peptidase-4 inhibitors in type 2 diabetes. *Lancet,* 368**,** 1696-705.

DUVILLIÉ, B., CORDONNIER, N., DELTOUR, L., DANDOY-DRON, F., ITIER, J.-M., MONTHIOUX, E., JAMI, J., JOSHI, R. L. & BUCCHINI, D. 1997.

Phenotypic alterations in insulin-deficient mutant mice. *Proceedings of the National Academy of Sciences,* 94**,** 5137-5140.

EKBLAD, E. & SUNDLER, F. 2002. Distribution of pancreatic polypeptide and peptide YY. *Peptides,* 23**,** 251-261.

ELAYAT, A. A., EL-NAGGAR, M. M. & TAHIR, M. 1995. An immunocytochemical and morphometric study of the rat pancreatic islets. *J Anat,* 186 (Pt 3)**,** 629-37.

ELFERS, C., RALSTON, M. & ROTH, C. L. 2011. Studies of different female rat models of hypothalamic obesity. *J Pediatr Endocrinol Metab,* 24**,** 131-7.

ELLINGSGAARD, H., HAUSELMANN, I., SCHULER, B., HABIB, A. M., BAGGIO, L. L., MEIER, D. T., EPPLER, E., BOUZAKRI, K., WUEEST, S., MULLER, Y. D., HANSEN, A. M. K., REINECKE, M., KONRAD, D., GASSMANN, M., REIMANN, F., HALBAN, P. A., GROMADA, J., DRUCKER, D. J., GRIBBLE, F. M., EHSES, J. A. & DONATH, M. Y. 2011. Interleukin-6 enhances insulin secretion by increasing glucagon-like peptide-1 secretion from L cells and alpha cells. *Nat Med,* 17**,** 1481-1489.

FLAMEZ, D., GILON, P., MOENS, K., VAN BREUSEGEM, A., DELMEIRE, D., SCROCCHI, L. A., HENQUIN, J. C., DRUCKER, D. J. & SCHUIT, F. 1999. Altered cAMP and Ca2+ signaling in mouse pancreatic islets with glucagon-like peptide-1 receptor null phenotype. *Diabetes,* 48**,** 1979-86.

FOURTNER, S. H., STANLEY, C. A. & KELLY, A. 2006. Protein-sensitive hypoglycemia without leucine sensitivity in hyperinsulinism caused by K(ATP) channel mutations. *J Pediatr,* 149**,** 47-52.

GAEDE, K., FERNER, H. & KASTRUP, H. 1950. [Second carbohydrate metabolism hormone of the pancreas (glucagon) and its origin in the alpha cells]. *Klin Wochenschr,* 28**,** 388-93.

GAO, F. & HU, X. F. 2006. Effect of somatostatin analogue octreotide injected into the third cerebral ventricle on pentagastrin-induced gastric acid secretion in rats. *World J Gastroenterol,* 12**,** 2767-9.

GELEGEN, C., CHANDARANA, K., CHOUDHURY, A. I., AL-QASSAB, H., EVANS, I. M., IRVINE, E. E., HYDE, C. B., CLARET, M., ANDREELLI, F., SLOAN, S. E., LEITER, A. B., WITHERS, D. J. & BATTERHAM, R. L. 2012. Regulation of hindbrain Pyy expression by acute food deprivation, prolonged caloric restriction and weight-loss surgery in mice. *American Journal of Physiology - Endocrinology And Metabolism*.

GELLING, R. W., DU, X. Q., DICHMANN, D. S., ROMER, J., HUANG, H., CUI, L., OBICI, S., TANG, B., HOLST, J. J., FLEDELIUS, C., JOHANSEN, P. B., ROSSETTI, L., JELICKS, L. A., SERUP, P., NISHIMURA, E. & CHARRON, M. J. 2003. Lower blood glucose, hyperglucagonemia, and pancreatic alpha cell hyperplasia in glucagon receptor knockout mice. *Proc Natl Acad Sci U S A,* 100**,** 1438-43.

GEROZISSIS, K. 2004. Brain insulin and feeding: a bi-directional communication. *European Journal of Pharmacology,* 490**,** 59-70.

GLAVAS, M. M., GRAYSON, B. E., ALLEN, S. E., COPP, D. R., SMITH, M. S., COWLEY, M. A. & GROVE, K. L. 2008. Characterization of brainstem peptide YY (PYY) neurons. *The Journal of Comparative Neurology,* 506**,** 194-210.

GONZÁLEZ-BARROSO, M. M., GIURGEA, I., BOUILLAUD, F., ANEDDA, A., BELLANNÉ-CHANTELOT, C., HUBERT, L., DE KEYZER, Y., DE LONLAY, P. & RICQUIER, D. 2008. Mutations in UCP2 in Congenital Hyperinsulinism Reveal a Role for Regulation of Insulin Secretion. *PLoS ONE,* 3**,** e3850.

GRANATA, R., SETTANNI, F., BIANCONE, L., TROVATO, L., NANO, R., BERTUZZI, F., DESTEFANIS, S., ANNUNZIATA, M., MARTINETTI, M., CATAPANO, F., GHÈ, C., ISGAARD, J., PAPOTTI, M., GHIGO, E. & MUCCIOLI, G. 2007. Acylated and Unacylated Ghrelin Promote Proliferation and Inhibit Apoptosis of Pancreatic β-Cells and Human Islets: Involvement of 3′,5′-Cyclic Adenosine Monophosphate/Protein Kinase A, Extracellular Signal-Regulated Kinase 1/2, and Phosphatidyl Inositol 3-Kinase/Akt Signaling. *Endocrinology,* 148**,** 512-529.

GRANDT, D., TEYSSEN, S., SCHIMICZEK, M., REEVE JR, J. R., FETH, F., RASCHER, W., HIRCHE, H., SINGER, M. V., LAYER, P., GOEBELL, H., HO, F. J. & EYSSELEIN, V. E. 1992. Novel generation of hormone receptor specificity by amino terminal processing of peptide YY. *Biochemical and Biophysical Research Communications,* 186**,** 1299-1306.

GREEN, B. D., GAULT, V. A., O'HARTE F, P. & FLATT, P. R. 2004. Structurally modified analogues of glucagon-like peptide-1 (GLP-1) and glucose-dependent insulinotropic polypeptide (GIP) as future antidiabetic agents. *Curr Pharm Des,* 10**,** 3651-62.

GREEN, E. D., MAFFEI, M., BRADEN, V. V., PROENCA, R., DESILVA, U., ZHANG, Y., CHUA, S. C., JR., LEIBEL, R. L., WEISSENBACH, J. & FRIEDMAN, J. M. 1995. The human obese (OB) gene: RNA expression pattern and mapping on the physical, cytogenetic, and genetic maps of chromosome 7. *Genome Res,* 5**,** 5-12.

GRILL, H. J. & KAPLAN, J. M. 2002. The Neuroanatomical Axis for Control of Energy Balance. *Frontiers in Neuroendocrinology,* 23**,** 2-40.

GRONDIN, G., HOOPER, N. M. & LEBEL, D. 1999. Specific Localization of Membrane Dipeptidase and Dipeptidyl Peptidase IV in Secretion Granules of Two Different Pancreatic Islet Cells. *Journal of Histochemistry & Cytochemistry,* 47**,** 489-497.

GUIDONE, C., MANCO, M., VALERA-MORA, E., IACONELLI, A., GNIULI, D., MARI, A., NANNI, G., CASTAGNETO, M., CALVANI, M. &

MINGRONE, G. 2006. Mechanisms of recovery from type 2 diabetes after malabsorptive bariatric surgery. *Diabetes,* 55**,** 2025-31.

HANSEN, L., DEACON, C. F., ØRSKOV, C. & HOLST, J. J. 1999. Glucagon-Like Peptide-1-(7–36)Amide Is Transformed to Glucagon-Like Peptide-1-(9–36)Amide by Dipeptidyl Peptidase IV in the Capillaries Supplying the L Cells of the Porcine Intestine. *Endocrinology,* 140**,** 5356-5363.

HARROLD, J. A. 2004. Hypothalamic control of energy balance. *Curr Drug Targets,* 5**,** 207-19.

HASLAM, D. 2010. Obesity and diabetes: the links and common approaches. . *Prim Care Diabetes,* 4 105 -112

HAUGE-EVANS, A. C., KING, A. J., CARMIGNAC, D., RICHARDSON, C. C., ROBINSON, I. C., LOW, M. J., CHRISTIE, M. R., PERSAUD, S. J. & JONES, P. M. 2009a. Somatostatin secreted by islet delta-cells fulfills multiple roles as a paracrine regulator of islet function. *Diabetes,* 58**,** 403-11.

HAUGE-EVANS, A. C., KING, A. J., CARMIGNAC, D., RICHARDSON, C. C., ROBINSON, I. C. A. F., LOW, M. J., CHRISTIE, M. R., PERSAUD, S. J. & JONES, P. M. 2009b. Somatostatin Secreted by Islet δ-Cells Fulfills Multiple Roles as a Paracrine Regulator of Islet Function. *Diabetes,* 58**,** 403-411.

HERRERA, P. L. 2000. Adult insulin- and glucagon-producing cells differentiate from two independent cell lineages. *Development,* 127**,** 2317-2322.

HETHERINGTON, A. W. & RANSON, S. W. 1940. Hypothalamic lesions and adiposity in the rat. *The Anatomical Record,* 78**,** 149-172.

HILL, J. O., WYATT, H. R., REED, G. W. & PETERS, J. C. 2003. Obesity and the Environment: Where Do We Go from Here? *Science,* 299**,** 853-855.

HINKE, S. A., POSPISILIK, J. A., DEMUTH, H. U., MANNHART, S., KUHN-WACHE, K., HOFFMANN, T., NISHIMURA, E., PEDERSON, R. A. & MCINTOSH, C. H. 2000. Dipeptidyl peptidase IV (DPIV/CD26) degradation of glucagon. Characterization of glucagon degradation products and DPIV-resistant analogs. *J Biol Chem,* 275**,** 3827-34.

HIRST, B. H. 2004. Secretin and the exposition of hormonal control. *J Physiol,* 560**,** 339.

HUE, L. 1982. [Hormonal control of liver gluconeogenesis]. *Rev Can Biol Exp,* 41**,** 73-6.

HUSSAIN, K. 2011. Investigations for neonatal hypoglycaemia. *Clinical Biochemistry,* 44**,** 465-466.

IMAI, Y., PATEL, H. R., HAWKINS, E. J., DOLIBA, N. M., MATSCHINSKY, F. M. & AHIMA, R. S. 2007. Insulin Secretion Is Increased in Pancreatic Islets of Neuropeptide Y-Deficient Mice. *Endocrinology,* 148**,** 5716-5723.

INAGAKI, N., GONOI, T., CLEMENT, J. P. T., NAMBA, N., INAZAWA, J., GONZALEZ, G., AGUILAR-BRYAN, L., SEINO, S. & BRYAN, J. 1995. Reconstitution of IKATP: an inward rectifier subunit plus the sulfonylurea receptor. *Science,* 270**,** 1166-70.

IRWIN, N. & FLATT, P. R. 2009. Therapeutic potential for GIP receptor agonists and antagonists. *Best Practice & Research Clinical Endocrinology & Metabolism,* 23**,** 499-512.

IRWIN, N., GAULT, V. & FLATT, P. R. 2010. Therapeutic potential of the original incretin hormone glucose-dependent insulinotropic polypeptide: diabetes, obesity, osteoporosis and Alzheimer's disease? *Expert Opin Investig Drugs,* 19**,** 1039-48.

JABRI, A. L. & BAYARD, C. 2004. Nesidioblastosis associated with hyperinsulinemic hypoglycemia in adults: review of the literature. *Eur J Intern Med,* 15**,** 407-410.

JACKEROTT, M., OSTER, A. & LARSSON, L. I. 1996. PYY in developing murine islet cells: comparisons to development of islet hormones, NPY, and BrdU incorporation. *Journal of Histochemistry & Cytochemistry,* 44**,** 809-17.

JACKSON, D. N., ELLIS, C. G. & SHOEMAKER, J. K. 2010. Estrogen modulates the contribution of neuropeptide Y to baseline hindlimb blood flow control in female Sprague-Dawley rats. *American Journal of Physiology - Regulatory, Integrative and Comparative Physiology,* 298**,** R1351-R1357.

JAMES, C., KAPOOR, R. R., ISMAIL, D. & HUSSAIN, K. 2009. The genetic basis of congenital hyperinsulinism. *Journal of medical genetics,* 46**,** 289-299.

JIANG, G. & ZHANG, B. B. 2003. Glucagon and regulation of glucose metabolism. *Am J Physiol Endocrinol Metab,* 284**,** E671-8.

JOHNSON, D. G., GOEBEL, C. U., HRUBY, V. J., BREGMAN, M. D. & TRIVEDI, D. 1982. Hyperglycemia of diabetic rats decreased by a glucagon receptor antagonist. *Science,* 215**,** 1115-6.

JOSHI, R. L., LAMOTHE, B., CORDONNIER, N., MESBAH, K., MONTHIOUX, E., JAMI, J. & BUCCHINI, D. 1996. Targeted disruption of the insulin receptor gene in the mouse results in neonatal lethality. *Embo j,* 15**,** 1542-7.

KAPOOR, R. R., HESLEGRAVE, A. & HUSSAIN, K. 2010. Congenital hyperinsulinism due to mutations in HNF4A and HADH. *Rev Endocr Metab Disord,* 11**,** 185-91.

KARCZ-SOCHA, I., ZWIRSKA-KORCZALA, K., ZEMBALA, M., BORGIEL-MAREK, H. & KARCZ, W. K. 2011. Ghrelin PYY 3-36 Serum Changes in Left Ventricular Hypertrophic, Insulin-Resistant, Hypertensive Obese Patients. *Obesity Facts,* 4**,** 386-392.

KARLSSON, S. & AHREN, B. 1996. A role for islet peptide YY in the regulation of insulin secretion. *Acta Physiologica Scandinavica,* 157**,** 305-306.

KARRA, E., CHANDARANA, K. & BATTERHAM, R. L. 2009. The role of peptide YY in appetite regulation and obesity. *Journal of Physiology-London,* 587**,** 19-25.

KEIRE, D. A., BOWERS, C. W., SOLOMON, T. E. & REEVE, J. R. 2002. Structure and receptor binding of PYY analogs. *Peptides,* 23**,** 305-321.

KIM, B.-J., CARLSON, O. D., JANG, H.-J., ELAHI, D., BERRY, C. & EGAN, J. M. 2005. Peptide YY Is Secreted after Oral Glucose Administration in a Gender-Specific Manner. *Journal of Clinical Endocrinology & Metabolism,* 90**,** 6665-6671.

KING, B. M. 2006. The rise, fall, and resurrection of the ventromedial hypothalamus in the regulation of feeding behavior and body weight. *Physiology & Behavior,* 87**,** 221-244.

KREYMANN, B., GHATEI, M. A., DOMIN, J., KANSE, S. & BLOOM, S. R. 1991. Developmental patterns of glucagon-like peptide-1-(7-36) amide and peptide-YY in rat pancreas and gut. *Endocrinology,* 129**,** 1001-5.

LAMONT, B. J., LI, Y., KWAN, E., BROWN, T. J., GAISANO, H. & DRUCKER, D. J. 2012. Pancreatic GLP-1 receptor activation is sufficient for incretin control of glucose metabolism in mice. *J Clin Invest,* 122**,** 388-402.

LARSSON, H. & AHREN, B. 2000. Glucose intolerance is predicted by low insulin secretion and high glucagon secretion: outcome of a prospective study in postmenopausal Caucasian women. *Diabetologia,* 43**,** 194-202.

LE ROUX, C. W., AYLWIN, S. J., BATTERHAM, R. L., BORG, C. M., COYLE, F., PRASAD, V., SHUREY, S., GHATEI, M. A., PATEL, A. G. & BLOOM, S. R. 2006. Gut hormone profiles following bariatric surgery favor an anorectic state, facilitate weight loss, and improve metabolic parameters. *Ann Surg,* 243**,** 108-14.

LE ROUX, C. W. & BLOOM, S. R. 2005. Peptide YY, appetite and food intake. *Proc Nutr Soc,* 64**,** 213-6.

LI, D.-S., YUAN, Y.-H., TU, H.-J., LIANG, Q.-L. & DAI, L.-J. 2009. A protocol for islet isolation from mouse pancreas. *Nat. Protocols,* 4**,** 1649-1652.

LIAO, Y.-T. M. J., JING-XING MS; YE, JIAN MS; QI, HUI MS; LI, FU-RONG 2012. A Novel Protocol for Mouse Islet Isolation.[Letter]. *Pancreas,* 41**,** 1134-1135.

LIU, C. D., NEWTON, T. R., ZINNER, M. J., ASHLEY, S. W. & MCFADDEN, D. W. 1997. Intraluminal peptide YY induces colonic absorption in vivo. *Diseases of the Colon & Rectum,* 40**,** 478-482.

LIU, G., ARNAUD-DABERNAT, S., KRITZIK, M., KAYALI, A., ZHANG, Y.-Q. & SARVETNICK, N. 2006. PYY in the expanding pancreatic epithelium. *Endocrine,* 30**,** 103-112.

MARSH, D. J., HOLLOPETER, G., KAFER, K. E. & PALMITER, R. D. 1998. Role of the Y5 neuropeptide Y receptor in feeding and obesity. *Nat Med,* 4**,** 718-21.

MARSK, R., JONAS, E., RASMUSSEN, F. & NASLUND, E. 2010. Nationwide cohort study of post-gastric bypass hypoglycaemia including 5,040 patients undergoing surgery for obesity in 1986-2006 in Sweden. *Diabetologia,* 53**,** 2307-11.

MCCLENAGHAN, N. H., FLATT, P. R. & BALL, A. J. 2006. Actions of glucagon-like peptide-1 on KATP channel-dependent and -independent effects of glucose, sulphonylureas and nateglinide. *J Endocrinol,* 190**,** 889-96.

MICHAEL CONLON, J. 2002. The origin and evolution of peptide YY (PYY) and pancreatic polypeptide (PP). *Peptides,* 23**,** 269-278.

MICHEL, M. C., BECK-SICKINGER, A., COX, H., DOODS, H. N., HERZOG, H., LARHAMMAR, D., QUIRION, R., SCHWARTZ, T. & WESTFALL, T. 1998. XVI. International Union of Pharmacology recommendations for the nomenclature of neuropeptide Y, peptide YY, and pancreatic polypeptide receptors. *Pharmacol Rev,* 50**,** 143-50.

MIHOLIC, J., ORSKOV, C., HOLST, J. J., KOTZERKE, J. & MEYER, H. J. 1991. Emptying of the gastric substitute, glucagon-like peptide-1 (GLP-1), and reactive hypoglycemia after total gastrectomy. *Dig Dis Sci,* 36**,** 1361-70.

MIYAWAKI, K., YAMADA, Y., YANO, H., NIWA, H., BAN, N., IHARA, Y., KUBOTA, A., FUJIMOTO, S., KAJIKAWA, M., KUROE, A., TSUDA, K., HASHIMOTO, H., YAMASHITA, T., JOMORI, T., TASHIRO, F., MIYAZAKI, J. & SEINO, Y. 1999. Glucose intolerance caused by a defect in the entero-insular axis: a study in gastric inhibitory polypeptide receptor knockout mice. *Proc Natl Acad Sci U S A,* 96**,** 14843-7.

MOENS, K., FLAMEZ, D., VAN SCHRAVENDIJK, C., LING, Z., PIPELEERS, D. & SCHUIT, F. 1998. Dual glucagon recognition by pancreatic beta-cells via glucagon and glucagon-like peptide 1 receptors. *Diabetes,* 47**,** 66-72.

MOORE, M. E., STUNKARD, A. & SROLE, L. 1962. Obesity, Social Class, and Mental Illness. *JAMA: The Journal of the American Medical Association,* 181**,** 962-966.

MORGAN, D. G., KULKARNI, R. N., HURLEY, J. D., WANG, Z. L., WANG, R. M., GHATEI, M. A., KARLSEN, A. E., BLOOM, S. R. & SMITH, D. M. 1998. Inhibition of glucose stimulated insulin secretion by neuropeptide Y is mediated via the Y1 receptor and inhibition of adenylyl cyclase in RIN 5AH rat insulinoma cells. *Diabetologia,* 41**,** 1482-1491.

MORTON, G. J., CUMMINGS, D. E., BASKIN, D. G., BARSH, G. S. & SCHWARTZ, M. W. 2006. Central nervous system control of food intake and body weight. *Nature,* 443**,** 289-295.

MURPHY, K. G. & BLOOM, S. R. 2006. Gut hormones and the regulation of energy homeostasis. *Nature,* 444**,** 854-859.

MYERS, M. G., JR., LEIBEL, R. L., SEELEY, R. J. & SCHWARTZ, M. W. 2010. Obesity and leptin resistance: distinguishing cause from effect. *Trends Endocrinol Metab,* 21**,** 643-51.

MYRSÉN-AXCRONA, U., EKBLAD, E. & SUNDLER, F. 1997. Developmental expression of NPY, PYY and PP in the rat pancreas and their coexistence with islet hormones. *Regulatory Peptides,* 68**,** 165-175.

NÄSLUND, E., BOGEFORS, J., SKOGAR, S., GRYBÄCK, P., JACOBSSON, H., HOLST, J. J. & HELLSTRÖM, P. M. 1999. GLP-1 slows solid gastric emptying and inhibits insulin, glucagon, and PYY release in humans. *American Journal of Physiology - Regulatory, Integrative and Comparative Physiology,* 277**,** R910-R916.

NAUCK, M., STÖCKMANN, F., EBERT, R. & CREUTZFELDT, W. 1986. Reduced incretin effect in Type 2 (non-insulin-dependent) diabetes. *Diabetologia,* 29**,** 46-52.

NAUCK, M. A., HEIMESAAT, M. M., ORSKOV, C., HOLST, J. J., EBERT, R. & CREUTZFELDT, W. 1993. Preserved incretin activity of glucagon-like peptide 1 [7-36 amide] but not of synthetic human gastric inhibitory polypeptide in patients with type-2 diabetes mellitus. *The Journal of Clinical Investigation,* 91**,** 301-307.

NIE, Y., NAKASHIMA, M., BRUBAKER, P. L., LI, Q.-L., PERFETTI, R., JANSEN, E., ZAMBRE, Y., PIPELEERS, D. & FRIEDMAN, T. C. 2000. Regulation of pancreatic PC1 and PC2 associated with increased glucagon-like peptide 1 in diabetic rats. *The Journal of Clinical Investigation,* 105**,** 955-965.

NIEUWENHUIZEN, A. G., KARLSSON, S., FRIDOLF, T. & AHRÉN, B. 1994. Mechanisms underlying the insulinostatic effect of peptide YY in mouse pancreatic islets. *Diabetologia,* 37**,** 871-878.

OBICI, S., FENG, Z., KARKANIAS, G., BASKIN, D. G. & ROSSETTI, L. 2002. Decreasing hypothalamic insulin receptors causes hyperphagia and insulin resistance in rats. *Nat Neurosci,* 5**,** 566-72.

OLIVAN, B., TEIXEIRA, J., BOSE, M., BAWA, B., CHANG, T., SUMME, H., LEE, H. & LAFERRERE, B. 2009. Effect of weight loss by diet or gastric bypass surgery on peptide YY3-36 levels. *Ann Surg,* 249**,** 948-53.

PARK, H. J., LEE, Y. L. & KWON, H. Y. 1993. Effects of pancreatic polypeptide on insulin action in exocrine secretion of isolated rat pancreas. *The Journal of Physiology,* 463**,** 421-429.

PARK, S., KAMEGAI, J., JOHNSON, T. A., FROHMAN, L. A. & KINEMAN, R. D. 2000. Modulation of pituitary somatostatin receptor subtype (sst1-5)

messenger ribonucleic acid levels by changes in the growth hormone axis. *Endocrinology,* 141**,** 3556-63.

PATTI, M. E., MCMAHON, G., MUN, E. C., BITTON, A., HOLST, J. J., GOLDSMITH, J., HANTO, D. W., CALLERY, M., ARKY, R., NOSE, V., BONNER-WEIR, S. & GOLDFINE, A. B. 2005. Severe hypoglycaemia post-gastric bypass requiring partial pancreatectomy: evidence for inappropriate insulin secretion and pancreatic islet hyperplasia. *Diabetologia,* 48**,** 2236-40.

PERLEY, M. J. & KIPNIS, D. M. 1967. Plasma Insulin Responses to Oral and Intravenous Glucose: Studies in Normal and Diabetic Subjects*. *The Journal of Clinical Investigation,* 46**,** 1954-1962.

PETERLI, R., WOLNERHANSSEN, B., PETERS, T., DEVAUX, N., KERN, B., CHRISTOFFEL-COURTIN, C., DREWE, J., VON FLUE, M. & BEGLINGER, C. 2009. Improvement in glucose metabolism after bariatric surgery: comparison of laparoscopic Roux-en-Y gastric bypass and laparoscopic sleeve gastrectomy: a prospective randomized trial. *Ann Surg,* 250**,** 234-41.

POSPISILIK, J. A., HINKE, S. A., PEDERSON, R. A., HOFFMANN, T., ROSCHE, F., SCHLENZIG, D., GLUND, K., HEISER, U., MCINTOSH, C. H. & DEMUTH, H. 2001. Metabolism of glucagon by dipeptidyl peptidase IV (CD26). *Regul Pept,* 96**,** 133-41.

POSPISILIK, J. A., MARTIN, J., DOTY, T., EHSES, J. A., PAMIR, N., LYNN, F. C., PITEAU, S., DEMUTH, H. U., MCINTOSH, C. H. & PEDERSON, R. A. 2003. Dipeptidyl peptidase IV inhibitor treatment stimulates beta-cell survival and islet neogenesis in streptozotocin-induced diabetic rats. *Diabetes,* 52**,** 741-50.

POULSEN, M. D., HANSEN, G. H., DABELSTEEN, E., HØYER, P. E., NORÉN, O. & SJÖSTRÖM, H. 1993. Dipeptidyl peptidase IV is sorted to the secretory granules in pancreatic islet A-cells. *Journal of Histochemistry & Cytochemistry,* 41**,** 81-8.

PULLEN, T. J., SYLOW, L., SUN, G., HALESTRAP, A. P., RICHTER, E. A. & RUTTER, G. A. 2012. Overexpression of monocarboxylate transporter-1 (SLC16A1) in mouse pancreatic beta-cells leads to relative hyperinsulinism during exercise. *Diabetes,* 61**,** 1719-25.

QINTAR, M., SIBAI, F. & TAHA, M. 2012. Hypoglycemia due to an adult-onset nesidioblastosis, a diagnostic and management dilemma.

RAHIER, J., GUIOT, Y. & SEMPOUX, C. 2000. Persistent hyperinsulinaemic hypoglycaemia of infancy: a heterogeneous syndrome unrelated to nesidioblastosis. *Arch Dis Child Fetal Neonatal Ed,* 82**,** F108-12.

RAMIREZ, J. L., GRANT, M., NORMAN, M., WANG, X. P., MOLDOVAN, S., DE MAYO, F. J., BRUNICARDI, C. & KUMAR, U. 2004. Deficiency of

somatostatin (SST) receptor type 5 (SSTR5) is associated with sexually dimorphic changes in the expression of SST and SST receptors in brain and pancreas. *Mol Cell Endocrinol,* 221**,** 105-19.

RAVN, P., MADHURANTAKAM, C., KUNZE, S., MATTHEWS, E., PRIEST, C., O'BRIEN, S., COLLINSON, A., PAPWORTH, M., FRITSCH-FREDIN, M., JERMUTUS, L., BENTHEM, L., GRUETTER, M. & JACKSON, R. H. 2013. Structural and Pharmacological Characterization of Novel Potent and Selective Monoclonal Antibody Antagonists of Glucose-dependent Insulinotropic Polypeptide Receptor. *Journal of Biological Chemistry,* 288**,** 19760-19772.

REID, T. 2012. Choosing GLP-1 Receptor Agonists or DPP-4 Inhibitors: Weighing the Clinical Trial Evidence. *Clinical Diabetes,* 30**,** 3-12.

RIGAMONTI, A. E., CELLA, S. G., BONOMO, S. M., MANCIA, G., GRASSI, G., PEROTTI, M., AGOSTI, F., SARTORIO, A., MÜLLER, E. E. & PINCELLI, A. I. 2011. Effect of somatostatin infusion on peptide YY secretion: studies in the acute and recovery phase of anorexia nervosa and in obesity. *European Journal of Endocrinology,* 165**,** 421-427.

ROCHELEAU, J. V., REMEDI, M. S., GRANADA, B., HEAD, W. S., KOSTER, J. C., NICHOLS, C. G. & PISTON, D. W. 2006. Critical Role of Gap Junction Coupled KATP Channel Activity for Regulated Insulin Secretion. *PLoS Biol,* 4**,** e26.

RODRIGUEZ-DIAZ, R. & CAICEDO, A. 2013. Novel approaches to studying the role of innervation in the biology of pancreatic islets. *Endocrinol Metab Clin North Am,* 42**,** 39-56.

RUBINO, F., FORGIONE, A., CUMMINGS, D. E., VIX, M., GNULI, D., MINGRONE, G., CASTAGNETO, M. & MARESCAUX, J. 2006. The mechanism of diabetes control after gastrointestinal bypass surgery reveals a role of the proximal small intestine in the pathophysiology of type 2 diabetes. *Ann Surg,* 244**,** 741-9.

SAINSBURY, A., SCHWARZER, C., COUZENS, M., FETISSOV, S., FURTINGER, S., JENKINS, A., COX, H. M., SPERK, G., HÖKFELT, T. & HERZOG, H. 2002a. Important role of hypothalamic Y2 receptors in body weight regulation revealed in conditional knockout mice. *Proceedings of the National Academy of Sciences,* 99**,** 8938-8943.

SAINSBURY, A., SCHWARZER, C., COUZENS, M., JENKINS, A., OAKES, S. R., ORMANDY, C. J. & HERZOG, H. 2002b. Y4 receptor knockout rescues fertility in ob/ob mice. *Genes & Development,* 16**,** 1077-1088.

SAM, A. H., GUNNER, D. J., KING, A., PERSAUD, S. J., BROOKS, L., HOSTOMSKA, K., FORD, H. E., LIU, B., GHATEI, M. A., BLOOM, S. R. & BEWICK, G. A. 2012. Selective ablation of peptide YY cells in adult mice reveals their role in beta cell survival. *Gastroenterology,* 143**,** 459-68.

SATO, D., MORINO, K., OHASHI, N., UEDA, E., IKEDA, K., YAMAMOTO, H., UGI, S., YAMAMOTO, H., ARAKI, S. & MAEGAWA, H. 2013. Octreotide improves early dumping syndrome potentially through incretins: a case report. *Endocr J,* 60**,** 847-53.

SCHALLY, A. V., HUANG, W. Y., CHANG, R. C., ARIMURA, A., REDDING, T. W., MILLAR, R. P., HUNKAPILLER, M. W. & HOOD, L. E. 1980. Isolation and structure of pro-somatostatin: a putative somatostatin precursor from pig hypothalamus. *Proc Natl Acad Sci U S A,* 77**,** 4489-93.

SCHIRRA, J., LEICHT, P., HILDEBRAND, P., BEGLINGER, C., ARNOLD, R., GOKE, B. & KATSCHINSKI, M. 1998. Mechanisms of the antidiabetic action of subcutaneous glucagon-like peptide-1(7-36)amide in non-insulin dependent diabetes mellitus. *J Endocrinol,* 156**,** 177-86.

SCHONHOFF, S., BAGGIO, L., RATINEAU, C., RAY, S. K., LINDNER, J., MAGNUSON, M. A., DRUCKER, D. J. & LEITER, A. B. 2005. Energy Homeostasis and Gastrointestinal Endocrine Differentiation Do Not Require the Anorectic Hormone Peptide YY. *Molecular and Cellular Biology,* 25**,** 4189-4199.

SCHWARTZ, M. W., WOODS, S. C., PORTE, D., SEELEY, R. J. & BASKIN, D. G. 2000. Central nervous system control of food intake. *Nature,* 404**,** 661-671.

SCOTT, M. M., WILLIAMS, K. W., ROSSI, J., LEE, C. E. & ELMQUIST, J. K. 2011. Leptin receptor expression in hindbrain Glp-1 neurons regulates food intake and energy balance in mice. *J Clin Invest,* 121**,** 2413-21.

SCROCCHI, L. A., BROWN, T. J., MACLUSKY, N., BRUBAKER, P. L., AUERBACH, A. B., JOYNER, A. L. & DRUCKER, D. J. 1996. Glucose intolerance but normal satiety in mice with a null mutation in the glucagon-like peptide 1 receptor gene. *Nat Med,* 2**,** 1254-8.

SEAQUIST, E. R., DAMBERG, G. S., TKAC, I. & GRUETTER, R. 2001. The effect of insulin on in vivo cerebral glucose concentrations and rates of glucose transport/metabolism in humans. *Diabetes,* 50**,** 2203-9.

SEINO, S., SHIBASAKI, T. & MINAMI, K. 2011. Dynamics of insulin secretion and the clinical implications for obesity and diabetes. *The Journal of Clinical Investigation,* 121**,** 2118-2125.

SENNIAPPAN, S., ARYA, V. & HUSSAIN, K. 2013. The molecular mechanisms, diagnosis and management of congenital hyperinsulinism. *Indian J Endocrinol Metab.* 17(1):19-30.

SERVICE, G. J., THOMPSON, G. B., SERVICE, F. J., ANDREWS, J. C., COLLAZO-CLAVELL, M. L. & LLOYD, R. V. 2005. Hyperinsulinemic Hypoglycemia with Nesidioblastosis after Gastric-Bypass Surgery. *New England Journal of Medicine,* 353**,** 249-254.

SHARP, G. W. 1996. Mechanisms of inhibition of insulin release. *Am J Physiol,* 271**,** C1781-99.

SHAW, J. E., SICREE, R. A. & ZIMMET, P. Z. 2010. Global estimates of the prevalence of diabetes for 2010 and 2030. *Diabetes Research and Clinical Practice,* 87**,** 4-14.

SHI, Y.-C., HÄMMERLE, C., LEE, I. C. J., TURNER, N., NGUYEN, A. D., RIEPLER, S. J., LIN, S., SAINSBURY, A., HERZOG, H. & ZHANG, L. 2012. Adult-onset PYY overexpression in mice reduces food intake and increases lipogenic capacity. *Neuropeptides*.

SHIOTA, C., LARSSON, O., SHELTON, K. D., SHIOTA, M., EFANOV, A. M., HØY, M., LINDNER, J., KOOPTIWUT, S., JUNTTI-BERGGREN, L., GROMADA, J., BERGGREN, P.-O. & MAGNUSON, M. A. 2002. Sulfonylurea Receptor Type 1 Knock-out Mice Have Intact Feeding-stimulated Insulin Secretion despite Marked Impairment in Their Response to Glucose. *Journal of Biological Chemistry,* 277**,** 37176-37183.

SINGH, E. & VELLA, A. 2012. Hypoglycemia After Gastric Bypass Surgery. *Diabetes Spectrum,* 25**,** 217-221.

SPEAKMAN, J. R. 2010. FTO effect on energy demand versus food intake. *Nature,* 464**,** E1-E1.

STOCK, S., LEICHNER, P., WONG, A. C. K., GHATEI, M. A., KIEFFER, T. J., BLOOM, S. R. & CHANOINE, J.-P. 2005. Ghrelin, Peptide YY, Glucose-Dependent Insulinotropic Polypeptide, and Hunger Responses to a Mixed Meal in Anorexic, Obese, and Control Female Adolescents. *Journal of Clinical Endocrinology & Metabolism,* 90**,** 2161-2168.

STROWSKI, M. Z., KOHLER, M., CHEN, H. Y., TRUMBAUER, M. E., LI, Z., SZALKOWSKI, D., GOPAL-TRUTER, S., FISHER, J. K., SCHAEFFER, J. M., BLAKE, A. D., ZHANG, B. B. & WILKINSON, H. A. 2003. Somatostatin receptor subtype 5 regulates insulin secretion and glucose homeostasis. *Mol Endocrinol,* 17**,** 93-106.

SUN, Y., WANG, P., ZHENG, H. & SMITH, R. G. 2004. Ghrelin stimulation of growth hormone release and appetite is mediated through the growth hormone secretagogue receptor. *Proc Natl Acad Sci U S A,* 101**,** 4679-84.

SZABO, O. & SZABO, A. J. 1975. Studies on the nature and mode of action of the insulin-sensitive glucoregulator receptor in the central nervous system. *Diabetes,* 24**,** 328-36.

SZECOWKA, J., GRILL, V., SANDBERG, E. & EFENDIC, S. 1982. Effect of GIP on the secretion of insulin and somatostatin and the accumulation of cyclic AMP in vitro in the rat. *Acta Endocrinol (Copenh),* 99**,** 416-21.

TATEMOTO, K., CARLQUIST, M. & MUTT, V. 1982. Neuropeptide Y a novel brain peptide with structural similarities to peptide YY and pancreatic polypeptide. *Nature,* 296**,** 659-660.

TATEMOTO, K. & MUTT, V. 1980. Isolation of two novel candidate hormones using a chemical method for finding naturally occurring polypeptides. *Nature,* 285**,** 417-418.

THORENS, B. 2012. Appetite Control. *Handbook of Experimental Pharmacology,* 209**,** Part 3, 277-294.

TIESJEMA, B., ADAN, R. A. H., LUIJENDIJK, M. C. M., KALSBEEK, A. & LA FLEUR, S. E. 2007. Differential Effects of Recombinant Adeno-Associated Virus-Mediated Neuropeptide Y Overexpression in the Hypothalamic Paraventricular Nucleus and Lateral Hypothalamus on Feeding Behavior. *The Journal of Neuroscience,* 27**,** 14139-14146.

TRUMPER, A., TRUMPER, K., TRUSHEIM, H., ARNOLD, R., GOKE, B. & HORSCH, D. 2001. Glucose-dependent insulinotropic polypeptide is a growth factor for beta (INS-1) cells by pleiotropic signaling. *Mol Endocrinol,* 15**,** 1559-70.

TSENG, C. C., ZHANG, X. Y. & WOLFE, M. M. 1999. Effect of GIP and GLP-1 antagonists on insulin release in the rat. *Am J Physiol,* 276**,** E1049-54.

UCHIDA, A., ZIGMAN, J. M. & PERELLO, M. 2013. Ghrelin and eating behavior: evidence and insights from genetically-modified mouse models. *Front Neurosci,* 7**,** 121.

UNGER, R. H. & EISENTRAUT, A. M. 1969. Entero-Insular Axis. *Arch Intern Med,* 123**,** 261-266.

UNSON, C. G., CYPESS, A. M., WU, C. R., GOLDSMITH, P. K., MERRIFIELD, R. B. & SAKMAR, T. P. 1996. Antibodies against specific extracellular epitopes of the glucagon receptor block glucagon binding. *Proceedings of the National Academy of Sciences,* 93**,** 310-315.

UPCHURCH, B. H., APONTE, G. W. & LEITER, A. B. 1994. Expression of peptide YY in all four islet cell types in the developing mouse pancreas suggests a common peptide YY-producing progenitor. *Development,* 120**,** 245-252.

UPCHURCH, B. H., FUNG, B. P., RINDI, G., RONCO, A. & LEITER, A. B. 1996. Peptide YY expression is an early event in colonic endocrine cell differentiation: evidence from normal and transgenic mice. *Development,* 122**,** 1157-1163.

VELLA, A. & SERVICE, F. J. 2007. Incretin hypersecretion in post-gastric bypass hypoglycemia--primary problem or red herring? *J Clin Endocrinol Metab,* 92**,** 4563-5.

WANG, Q., BING, C., AL-BARAZANJI, K., MOSSAKOWASKA, D. E., WANG, X. M., MCBAY, D. L., NEVILLE, W. A., TADDAYON, M., PICKAVANCE, L., DRYDEN, S., THOMAS, M. E., MCHALE, M. T., GLOYER, I. S., WILSON, S., BUCKINGHAM, R., ARCH, J. R., TRAYHURN, P. & WILLIAMS, G. 1997. Interactions between leptin and

hypothalamic neuropeptide Y neurons in the control of food intake and energy homeostasis in the rat. *Diabetes,* 46**,** 335-41.

WHEELER, M. B., GELLING, R. W., MCINTOSH, C. H., GEORGIOU, J., BROWN, J. C. & PEDERSON, R. A. 1995. Functional expression of the rat pancreatic islet glucose-dependent insulinotropic polypeptide receptor: ligand binding and intracellular signaling properties. *Endocrinology,* 136**,** 4629-39.

WHIM, M. D. 2011. Pancreatic Beta Cells Synthesize Neuropeptide Y and Can Rapidly Release Peptide Co-Transmitters. *PLoS ONE,* 6**,** e19478.

WHO. 2013. *Obesity* [Online]. Available: http://www.who.int/topics/obesity/en/ 2013].

WILLIAMS, D. L. & SCHWARTZ, M. W. 2011. Neuroanatomy of body weight control: lessons learned from leptin. *J Clin Invest,* 121**,** 2152-5.

WONG, I. P. L., DRIESSLER, F., KHOR, E. C., SHI, Y.-C., HÖRMER, B., NGUYEN, A. D., ENRIQUEZ, R. F., EISMAN, J. A., SAINSBURY, A., HERZOG, H. & BALDOCK, P. A. 2012. Peptide YY Regulates Bone Remodeling in Mice: A Link between Gut and Skeletal Biology. *PLoS One,* 7**,** e40038.

XU, G., STOFFERS, D. A., HABENER, J. F. & BONNER-WEIR, S. 1999. Exendin-4 stimulates both beta-cell replication and neogenesis, resulting in increased beta-cell mass and improved glucose tolerance in diabetic rats. *Diabetes,* 48**,** 2270-6.

XU, J., MCNEARNEY, T. A. & CHEN, J. D. Z. 2011. Impaired postprandial releases/syntheses of ghrelin and PYY3-36 and blunted responses to exogenous ghrelin and PYY3-36 in a rodent model of diet-induced obesity.

XU, Z. D., YU, H. F., SANG, Y. M., ZHANG, Y. N., YAN, J., WU, Y. J., ZHU, C. & NI, G. C. 2013. [ABCC8, KCNJ11 and GLUD1 gene mutation analysis in congenital hyperinsulinism pedigree]. *Zhonghua Yi Xue Za Zhi,* 93**,** 1089-92.

YANG, S. K., PARKINGTON, H. C., BLAKE, A. D., KEATING, D. J. & CHEN, C. 2005. Somatostatin increases voltage-gated K+ currents in GH3 cells through activation of multiple somatostatin receptors. *Endocrinology,* 146**,** 4975-84.

YORIFUJI, T., KAWAKITA, R., HOSOKAWA, Y., FUJIMARU, R., MATSUBARA, K., AIZU, K., SUZUKI, S., NAGASAKA, H., NISHIBORI, H. & MASUE, M. 2013. Efficacy and safety of long-term, continuous subcutaneous octreotide infusion for patients with different subtypes of KATP-channel hyperinsulinism. *Clinical Endocrinology,* 78**,** 891-897.

YOUOS, J. G. 2011. The role of alpha-, delta- and F cells in insulin secretion and action. *Diabetes Res Clin Pract,* 93 Suppl 1**,** S25-6.

ZHANG, L., NGUYEN, A. D., LEE, I. C. J., YULYANINGSIH, E., RIEPLER, S. J., STEHRER, B., ENRIQUEZ, R. F., LIN, S., SHI, Y. C., BALDOCK, P.

A., SAINSBURY, A. & HERZOG, H. 2012. NPY modulates PYY function in the regulation of energy balance and glucose homeostasis. *Diabetes, Obesity and Metabolism,* 14**,** 727-736.

ZHANG, Y., OLBORT, M., SCHWARZER, K., NUESSLEIN-HILDESHEIM, B., NICOLSON, M., MURPHY, E., KOWALSKI, T. J., SCHMIDT, I. & LEIBEL, R. L. 1997. The leptin receptor mediates apparent autocrine regulation of leptin gene expression. *Biochem Biophys Res Commun,* 240**,** 492-5.

ZHAO, T. J., LIANG, G., LI, R. L., XIE, X., SLEEMAN, M. W., MURPHY, A. J., VALENZUELA, D. M., YANCOPOULOS, G. D., GOLDSTEIN, J. L. & BROWN, M. S. 2010. Ghrelin O-acyltransferase (GOAT) is essential for growth hormone-mediated survival of calorie-restricted mice. *Proc Natl Acad Sci U S A,* 107**,** 7467-72.

ZHOU, J., MONTROSE-RAFIZADEH, C., JANCZEWSKI, A. M., PINEYRO, M. A., SOLLOTT, S. J., WANG, Y. & EGAN, J. M. 1999. Glucagon-like peptide-1 does not mediate amylase release from AR42J cells. *J Cell Physiol,* 181**,** 470-8.

Appendices

Appendix I: Solutions

Tail lysis buffer (per 100ml): 67 mM Tris-HCl pH 8.8, 16.6 mM $(NH_4)_2SO_4$, 6.7 mM $MgCl_2$, 0.5 % v/v Triton X-100, 1 % v/v beta mercaptoethanol

2X KRB stock solution: 136 mM NaCl, 4.7 mM KCl, 1.2 mM KH_2PO_4, 5 mM $NaHCO_3$, 1.2 mM $MgSO_4$ ($7H_2O$)

Quenching buffer (1x KRB): 2x KRB stock solution, 10 mM Hepes, 1 mM $CaCl_2$, 2 mM D-glucose, pH to 7.4 and filter the solution

Pancreatic digestion solution: filtered 1x KRB solution (pH 7.4) with 100 units/ml penicillin + 100 μg/ml streptomycin and 0.225 mg/ml Liberase RI (Roche, West Sussex, UK) (2.5 mg/ml stock solution)

Antigen-retrieval solution: 10% Dako antigen retrieval solution concentrate (Dako, Cambridgeshire, UK) in 1x PBS (v/v)

Blocking solution: (1) *for unconjugated primary antibodies:* 10% normal goat serum in 1x PBS (v/v) and (2) *for the biotin-conjugated antibodies:* incubation with 2 drops of avidin for 10 minutes, followed by 2 drops of biotin for 10 minutes and finally 0.1% Dako serum-free protein block in 1x PBS (v/v).

Appendix II: Supplementary IHC images for Chapter 3

Representative z-stacked IHC images of C57BL/6 male mice aged 10-12 weeks:

Islet immunostaining of:

(A1) DPP-4 (green) and DAPI (blue) x 100.

(A2) DPP-4 (green) and DAPI (blue) x 63.

(A3) DPP-4 (green), Ins (red) and DAPI (blue) x 20.

(A4) DPP-4 (green), Ins (red) and DAPI (blue) x 100.

(A5) DPP-4 (green), GCG (red) and DAPI (blue) x 40.

(A6) DPP-4 (green), GCG (red) and DAPI (blue) x 100.

(A7) DPP-4 (green), SST (red) and DAPI (blue) x 40.

(A8) DPP-4 (green), PYY (red) and DAPI (blue) x 40.

(A9) Y1R (green), Ins (red) and DAPI (blue) x 40.

(A10) DPP-4 (green), Y1R (red) and DAPI (blue) x 40.

(Image quality best with RealPlayer Software)

Appendix III: Presentations, Awards & Publications

PRESENTATIONS

1. **S. A. Rahman.** Obesity: Why is it such a 'BIG' issue in our society? St Marys Hospital Physiotherapy Department, London, UK. January 2011.
2. **S. A. Rahman.** Investigating the Role and Regulation of Intra-islet Peptide YY. GlaxoSmithKline, North Carolina, USA. December 2011.
3. **S. A. Rahman.** Division of Medicine Seminar series: Investigating the Physiological Role and Regulation of Intra-islet Peptide YY. University College London, UK. May 2012.
4. M-J Brassill, **SA Rahman,** A Boyde, RL Batterham, GR Williams, JHD Bassett. Peptide YY regulates bone mineral content and strength. Society for Endocrinology BES 2013. Harrogate, UK. March 2013

POSTER PRESENTATIONS

1. **S. A. Rahman,** Efthimia Karra and Khalid Hussain**.** Characterising the role and regulation of dipeptidyl peptidase-4 in congenital hyperinsulinism. UCL Division of Medicine PhD Student Summer Meeting. University College London, UK. June 2013.
2. **S. A. Rahman,** Efthimia Karra and Khalid Hussain**.** Characterising the role and regulation of dipeptidyl peptidase-4 in congenital hyperinsulinism. 9th Joint Meeting of Paediatric Endocrinology, Milan, Italy. 21 September 2013.
3. Azizun Nessa, Alison Thomas, Qadeer H. Aziz, Steve Harmer, Amanda Heslegrave, Chela James, Ved B. Arya, **Sofia Rahman**, Maha Sherif, Sarah E. Flanagan, Ritika R. Kapoor, Sian S. Ellard, Andrew Tinker, Khalid Hussain. Understanding the molecular basis of congenital hyperinsulinism due to autosomal dominant ABCC8 and KCNJ11 mutation. 9th Joint Meeting of Paediatric Endocrinology, Milan, Italy. 21 September 2013.
4. Ved Bhushan Arya, Syeda Alam, Senthil Senniappan, Azizun Nessa, **Sofia Rahman,** Maha Sherif, Sarah E. Flanagan, Sian Ellard, Khalid Hussain. Long-term endocrine and exocrine outcome of medically unresponsive diffuse congenital hyperinsulinism managed with near-total pancreatectomy: 18-years' experience. 9th Joint Meeting of Paediatric Endocrinology, Milan, Italy. 21 September 2013.
5. Maha Mohamed Sherif, Ibtisam Hadeed, Azizun Nessa, **Sofia A. Rahman**, Ved B. Arya, Senthil Senniappan, Mehul Dattani, Khalid Hussain. Two families with diabetes mellitus and sensorineural deafness. 9th Joint Meeting of Paediatric Endocrinology, Milan, Italy. 21 September 2013.
6. **S. A. Rahman,** Efthimia Karra and Khalid Hussain**.** Characterising the role and regulation of dipeptidyl peptidase-4 in congenital hyperinsulinism. Institute of Child Health Postgraduate Poster Competition. 20 November 2013.

AWARDS

1. SfE Career Development worskshop, residential course, Oxfordshire, UK (Oct 2013).
2. UCL Institute of Child Health Conference grant September 2013 (£250).
3. BES travel grant December 2008- 2010, 2012-2013 (£500) and December 2011 (£750).
4. 3-month GSK international internship, Research Triangle Park, North Carolina, USA (2011).

Appendix IV: Publications

1. Hameed, Saira., Dhillo, Waljit S., Patterson, Michael., Bloom, Stephen R., **Rashid, Sofia**., Bassett, J.H. Duncan., Williams, Graham R. & Gardiner. James V. (2009). The central regulation of food intake and energy expenditure by thyroid hormones. Hot Thyroidology E-book, pages 1-31.

2. Karra, E., O. G. Daly, A. I. Choudhury, A. Yousseif, S. Millership, M. T. Neary, W. R. Scott, K. Chandarana, S. Manning, M. E. Hess, H. Iwakura, T. Akamizu, Q. Millet, C. Gelegen, M. E. Drew, **S. Rahman,** J. J. Emmanuel, S. C. R. Williams, U. U. Ruther, J. C. Bruning, D. J. Withers, F. O. Zelaya and R. L. Batterham (2013). "A link between FTO, ghrelin, and impaired brain food-cue responsivity." The Journal of Clinical Investigation 123(8): 3539-3551.

3. Ved Bhushan Arya*, **Sofia Rahman*,** Senthil Senniappan, Sarah E. Flanagan, Sian Ellard and Khalid Hussain. HNF4A Mutation: Switch from Hyperinsulinaemic Hypoglycaemia to Maturity Onset Diabetes of Young and Incretin Response. * Joint first authors. Diabetic Medicine. 2013 Dec 3. doi: 10.1111/dme.12369. [Epub ahead of print].

4. A Yousseif. E Karra, **S Rahman** & RL Batterham 2014. 'Obesity' in PE Harria & PG Bouloux (Second Edition), *Endocrinology in Clinical Practice.* Taylor & Francis Publishing. London, UK, pp. 491-509.